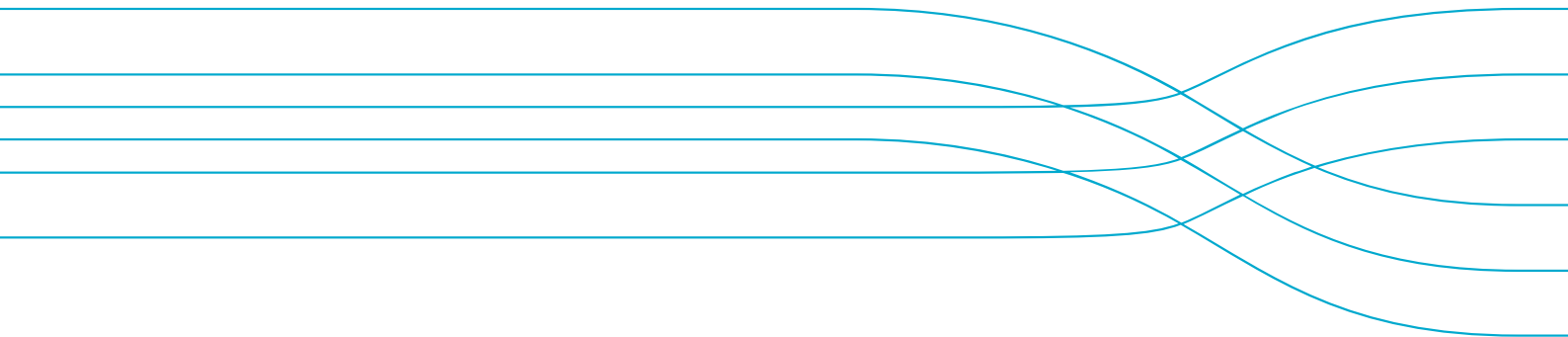


Potential impacts on groundwater resources from conventional gas in the South East of SA

Rebecca Doble, Trevor Pickett, Sreekanth Janardhanan, Russell Crosbie, Dennis Gonzalez



ISBN (print): 978-1-4863-1473-7

ISBN (online): 978-1-4863-1474-4

Citation

Rebecca Doble, Trevor Pickett, Sreekanth Janardhanan, Russell Crosbie, Dennis Gonzalez (2020)

Potential impacts on groundwater resources from conventional gas in the South East of SA, CSIRO Land and Water.

Copyright

© Commonwealth Scientific and Industrial Research Organisation 2020. To the extent permitted by law, all rights are reserved and no part of this publication covered by copyright may be reproduced or copied in any form or by any means except with the written permission of CSIRO.

Important disclaimer

CSIRO advises that the information contained in this publication comprises general statements based on scientific research. The reader is advised and needs to be aware that such information may be incomplete or unable to be used in any specific situation. No reliance or actions must therefore be made on that information without seeking prior expert professional, scientific and technical advice. To the extent permitted by law, CSIRO (including its employees and consultants) excludes all liability to any person for any consequences, including but not limited to all losses, damages, costs, expenses and any other compensation, arising directly or indirectly from using this publication (in part or in whole) and any information or material contained in it.

CSIRO is committed to providing web accessible content wherever possible. If you are having difficulties with accessing this document, please contact csiroenquiries@csiro.au.

Contents

Acknowledgments.....	vi
Executive summary	vii
1 Introduction	9
2 Child MODFLOW model development and calibration	10
2.1 Materials and methods	10
3 Uncertainty analysis.....	26
3.1 History matching	26
3.2 PEST-IES set-up	31
3.3 Results of calibration and uncertainty analysis.....	31
4 Probabilistic water balance and scenario analysis	41
4.1 Scenarios.....	41
4.2 Groundwater heads.....	42
4.3 Drawdown	44
4.4 Well pumping rates	46
4.5 Water balance	47
4.6 Net recharge	49
5 Conclusions	52
6 Appendices	54
6.1 Land use change	54
6.2 Average annual NetRcurves	66
7 References	68

Figures

Figure 1: Study area, the South East subregion and locations of the exploration gas wells.....	11
Figure 2: Geological and hydrogeological conceptual model of the South East (after Morgan et al., 2015).....	12
Figure 3: 3D view of the model showing outcropping model layers, looking north (grid indicated by blue lines) Z-axis exaggeration is 10x.....	13
Figure 4 Heads in the Gambier Limestone aquifer (Layer 1) of the regional groundwater model (Wood and Pierce, 2015), showing the extent of the child model. New gas wells indicated in dark red.....	15
Figure 5 Heads in the Tertiary Confined aquifer (Layer 3) of the regional groundwater model (Wood and Pierce, 2015), showing the extent of the child model. New gas wells indicated in dark red.....	16
Figure 6 Drain base elevations used in Layer 1 of the child model.	17
Figure 7 Groundwater model developed in FloPy showing drains (yellow), extraction wells (red), and observation wells (blue).....	18
Figure 8 Average monthly rainfall for (a) Penola and (b) Mt Burr.....	19
Figure 9 Changes in land cover from 1987 to 2015 for the child model extent.....	21
Figure 10 Most likely land cover for the child model from 2010 to 2015	22
Figure 11 Clay content in the top two metres of soil, developed from the Australian Soil Resources Information System (ASRIS) Atlas of Australian Soils database (Johnston, et al., 2003).	23
Figure 12 Annual average NetR curves for Penola, for each soil type, showing crops, pasture, native vegetation and forestry land uses.	24
Figure 13 Six monthly historical NetR curves developed for forestry areas with soil type 3 (15 – 25% clay) using WAVES. Each grey line represents the NetR curve for one six-month stress period and the blue line is an indicative NetR curve representing summer (a) and winter (b) conditions. Summer net recharge curves are dominated by evapotranspiration, especially when groundwater is shallow, while the winter curves are dominated by recharge.....	25
Figure 14 Drain gauges that were used for the calibration of the child model, showing the contributing drains. Drain gauge numbers are the Water Connect identifiers.....	28
Figure 15 Drain discharge data from A2391001 Bakers Range South Drain at Phillips Road	29
Figure 16 Drain discharge data from A2390536 Drain C at upstream of Coonawarra.....	29
Figure 17 Drain discharge data from A2390515 Bakers Range South Drain at Robe-Penola Road	30
Figure 18 Two parameters used to vary the NetR curves (a) H-stretch (+/- 20%) and (b) V-stretch (+/- 40%).....	31

Figure 19: Prior and posterior distribution of hydraulic properties at the pilot points in the aquifer layers	32
Figure 21 One realization of Kh values for layer 1 and 3 interpolated from the pilot points.	33
Figure 22: Distribution of horizontal and vertical conductivity realization for the aquitard layer (Layer 2)	34
Figure 23 One realization of Ss values for layer 1 and 3 interpolated from the pilot points.	34
Figure 24 One realization of Sy values for layer 1 and 3 interpolated from the pilot points.....	35
Figure 25: Distribution of specific yield parameter at 9 pilot points in model layer 1.....	35
Figure 26: Prior and posterior distributions of drain conductance.	36
Figure 27: Time series of observed and modelled groundwater levels in selected bores where observations span across different lengths of periods.....	37
Figure 28: Prior and posterior distribution of str_d parameter for the NetR package. The str_d is a unitless multiplier for the depth component of the NetR function.	38
Figure 29: Prior and posterior distribution of the str_f parameter for the NetR package. The str_f is a unitless multiplier for the flux component of the NetR function.	38
Figure 30: Prior and posterior distribution of objective function obtained from the Monte Carlo simulation using the NetR package.....	39
Figure 31 Modelled and observed drain fluxes for drain gauges (a) A2391001 Bakers Range South Drain at Phillips Road (b) A2390536 Drain C at upstream of Coonawarra and (c) A2390515 Bakers Range South Drain at Robe-Penola Road.....	40
Figure 29 Groundwater extraction scenario for the three gas wells.....	42
Figure 30 Groundwater heads for one realisation of the South East child model, unconfined aquifer, (a) Layer 1 and (b) Layer 3.	42
Figure 33 One realisation of the groundwater heads at the location of the gas wells, Dombey (a), Haselgrove 4 (b) and Nangwarry (c)	44
Figure 34 Drawdown at the three well sites showing the average drawdown in blue, and uncertainty bands in grey, for Dombey (a), Haselgrove 4 (b) and Nangwarry (c).....	45
Figure 35 Drawdown at a distance of 500 m (a, c and e) and one km (b, d and f) from each of the three well sites showing the average drawdown in blue, and uncertainty bands in grey, for Dombey (a,d), Haselgrove 4 (b,e) and Nangwarry (c,f).	46
Figure 36 Histogram of the summer pumping rates from existing irrigation, stock and domestic wells within the child model extent, and the expected summer pumping rates at the Dombey, Haselgrove 4 and Nangwarry wells. Note that this only includes existing wells from within the child model extent, and not for the whole of the South East.	47
Figure 37 Water balance for the child model extent comparing the gas well extraction rate for the single year of construction to the annual average water balance over the 100-year model run time. It includes changes in groundwater storage (storage in and out), flows across the general head boundaries (GHB in and out), net Recharge NetR in and out), groundwater	

intercepted by the drains (drains), pumping from existing wells (wells) and pumping from the Dombey, Haselgrove 4 and Nangwarry wells (gas_wells).	48
Figure 38 Water balance for the child model extent comparing the gas well extraction rate for the single year of construction to the annual average water balance over the 100-year model run time shown as inflows to the child model and outflows. The groundwater extraction for the gas wells makes up 1.7% of the total for the year of construction, and 0% for all other years... 49	49
Figure 39 One realisation of the net recharge for the child model extent during the dry summer season (a) and the wet winter season (b). Note the change from ET dominant conditions (a) to recharge dominant conditions (b) and the NW-SE line demarking the change between Mount Burr and Penola climate data in (b).	50
Figure 40 Depth to groundwater in stress period 33 of the model for the same realisation in Figure 39.....	50
Figure 41 One realisation of the net recharge for the child model extent (summer season, ET dominant) in 1970 (a) and 2016 (b). Red ovals indicate areas where forestry development has taken place.	50
Figure 42 Water balance from the groundwater model with seasonally changing NetR curves, for the last 18 stress periods of the history matching period (2000 - 2019). Net recharge inflows and outflows and changes in storage are relatively larger due to the seasonally changing NetR curves.	51
Figure 43 Water balance from the groundwater model with annually changing NetR curves, for the last 18 stress periods of the history matching period (2000 - 2019). Net recharge inflows and outflows are relatively larger due to the seasonally changing NetR curves.	51
Figure 44 Most likely land cover for the Penola region from 1987 to 1990.....	54
Figure 45 Most likely land cover for the Penola region from 1990 to 1995.....	55
Figure 46 Most likely land cover for the Penola region from 1995 to 2000.....	56
Figure 47 Most likely land cover for the Penola region from 2000 to 2005.....	57
Figure 48 Most likely land cover for the Penola region from 2005 to 2010.....	58
Figure 49 Most likely land cover for the Penola region from 2010 to 2015.....	59
Figure 50 Most likely land cover aggregated for the child model from 1987 to 1990.....	60
Figure 51 Most likely land cover aggregated for the child model from 1990 to 1995.....	61
Figure 52 Most likely land cover aggregated for the child model from 1995 to 2000.....	62
Figure 53 Most likely land cover aggregated for the child model from 2000 to 2005.....	63
Figure 54 Most likely land cover aggregated for the child model from 2005 to 2010.....	64
Figure 55 Most likely land cover aggregated for the child model from 2010 to 2015.....	65

Tables

Table 1 Aggregation of the seventeen South Australian Land Cover types into seven most common land cover types, and areas of cover based on 2010 – 2015 data.	20
Table 2 Area of each of the land cover types within the child model region (km ²). General trends show a decrease in dryland agriculture and native vegetation, and increases in forestry, particularly hardwood, and irrigated agriculture.	20
Table 3 Gas well locations, and locations of potentially greatest drawdown.	41

Acknowledgments

The authors acknowledge the funding provided by the CSIRO Gas Industry Social and Environmental Research Alliance (GISERA) for undertaking this study. We acknowledge the South Australia Department of Energy and Mining (SA DEM) for providing support and advice in designing the scenarios analysed in this study for contamination risk assessment. We acknowledge SA Department of Environment and Water for the provision of the regional scale groundwater model, pertaining data sets for the child model used in this study. We also acknowledge the co-operation of Beach Energy in this study by providing relevant data and reports from their EIS studies. Representatives from SA DEM, DEW, Beach Energy, CSIRO Energy, CSIRO Land and Water contributed to the initial stakeholder workshop of this study and their contributions are also greatly appreciated.

Executive summary

Conventional gas and petroleum operations in the Otway Basin located in south eastern Australia require groundwater resources for construction of wells. The water use is in conjunction with other uses in the region such as irrigated agriculture and industry. For these reasons, community and other stakeholders express significant concerns regarding the effects that the onshore gas industry may have specifically on water resources and on the environment in general.

Conventional petroleum production occurs at large depths and is often separated from surface and groundwater resources by layers of impermeable rock that are several kilometres thick. Hence, it is unlikely that depressurising gas reservoirs would lead to drawdown in the surficial aquifers. However, it is possible that direct groundwater extraction for the construction and operation of gas and petroleum wells may have a localised adverse impact on aquifers due to enhanced drawdown, especially if extraction rates are high. Hence it is useful to quantify the potential drawdown and water balance impacts due to onshore gas operations.

This study aims to probabilistically quantify the overall water balance and drawdown of aquifers for an area of the South East of South Australia (“South East”) near Penola following the development of three new conventional gas wells (natural gas and carbon dioxide). It also aims to develop a detailed understanding of the groundwater flow regimes in these aquifers, including the identification of flow paths and flow rates that underpin the modelling of solute transport conducted in the companion South Australia GISERA water quality research project (<https://gisera.csiro.au/project/water-contamination-causes-pathways-and-risks/>).

The South East regional water balance groundwater model that has been developed by the Department for Environment and Water was used and a child model was developed as its subset, with a finer scale and more refined representation of surface-water groundwater interactions through a net recharge (NetR) boundary condition. The model extended 36 km east-west and 42 km north-south thus covering a total area of 1512 km². The model domain was conceptualised as a three-layer system, comprising of the unconfined Tertiary Limestone Aquifer, the Upper Tertiary Aquitard, and the Tertiary Confined Sands Aquifer. The model history matching period spanned from May 1970 to May 2019. The future scenario runs extended for a period of 149 years, which comprised 49 years of historical development and one year for well construction, an operational lifetime of 40 years within a total potential duration of impact of 100 years.

The water balance impacts in the South East arising from the construction and operation of the conventional gas wells were found to be minimal. The maximum drawdown under the planned extraction scenario in the unconfined Tertiary Limestone Aquifer at the Dombey 1 and Haselgrove 4 sites, had a 95% chance of being less than 14 cm. The maximum drawdown in the Tertiary Confined Sands Aquifer for the Nangwarry 1 site had a 95% chance of being less than 4 cm. Further than one kilometre away from the extraction wells, the drawdown had a 95% chance of being less than 9 cm, 7 cm and 3 cm for Dombey 1, Haselgrove 4 and Nangwarry 1 respectively.

The magnitude of drawdown for each of the wells was comparable to the seasonal changes in groundwater elevation with a recovery of groundwater heads occurring within a ten-year period. Looking at the water balance for the child model extents, the volumes of water proposed to be

extracted for the three wells represented only 1.7% of the water balance outflows for a one-year construction period. At the scale of the entire Otway Basin, the extraction volumes for the gas wells would be much less than 1.7% of the water budget outputs.

The drawdown and water balance changes arising from the construction of these wells are therefore unlikely to impact any groundwater dependent assets in the region.

The use of the NetR package allowed the incorporation of spatial and temporal changes in rainfall, soil types and land cover into the model to better capture recharge and ET processes especially in areas where groundwater is shallow. The project demonstrated the functionality of the NetR package in a fully transient mode with changing land use and climate data for the first time. The NetR curves were also included in the model calibration.

The refined model scale and net recharge processes used to improve the representation of the shallow groundwater behaviour provided the basis to model particle tracking thus providing crucial input data that underpins the modelling of solute transport conducted in the companion South Australia GISERA water quality project and reported in the final report of that project (Rassam et al, 2020).

1 Introduction

Petroleum and conventional gas operators often extract groundwater in the process of producing petroleum and gas both during well construction and the production process itself. Groundwater use by petroleum and gas operators in the Otway basin occurs in conjunction with other water uses including industry, forestry and irrigated agriculture. Groundwater in many parts of the Otway basin is shallow and groundwater dependent ecosystems such as wetlands are commonly found. For these reasons community and other stakeholders express significant concerns about the effect the onshore gas industry may have on the environment and water resources.

Conventional petroleum production occurs at very large depths and are often separated from the surface and groundwater sources by layers of impermeable rock that are several kilometres thick. It has been shown that conventional gas production is not expected induce drawdown in surficial aquifers from depressurisation of gas reservoirs (Cook, et al., 2016). Groundwater may be used by industry for their operations; however, they do require a licence from the relevant State regulators before they allowed to extract. Risks to water quantity from gas production are only likely to occur in the South East of South Australia (hereafter referred to as the 'South East') if the conventional gas industry becomes a user of significant volumes of water, which is dependent on the type and scale of resource development. However, understanding the status quo of the groundwater resource is important for this region considering that multiple competing uses of water (irrigation, forestry, gas) exist and that water levels have been declining over the years.

The first objective of the study is therefore to probabilistically quantify the overall water balance of aquifers and groundwater impacts arising from the development of three new conventional gas wells near Penola in the South East. Understanding the hydrogeology and status of groundwater resources in areas with existing and potential onshore gas activities is important to ascertain the characteristics of the resource and evaluate any potential changes induced by the industry. Evidence-based scientific analysis is required to underpin these assessments which can assist stakeholders make informed decisions regarding the presence or absence of relative risks to the environment and water resources.

The second objective is to provide the model-basis to develop a detailed understanding of groundwater flow regimes and flow velocities in these aquifers to underpin contaminant transport studies in the companion South Australia GISERA water quality research project (Rassam, et al., 2020). A detailed understanding of groundwater flow directions and velocities derived from a groundwater flow model is essential to quantify potential water quality effects induced by different activities associated with onshore gas development.

2 Child MODFLOW model development and calibration

2.1 Materials and methods

To assess the groundwater impacts of conventional gas well development, a child groundwater model that incorporated a subset of the region surrounding Penola was developed from existing regional groundwater models of the South East. The child groundwater model was developed for two purposes: (i) to assess the likelihood that water extraction for the development and operation of three conventional gas wells would negatively impact groundwater resources in the area, and (ii) to allow particle tracking analyses that identify potential pathways through the groundwater system of any contaminants that may be spilled at the surface. It was developed as a probabilistic model, so that impacts could be reported in terms of likelihood and probability.

The model developed solutions for:

- Drawdown in the unconfined and confined aquifers from water extraction used for the construction and operation of a conventional gas well
- Groundwater balance change in the study area caused by the extraction for gas well drilling purposes
- Regional groundwater flow directions and rates that influence contaminant transport in aquifers (reported in the companion South Australia GISERA water quality research project report (Rassam, et al., 2020)).

2.1.1 Study area and hydrogeology

The South East of South Australia is a relatively flat region, characterised by a limestone geology overlain by sandy soils (Figure 3). The area is characterised by dunes and interdunal flats from previous ocean ingressions. The major aquifers are the unconfined Tertiary Limestone Aquifer (TLA) and confined Tertiary Confined Sands Aquifer (TCSA) (Figure 4). Near Penola, the majority of groundwater extraction is sourced from the TLA. Karst features are known to be present in the TLA south of Mount Burr, however these were not explicitly included in the modelling.

The water table in the low-lying areas has been artificially lowered using agricultural drains, the first of which was constructed in 1863, while the majority of drains were developed from 1949 to 1972. The area has a large number of lakes and wetlands many of which are dependent on groundwater inflows to maintain water levels for part or all of the year. Predominant land uses include dryland grazing, irrigated pasture and viticulture, softwood and hardwood forestry and native vegetation.

Petroleum and conventional gas wells have been developed in the region around Penola since 1987 with the commercialisation of the Katnook and then the Ladbroke Grove fields. Three

additional gas wells have been drilled in this region, namely, Nangwarry 1 (for carbon dioxide, CO₂), Haselgrove 4 and Dombey 1.

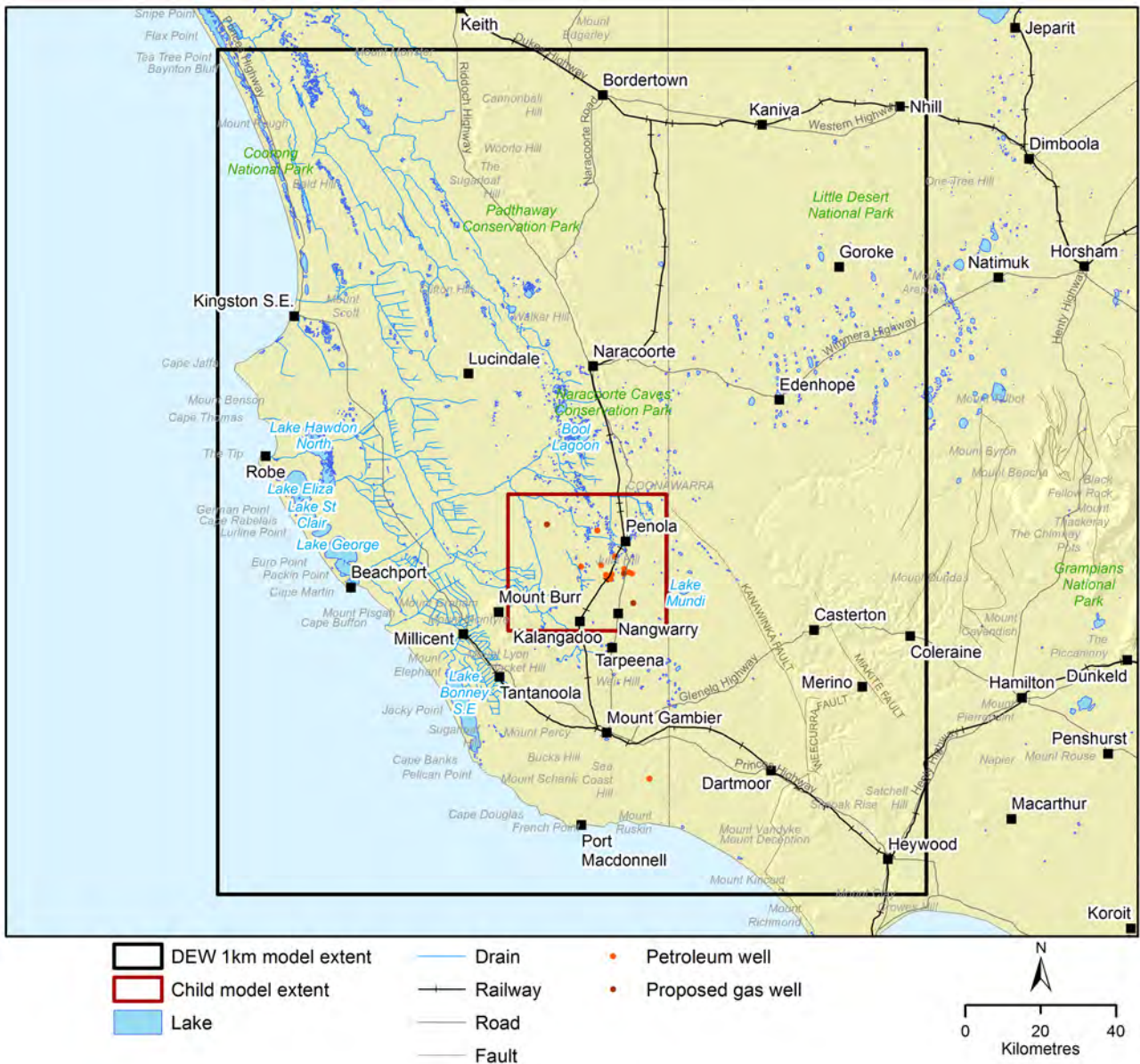


Figure 1: Study area, the South East subregion and locations of the exploration gas wells.

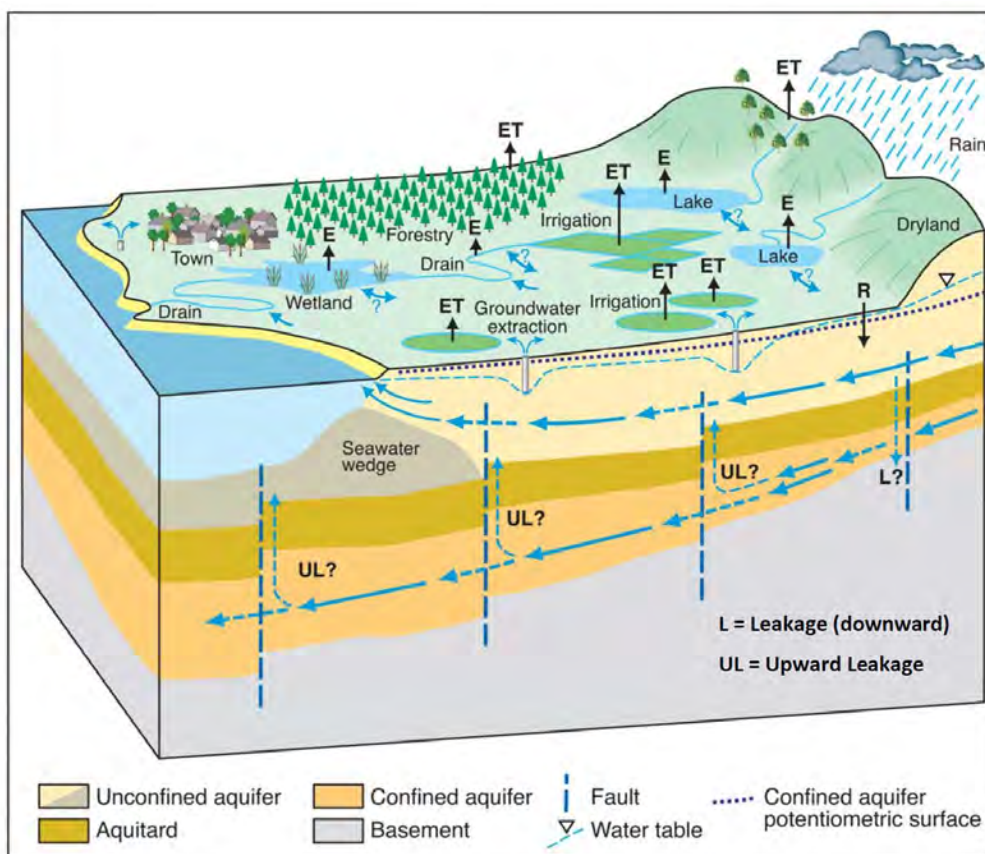


Figure 2: Geological and hydrogeological conceptual model of the South East (after Morgan et al., 2015)

2.1.2 Previous groundwater models

Previous groundwater models of the region include the Wattle Range groundwater model, a one-layer model of the upper South East, north of and including some of the area of interest (Wood, 2017). This model was developed to model forestry impacts in the Gambier Limestone aquifer and does not incorporate the Tertiary Confined Aquifer.

The South East regional water balance model was developed in 2014 (Morgan, et al., 2015), based on work by Brown et al. (2006). This model covers an area of 42,000 km, and includes the entire child model region, albeit at a coarser scale. Cell sizes are 1 km x 1 km, and the model incorporates the Gambier Limestone and Tertiary Confined aquifers, and the aquitard that separates them.

More recently the South East regional water balance model was recalibrated for a water resource assessment in the Kingston area (Wood, 2017). Although the South East regional water balance model is currently being recalibrated, the Kingston calibration was the best available calibrated regional model at the time of the study.

2.1.3 Numerical model design and implementation

A child model with a finer spatial resolution was developed in this study based on the regional water balance model. The child groundwater model was developed based on the hydro-stratigraphy and parameterisation of the Wattle Range groundwater model (Wood, 2017) and the Kingston calibration of the South East regional water balance model (Morgan, et al., 2015, Wood and Pierce, 2015).

The model was developed using FloPy (Bakker, et al., 2016), a Python based interface for the USGS MODFLOW 2005 groundwater flow model (Harbaugh, 2005). The FloPy interface allows for transparency and reproducibility in modelling (Hutton, et al., 2016, Ince, et al., 2012). It facilitates rapid and flexible model development that may be readily altered as data is upgraded or modelling intent changes. The model was visualised in ParaView (Ahrens, et al., 2005) and in Python.

The model was located in a region near Penola that included the sites for the Haselgrove 4, Nangwarry 1 and Dombey 1 wells. It extended 36 km east-west and 42 km north-south, covering a total area of 1512 km². The flow domain was conceptualised as a three-layer system, comprising of an unconfined aquifer (Tertiary Limestone Aquifer), an aquitard (Upper Tertiary Aquitard) and a confined aquifer (Tertiary Confined Sand Aquifer) (Figure 5).

The model run included a 49-year history matching period from May 1970 to May 2019. Six-month long stress periods allowed groundwater extraction to vary between summer when irrigation extraction is high, and winter when extraction is very low. Each stress period comprised ten time steps with a 1.5 multiplier that provides smaller time steps immediately following a stress period change.

Future scenario analysis runs were for a period of 149 years extending from 1970 to 2119. This assumed a historical warm up period of 49 years with a gas well development period of one year, operational lifetime of 40 years within a duration of potential impact of 100 years.

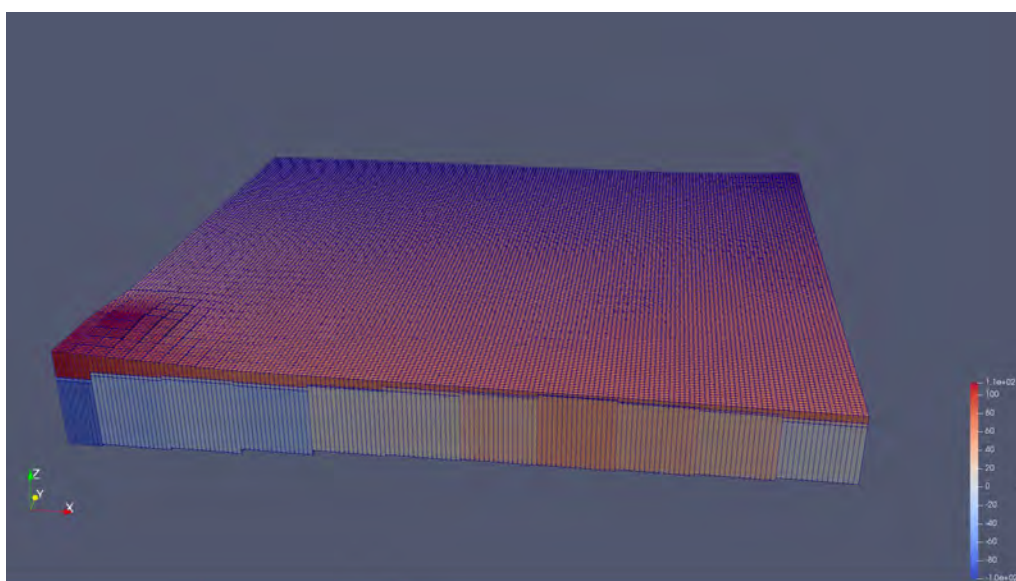


Figure 3: 3D view of the model showing outcropping model layers, looking north (grid indicated by blue lines) Z-axis exaggeration is 10x.

The land surface information was developed from the 1-second DEM data, upscaled to the 250-m cell size. Accurate and detailed land surface information was critical to appropriately capture the surface-groundwater interaction behaviour that was dominant in this shallow groundwater environment. Base elevations for Layers 1 to 3 were adopted from the SE regional groundwater model.

2.1.4 Boundary and initial conditions

The South East child model represents a small subset of the South East regional water balance model, and none of the boundaries are represented by a no flow boundary condition (used where flow is parallel to the boundary, or at natural hydrogeological boundaries) or specified head boundaries that would commonly be used for coastal boundaries. All four boundaries are dependent on the head and flow conditions in the parent regional model.

Head boundaries were extracted from the Kingston version of the South East Regional Water Balance Model (Figure 7 and Figure 8). To give the child model a degree of independence and flexibility from the parent model, a general head boundary condition was used. Groundwater heads at a distance of 2 km from the boundaries were specified from those locations within the regional groundwater model for Layers 1 and 3. Conductance, C , was calculated for each of the cells based on the 2 km distance between the boundary and specified head, the cell dimensions and hydraulic conductivity at that location.

$$C = \frac{kA}{x_1 - x_0}$$

Where: k is the hydraulic conductivity of the boundary cell, A is the cross-sectional area of the cell that forms the model boundary, and $(x_1 - x_0)$ is the distance between the cell edge and the point at which the GHB is measured.

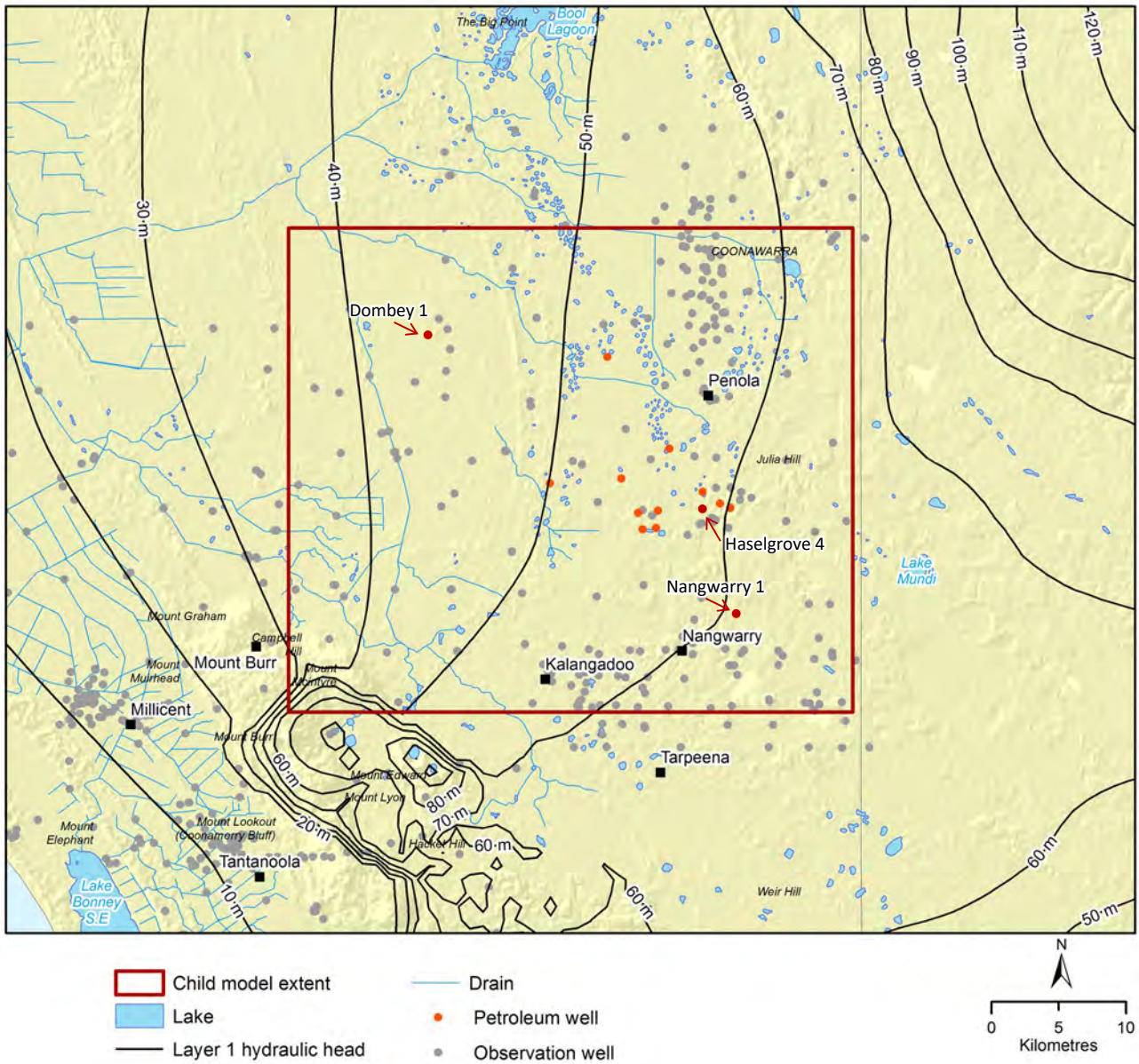


Figure 4 Heads in the Gambier Limestone aquifer (Layer 1) of the regional groundwater model (Wood and Pierce, 2015), showing the extent of the child model. New gas wells indicated in dark red.

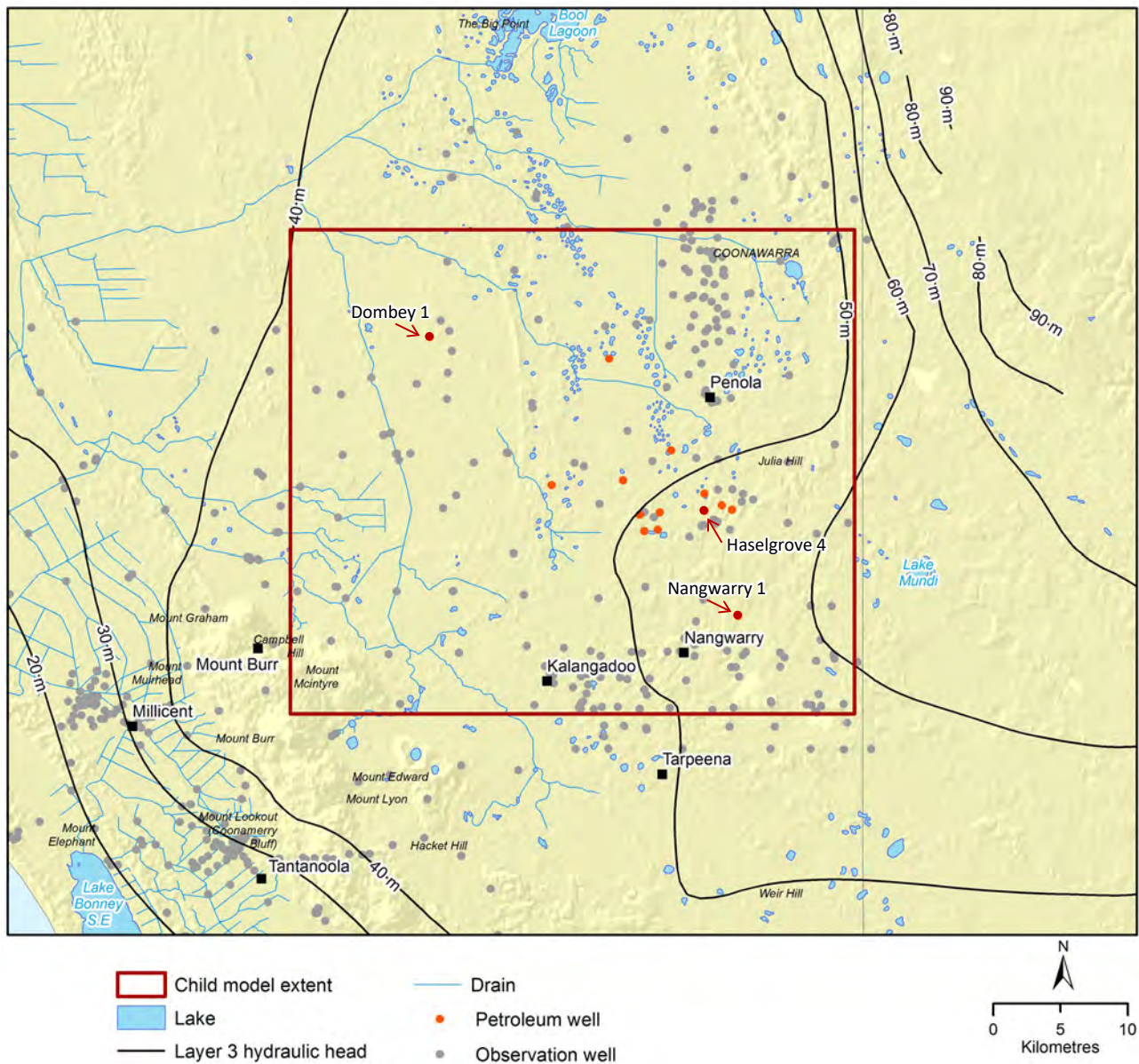


Figure 5 Heads in the Tertiary Confined aquifer (Layer 3) of the regional groundwater model (Wood and Pierce, 2015), showing the extent of the child model. New gas wells indicated in dark red.

Well extraction data was based on a subset of the input data for the Kingston version of the South East Regional Water Balance Model. The extraction rates were aggregated temporally to the six-monthly stress period of the child model; they were also aggregated spatially where more than one well was located within a cell. Water extraction was represented using the MODFLOW 2005 wells package.

Agricultural drains used to remove surface water and shallow groundwater were developed for the child model from a DEM based on LiDAR data flown for the region in 2011 (Wood and Way, 2011) (Figure 9). Information in the drain file of the SE Regional Groundwater Model was at a 1000 m resolution, which was too coarse for the child model. As there were inconsistencies of more than ten metres between the LIDAR drain data which provided the base elevation of the drain and the 9 second DEM that provided the land surface, the drain locations were derived from the LIDAR data, and the base elevation was defined to be one metre below the land surface. This relative drain depth was consistent with that of the LIDAR data.

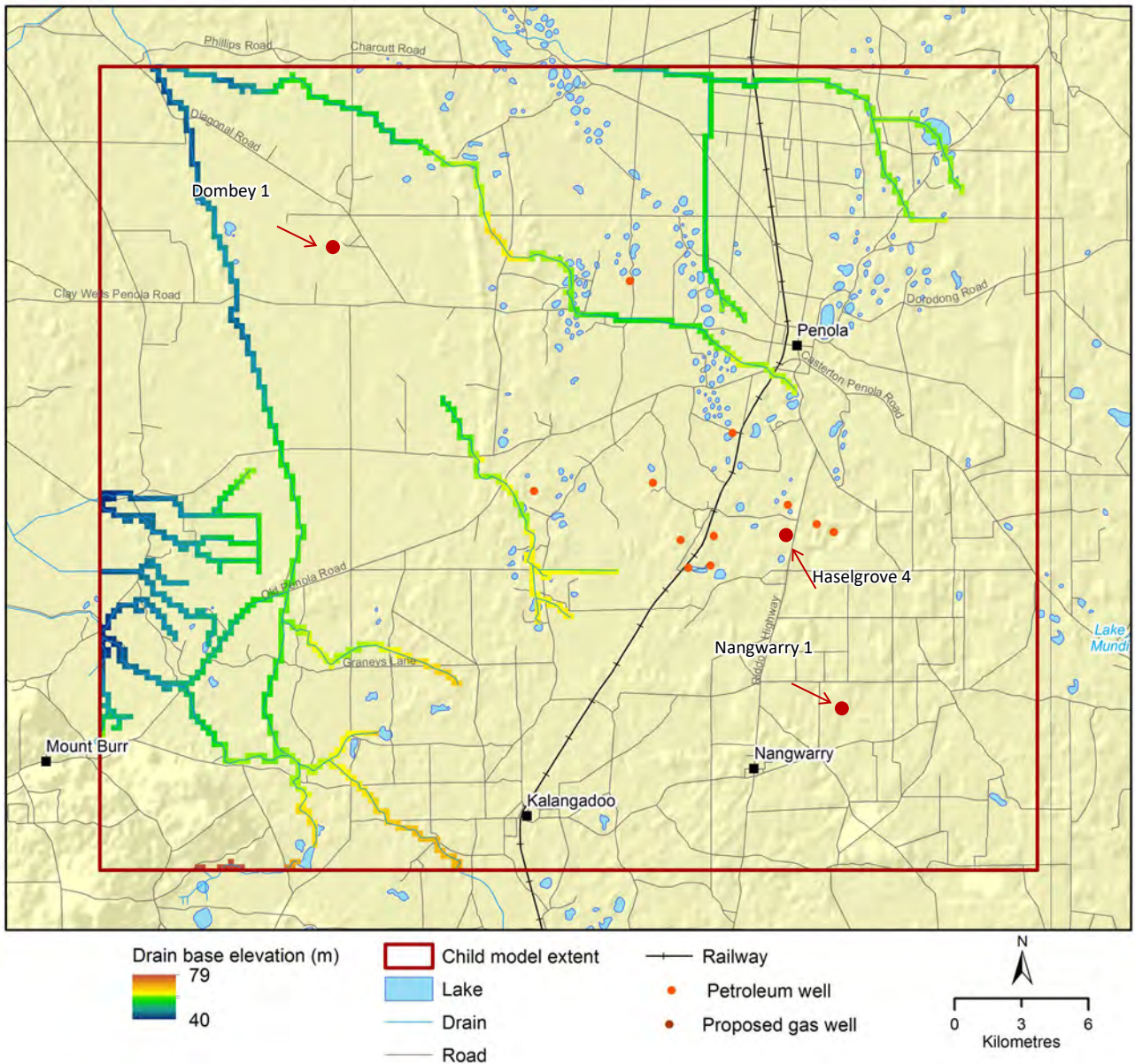


Figure 6 Drain base elevations used in Layer 1 of the child model.

Recharge was represented using the NetR package, previously developed for the South East region, with some modifications and aggregations of land use types (Doble, et al., 2015, Doble, et al., 2017). This is discussed further in following sections.

Initial heads were initially extracted from the Kingston version of the South East Regional Water Balance Model (Wood and Pierce, 2015). After model calibration, the initial heads were derived from a steady state model run, prior to the transient modelling.

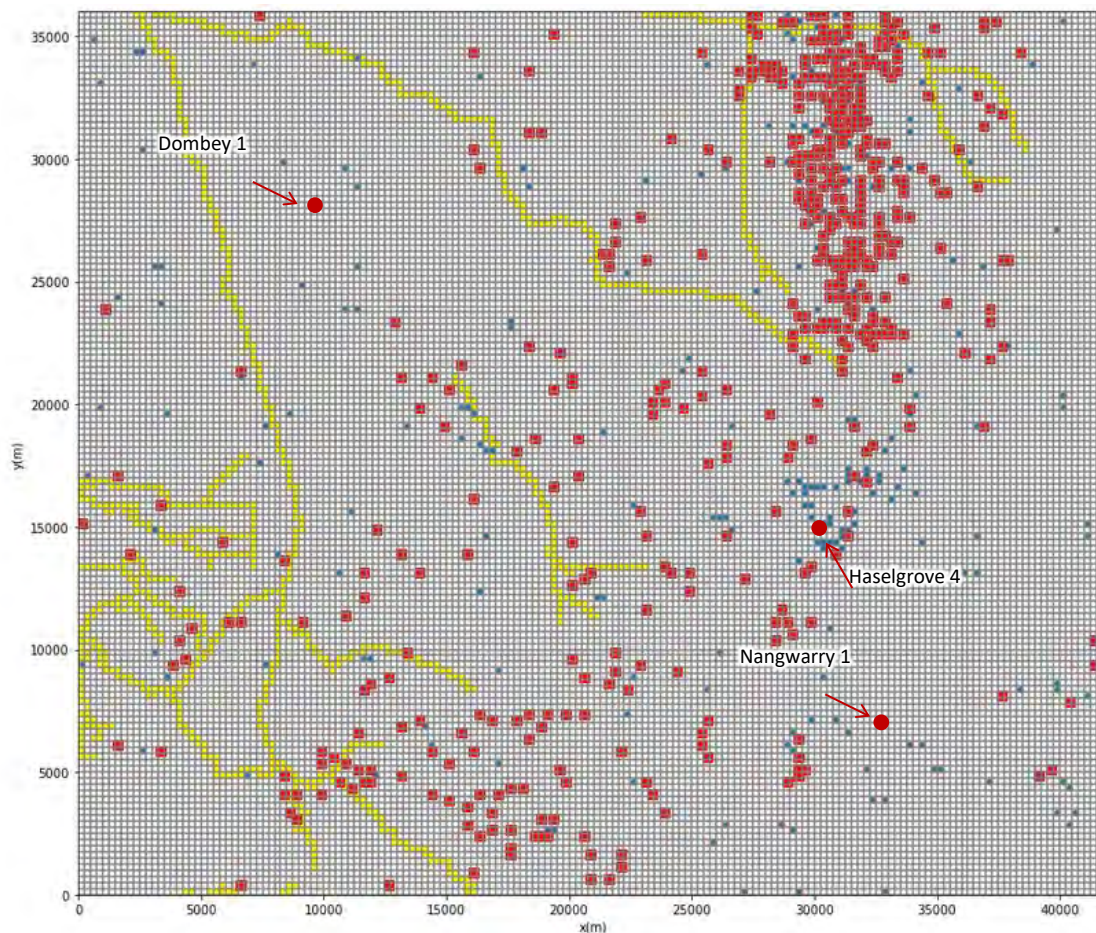


Figure 7 Groundwater model developed in FloPy showing drains (yellow), extraction wells (red), and observation wells (blue)

2.1.5 Net recharge inputs

The NetR package was originally developed by Doble et al. (2015 and 2017) to emulate the unsaturated zone processes of recharge and evapotranspiration in a simple lookup table format. The package develops relationships between net recharge (recharge minus evapotranspiration directly from groundwater) and depth to groundwater using the unsaturated zone model WAVES (Dawes, et al., 2004). The WAVES model uses inputs of climate, vegetation cover and soil type to develop the net recharge – depth to water table curves.

Climate

Climate data was obtained from the Bureau of Meteorology Penola and Mount Burr automated weather stations. Data for rainfall, minimum and maximum temperature, vapour pressure deficit and incoming solar radiation were used to populate the WAVES model climate input files (Dawes, et al., 2004). Model cells were allocated climate data based on their proximity to the weather station.

Average annual rainfall and PET for Penola was 645 mm and 1021 mm, respectively. Average annual rainfall and PET for Mt Burr was 781 mm and 965 mm, respectively. Monthly rainfall distributions are shown in Figure 8.

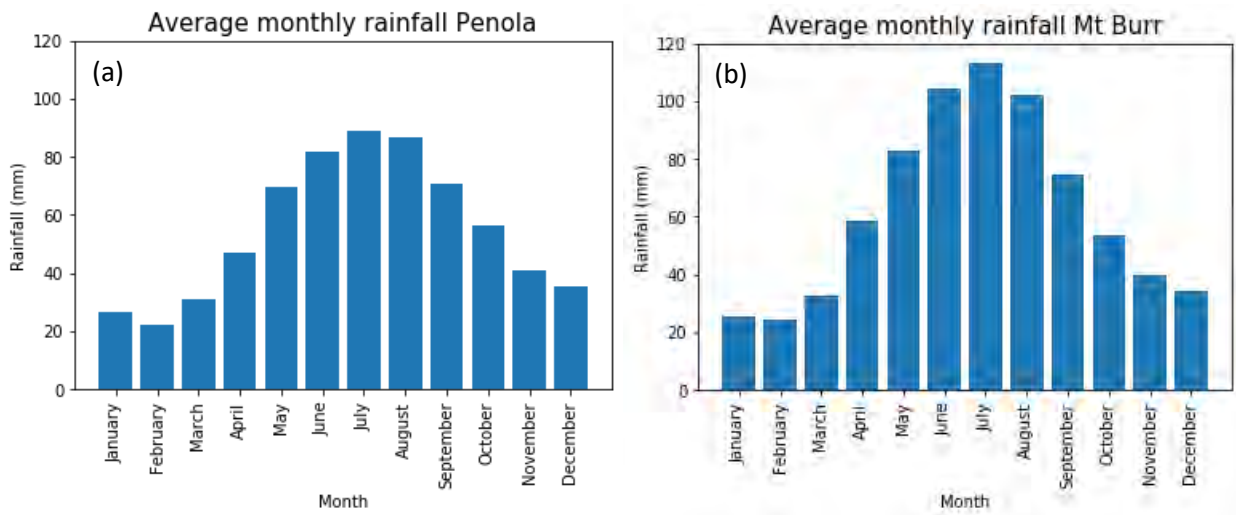


Figure 8 Average monthly rainfall for (a) Penola and (b) Mt Burr.

Land cover

The most likely five-year average land use information was obtained for the period 1987 to 2015 from the South Australian Land Cover Layers (Willoughby, et al., 2018). This data provided seventeen land cover types, which were aggregated into the seven most common land uses for the South East (Table 1). The most common land use type was dryland agriculture, which decreased by 20% over the modelling period. Both forestry (hardwood in particular) and irrigation land use areas increased, while native vegetation and ‘other’ land uses decreased (Table 2, Figure 11). Most likely land cover for 2010 to 2015 is shown in Figure 10.

Table 1 Aggregation of the seventeen South Australian Land Cover types into seven most common land cover types, and areas of cover based on 2010 – 2015 data.

South Australian Land Cover Layer type	Area (km2)	Area (%)	Aggregated GISERA SE land cover type	Area (km2)	Area (%)
Woody Native Vegetation	231.24	15.3%	Native vegetation		
Non-Woody Native Vegetation	2.22	0.1%	Native vegetation		
Saltmarsh Vegetation	0.01	0.0%	Native vegetation		
Wetland Vegetation	35.40	2.3%	Native vegetation		
Natural Low Cover	0.54	0.0%	Native vegetation		
Exotic Vegetation	8.63	0.6%	Native vegetation	278.03	18.4%
Dryland Agriculture	754.74	49.9%	Dryland Agriculture	754.74	49.9%
Irrigated Non-Woody	26.46	1.8%	Irrigated		
Orchards/ Vineyards	32.70	2.2%	Irrigated	59.16	3.9%
Plantation (Softwood)	220.26	14.6%	Plantation (Softwood)	220.26	14.6%
Plantation (Hardwood)	190.36	12.6%	Plantation (Hardwood)	190.36	12.6%
Urban Area	5.53	0.4%	Other		
Built-up Area	0.31	0.0%	Other		
Disturbed Ground / Outcrop	3.32	0.2%	Other	9.17	0.6%
Water Unspecified	0.02	0.0%	Water	0.02	0.0%

Table 2 Area of each of the land cover types within the child model region (km²). General trends show a decrease in dryland agriculture and native vegetation, and increases in forestry, particularly hardwood, and irrigated agriculture.

Land cover type	Area within child model extent (km2)					
	1987 - 1990	1990 - 1995	1995 - 2000	2000 - 2005	2005 - 2010	2010 - 2015
Dryland agriculture	926.09	955.98	939.81	808.92	793.72	755.22
Plantation (Softwood)	154.35	176.43	196.53	213.94	215.60	220.26
Plantation (Hardwood)	11.25	13.65	16.82	124.89	138.95	190.33
Water	0.07	0.01	0.02	0.02	0.02	0.02
Native vegetation	345.46	310.29	294.79	294.90	291.25	277.19
Other	51.97	25.39	18.67	11.76	9.72	9.85
Irrigated	22.82	30.24	45.36	57.57	62.74	59.13

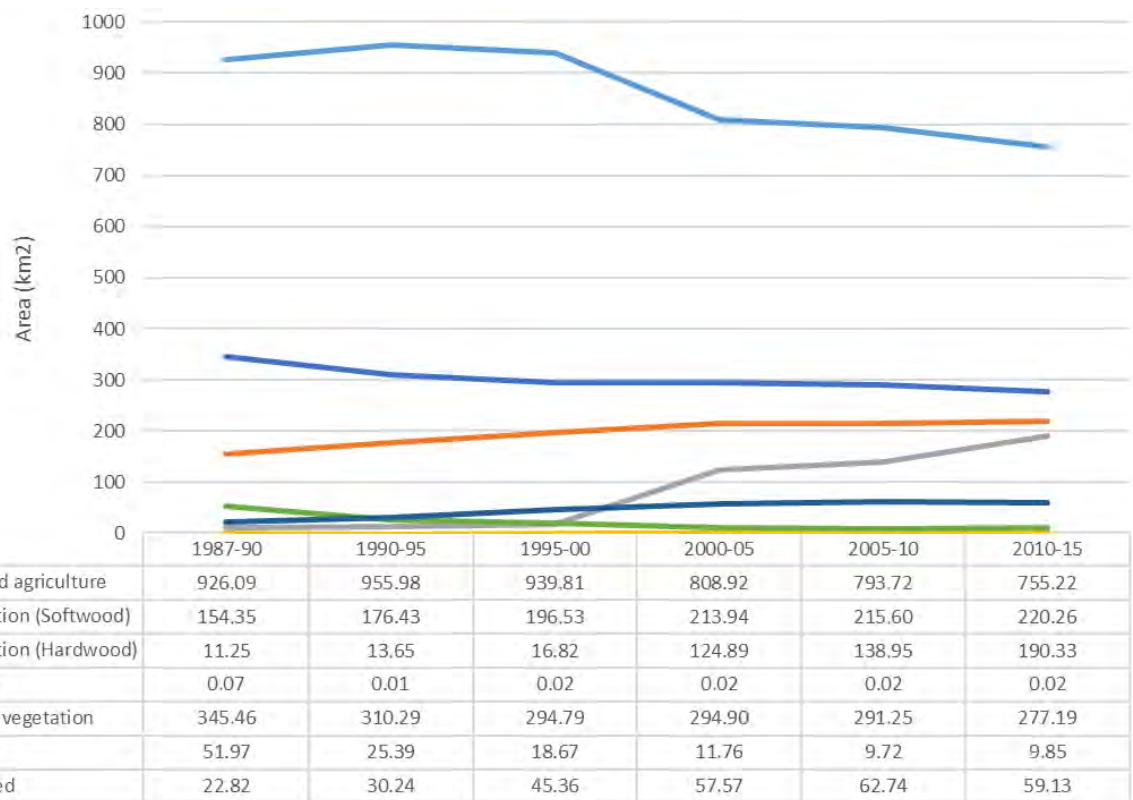


Figure 9 Changes in land cover from 1987 to 2015 for the child model extent.

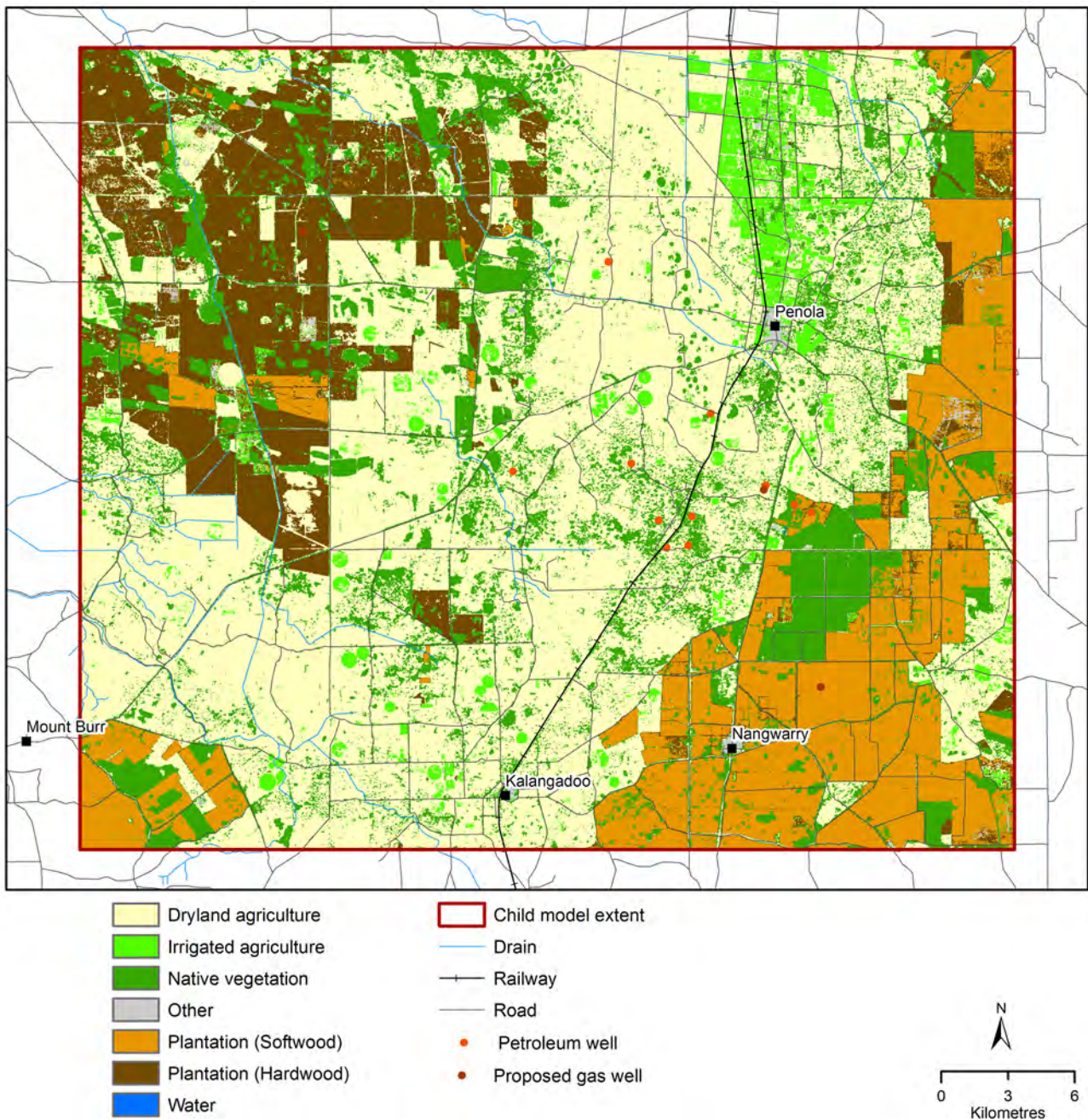


Figure 10 Most likely land cover for the child model from 2010 to 2015

Soils

The soil characteristics required to estimate net recharge were represented by the percentage of clay in the top two metres of the soil profile. Clay content was estimated from the ASRIS Atlas of Australian Soils (Johnston, et al., 2003), aggregated to the top two metres (Figure 11).

Clay content was aggregated into seven categories: 5 – 10%, 10 – 15%, 15 – 25%, 25 – 35%, 35 – 45% and >45%.

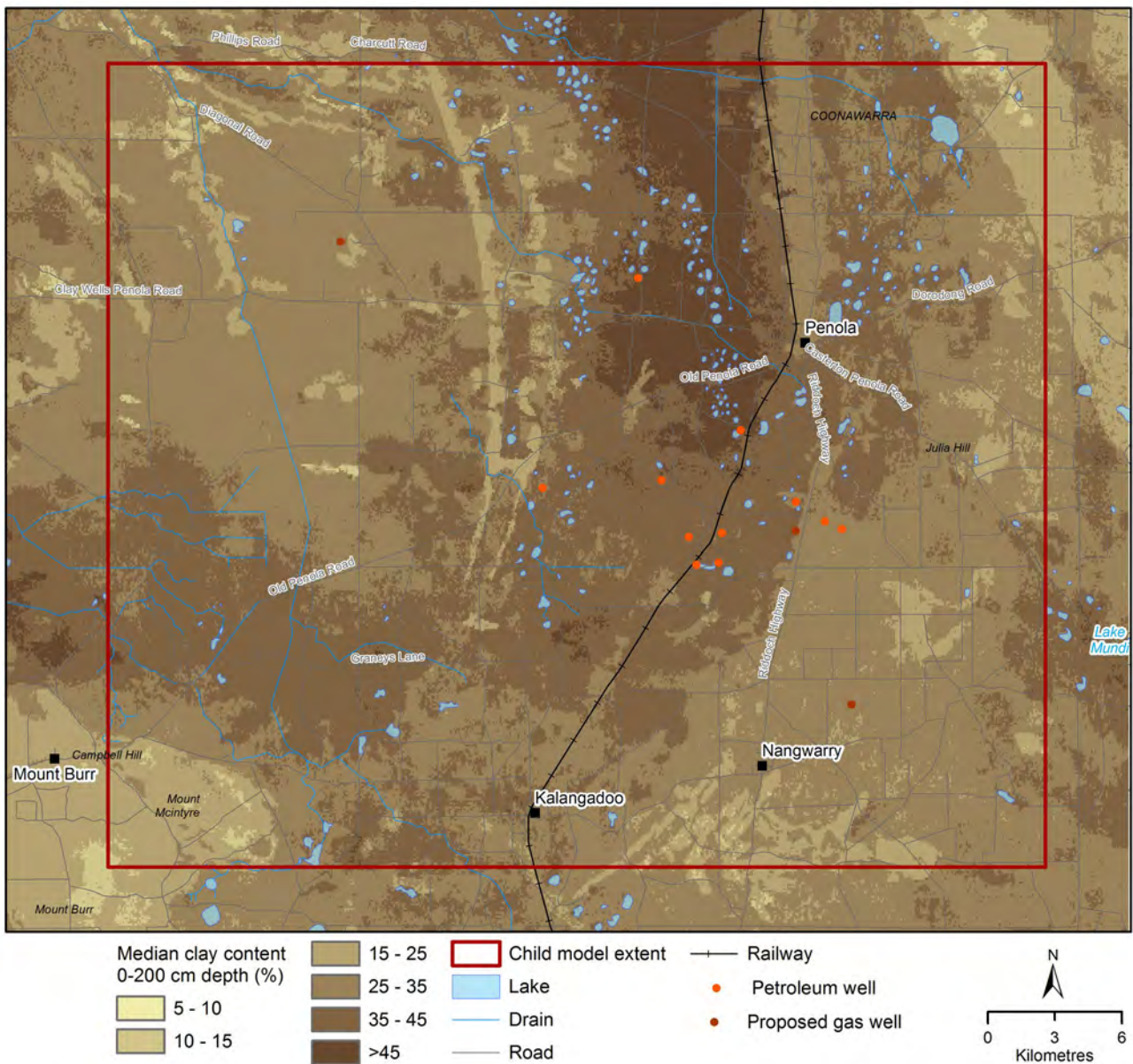


Figure 11 Clay content in the top two metres of soil, developed from the Australian Soil Resources Information System (ASRIS) Atlas of Australian Soils database (Johnston, et al., 2003).

NetR curves

Annual average net recharge curves for the Penola climate for the four land use types and seven soil types are shown in Figure 12. Curves were also produced for the long-term average summer dry season climate (November to April) and winter wet season climate (May to October), and a historical record of six-month periods from 1970 to 2019 (Figure 13). For this study, the six-monthly historical record curves were used. Figure 13 shows an example curve for summer (a) and winter (b) overlying the 49 years of historical summer and winter curves.

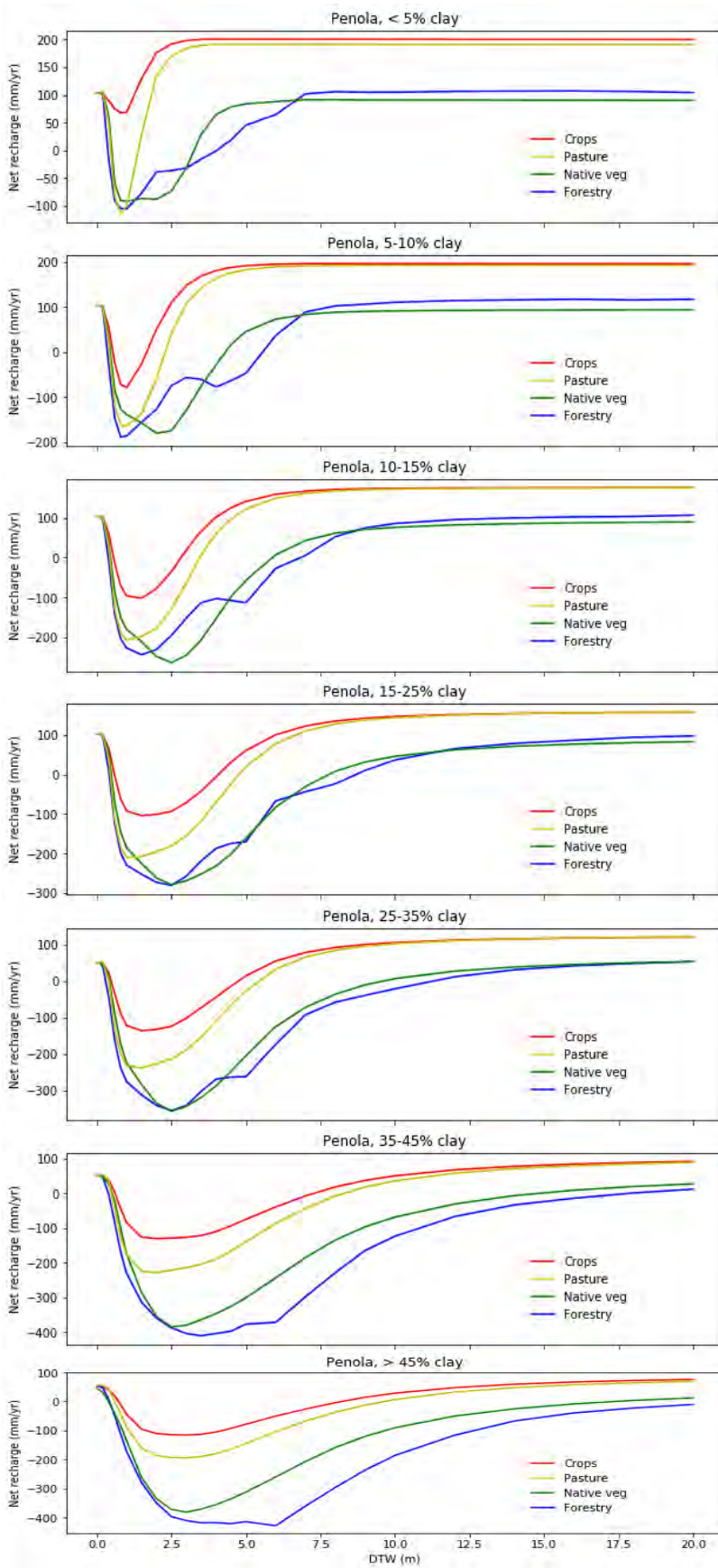


Figure 12 Annual average NetR curves for Penola, for each soil type, showing crops, pasture, native vegetation and forestry land uses.

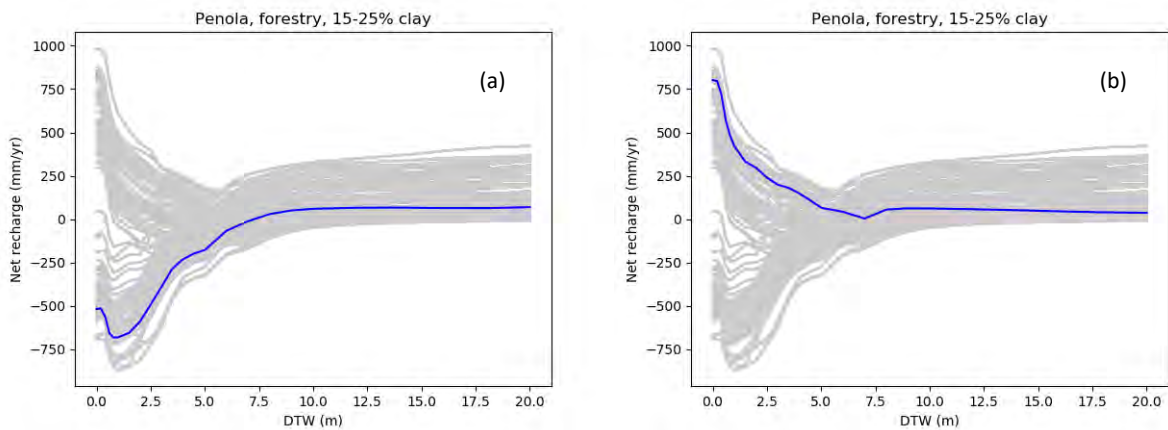


Figure 13 Six monthly historical NetR curves developed for forestry areas with soil type 3 (15 – 25% clay) using WAVES. Each grey line represents the NetR curve for one six-month stress period and the blue line is an indicative NetR curve representing summer (a) and winter (b) conditions. Summer net recharge curves are dominated by evapotranspiration, especially when groundwater is shallow, while the winter curves are dominated by recharge.

2.1.6 MODFLOW-NWT NetR package

The NetR package was developed to emulate recharge and evapotranspiration processes in shallow groundwater using a lookup table approach (Doble, et al., 2015, Doble, et al., 2017). NetR allows users to model recharge and evapotranspiration as one process, where both evapotranspiration and recharge can vary with depth to water table, and results can be compared with field measures of net recharge such as the chloride mass balance (CMB) approach. Previous application of the NetR method has used MODFLOW-2000, which has been superseded by more recent MODFLOW models (MODFLOW-2005, MODFLOW 6 and MODFLOW-USG). This project coded the NetR package into MODFLOW 2005 (Harbaugh, 2005) using the MODFLOW-NWT Newton solver which better manages non-linear drying and rewetting of unconfined aquifers (Niswonger, et al., 2011). MODFLOW-NWT was observed to produce more stable results for the modelling and while it took longer to run, it was able to skip over temporary non-convergence problems rather than stopping model runs completely. This gave a higher rate of successful models in the uncertainty analysis.

3 Uncertainty analysis

Model calibration and uncertainty analysis was undertaken using the Iterative Ensemble Smoother approach (White, 2018) using the PEST++ software suite. The software tool implements the ensemble-smoother form of The Gauss-Levenberg-Marquardt algorithm for the minimisation problem. The PEST-IES software utility enables the use of the PEST model interface utilities and has built-in parallel run manager and model run failure tolerance. This enables it to be a useful tool to undertake groundwater model calibration and uncertainty analysis. The Gauss-Levenberg-Marquardt algorithm used in calibration tools like PEST relies on the filling of the Jacobian Matrix that comprises the finite-difference approximation of the first derivative of model-generated observations with respect to the input model parameters. In this approach, the number of model runs undertaken for the inversion is directly proportional to the number of model parameters and poses a significant challenge when used in highly parameterised models like that used in this study.

In this study, we used pilot points to represent the spatial heterogeneity of hydraulic properties resulting in a total of 2694 model parameters. Each hydraulic characteristic – horizontal hydraulic conductivity, vertical hydraulic conductivity, specific yield and specific storage (K_h , K_v , S_y , S_s) for each model layer was represented by 224 pilot points. This implied that each iteration of the model calibration using the GLM algorithm will need the model to be run 2695 times to populate the Jacobian Matrix. Model failure during computation of Jacobian matrix can also create problems.

However, the PEST-IES offers an alternative approach for using the Jacobian matrix derived empirically from an ensemble of random parameter sets using the formulation proposed by Chen and Oliver (2012). Using this formulation, the model needs to be run only as many times as the size of the ensemble chosen thus eliminating the computational burden induced by the large number of parameters. This approach also enables the quantification of model parameter uncertainty. Since an ensemble of parameters are propagated through the algorithm until acceptable objective function values are attained, the calibration process ends up with an ensemble of model parameter sets that can all calibrate the model. This provides an estimate of the posterior parameter distribution constrained by the available observations (White, 2018).

3.1 History matching

History matching for the period 1970 to 2019 was completed using PEST-IES. It involved changing 2694 parameters based on 5761 observations of groundwater head. Initial values of the parameters were specified based on values obtained from the regional groundwater model (Wood, 2017). Calibration and uncertainty analysis were undertaken initially with a version of the model that used the Recharge Package rather than NetR. The parameters calibrated in this run comprised the hydraulic property pilot points corresponding to K_h , K_v , S_y and S_s also in addition to the hydraulic conductance of the drains. A subsequent round of uncertainty analysis was also undertaken with the version of the model using the NetR package to explore the uncertainty of the NetR parameters. In this uncertainty analysis run, we used the NetR package to represent the

net recharge. In this run the calibration parameters additionally included two parameters corresponding to the NetR package.

3.1.1 Parameters

Parameters included in the uncertainty analysis included the horizontal and vertical hydraulic conductivities (K_h and K_v), specific storage (SS) and specific yield (S_y) for each layer. These hydraulic properties were considered as heterogeneous spatial fields. The spatial fields were generated by interpolating from pilot points at 224 model cells. The interpolation was undertaken for each model layer with values at pilot points using ordinary Kriging with a spherical variogram. The spherical variogram used a nugget value of 0.327 and sill value of 0.764 with a log transformation of the hydraulic properties and the value of range used was 5000 m. Given that the available estimates of hydraulic properties from previous models were homogeneous or zone-wise heterogeneous, the above parameters were used primarily to model the effect of spatial heterogeneity. Alternative models could be developed, and parameters values could be further explored when spatial estimates of hydraulic property values are available from pump tests, other field measurements, or modelled estimates.

The parameters included in model calibration also included the hydraulic conductance of the drain network. Four separate drain conductance parameters were considered corresponding to four different reaches of the drain (Figure 17). In the second run of the model calibration, the net recharge package was parameterised using two additional parameters.

Spatially varying parameters included well fluxes in Layers 1 and 3, drain conductance and base elevation, general head boundary heads and conductance. Temporally varying parameters consisted of well fluxes and general head boundary conditions.

The NetR parameters were varied as a single bulk parameter across the catchment but could be varied in zones or with pilot points.

3.1.2 Observations

Field observations used in the model uncertainty analysis and calibration consisted of 318 observation wells (Figure 7) with a total of 5761 observations. Discharge in the drains at three gauging stations were also available. The three drain flux locations (Figure 14) consisted of 112 six-monthly observations (Figure 15, Figure 16 and Figure 17). The modelled groundwater flux to the drain cells in the three gauged drains were summed and compared with the gauged flux.

Note that the modelled flux did not account for any channel losses or evaporation from the drains. Furthermore, not all of the minor drains captured in the drain networks were modelled. For this reason, and due to discontinuous and the limited nature of the data set and coarse temporal resolution of the model stress periods, the gauged drain fluxes were not used as calibration targets but used in a post-calibration comparison of modelled to observed fluxes at the drain gauges.

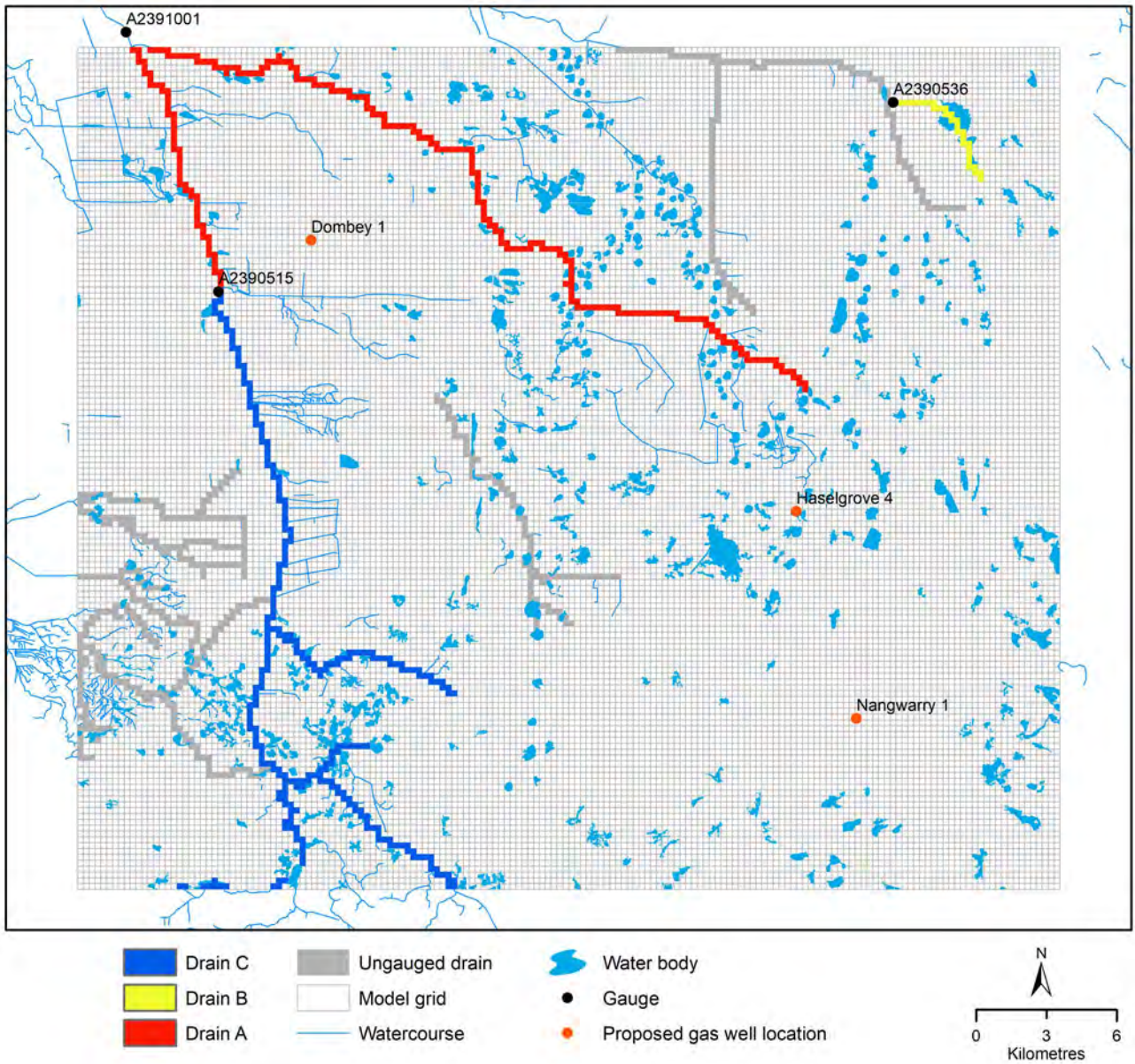


Figure 14 Drain gauges that were used for the calibration of the child model, showing the contributing drains. Drain gauge numbers are the Water Connect identifiers.

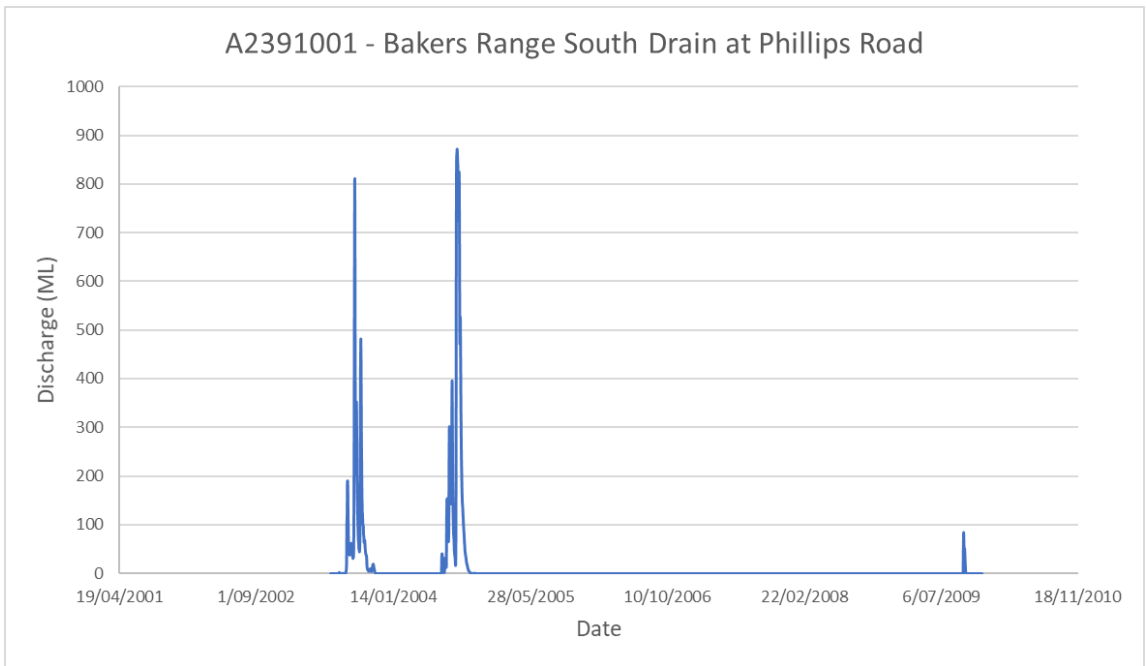


Figure 15 Drain discharge data from A2391001 Bakers Range South Drain at Phillips Road

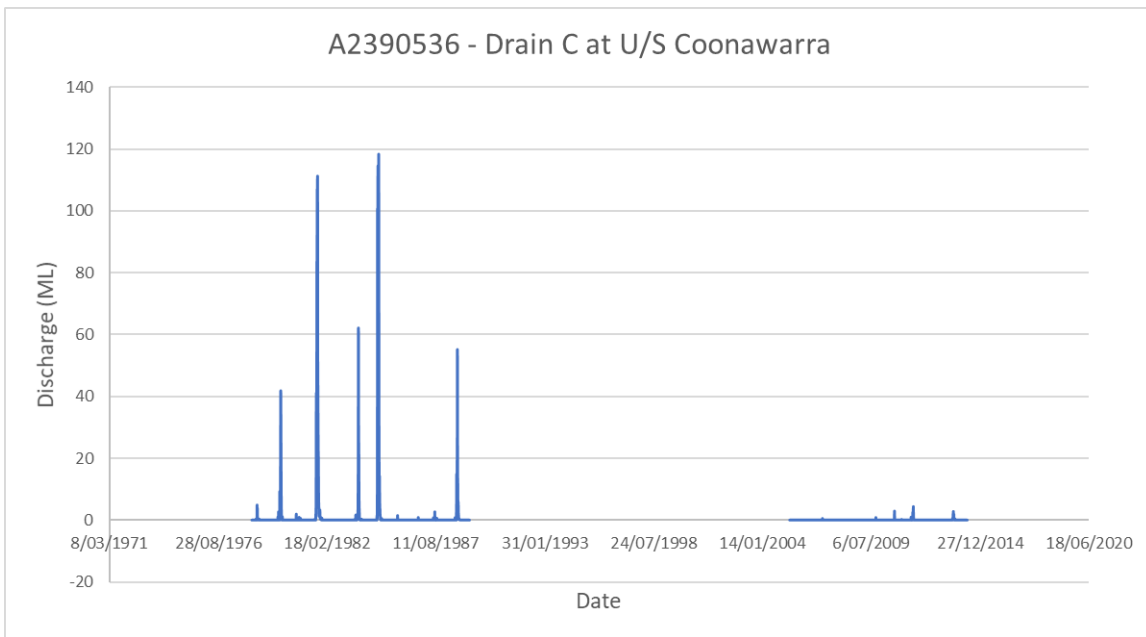


Figure 16 Drain discharge data from A2390536 Drain C at upstream of Coonawarra

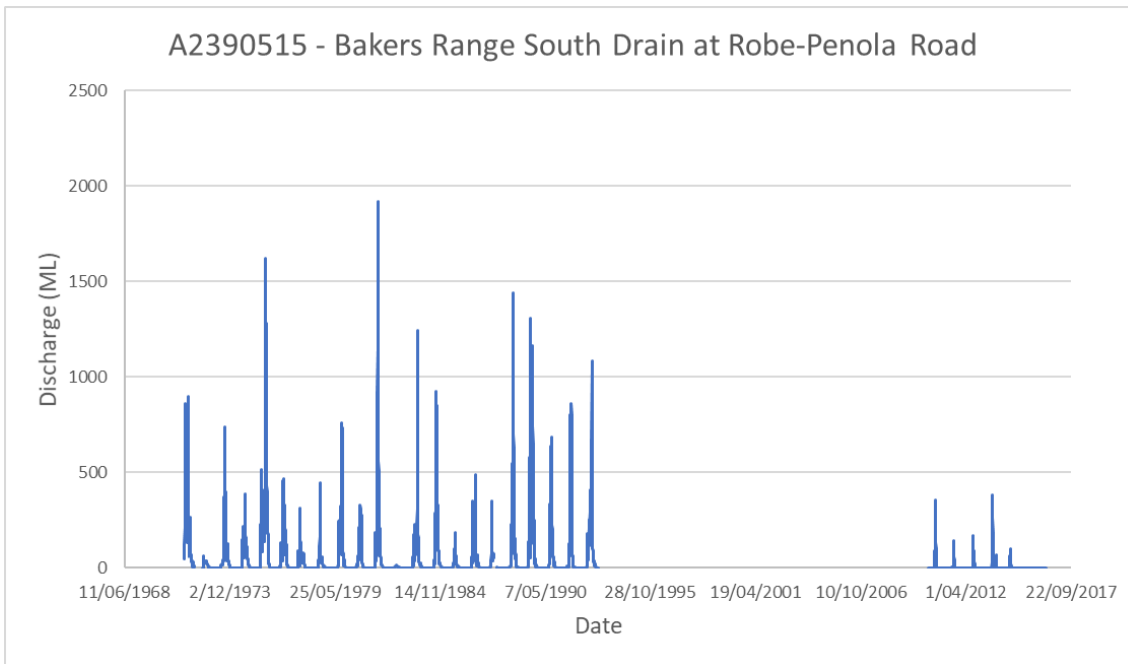
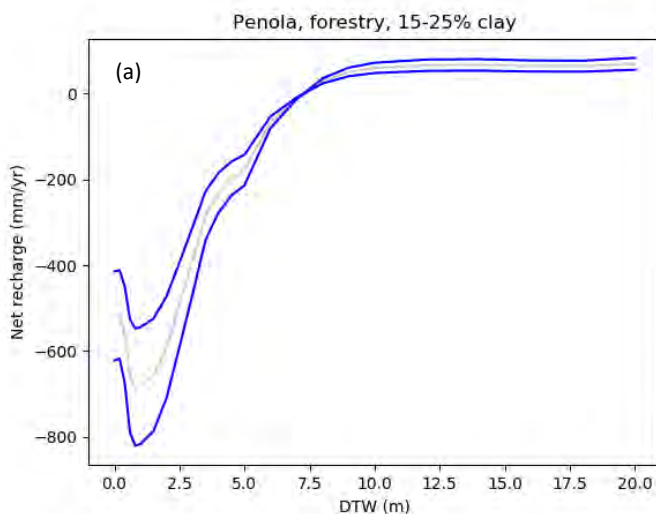


Figure 17 Drain discharge data from A2390515 Bakers Range South Drain at Robe-Penola Road

3.1.3 NetR curves

To calibrate and vary the NetR curves, two parameters were used to stretch and shift the curves relative to the original. These two parameters were introduced as a parsimonious solution for the calibration of the hundred plus parameters that are used in the WAVES modelling. The H-stretch increased or decreased the maximum recharge or ET near the soil surface (Figure 21a), whereas the V-stretch stretched or contracted the curve in the direction of groundwater depth, altering the conceptual rooting depth (Figure 21b). These two parameters were included in the probabilistic water balance and scenario analysis section (Section 5).



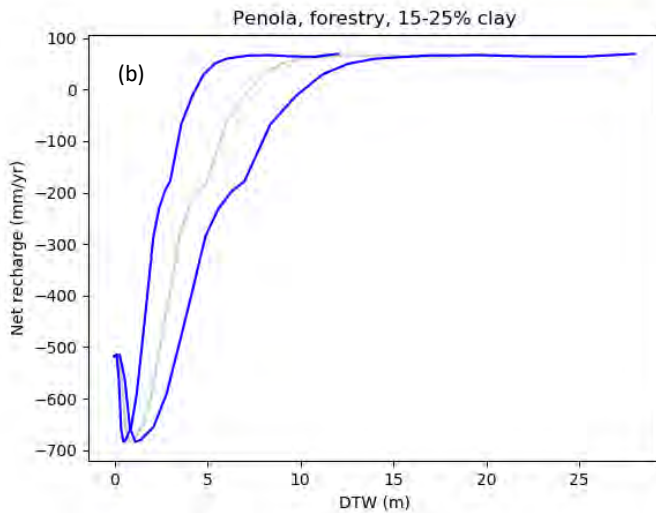


Figure 18 Two parameters used to vary the NetR curves (a) H-stretch (+/- 20%) and (b) V-stretch (+/- 40%).

3.2 PEST-IES set-up

An initial ensemble size of 500 was selected for initiating the calibration and uncertainty analysis model runs using PEST-IES. This meant that 500 sets of model parameters were generated during each iteration of the calibration run with the Jacobian matrix populated by these 500 models runs using the empirical approach. Initial bounds of the model parameters were specified in the PEST file based on values and ranges obtained from previous studies and the literature. As the calibration procedure progressed, some of the parameters that were informed by the available observations became progressively constrained yielding the posterior distribution for these parameters. Other parameters that were not informed by the observations retained the prior distribution in the final ensemble of parameters.

3.3 Results of calibration and uncertainty analysis

The prior and posterior distribution of hydraulic properties at the pilot points for the Tertiary Limestone Aquifer (Layer 1) and the Tertiary Confined Sands Aquifer (Layer 3) obtained from the initial calibration run with the recharge package are shown in Figure 19.

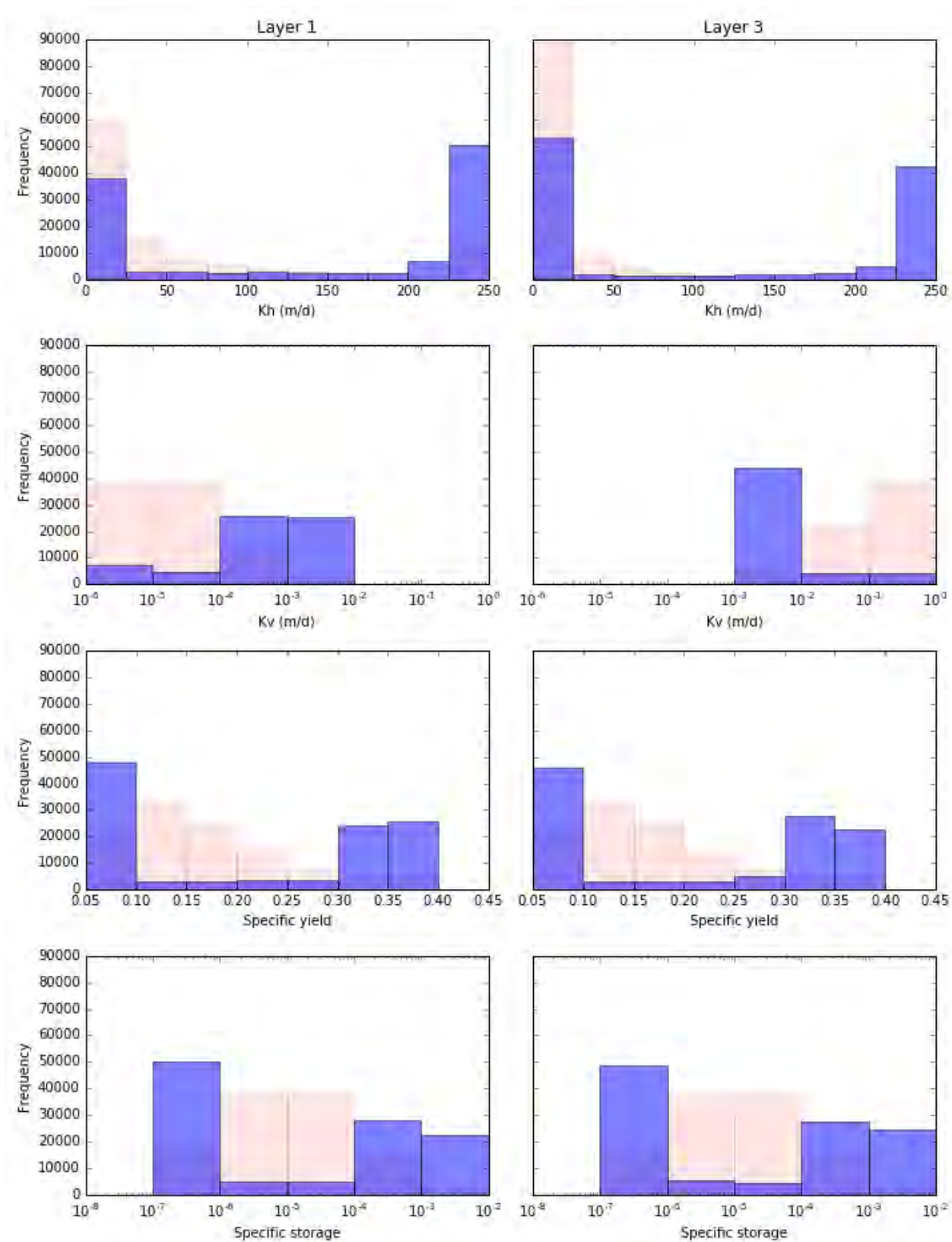


Figure 19: Prior and posterior distribution of hydraulic properties at the pilot points in the aquifer layers

It should be noted that the pilot points of hydraulic conductivity for both aquifers assume values from the extreme ends of the range (Figure 19). This does not imply that the distribution of that hydraulic property is bimodal. Instead, it just means that some of the pilot points assumed high

values in many realisations. This indicates the possibility that properties may have a wider range than what was assumed in the calibration runs. The distribution of Kh in Layer 1 and Layer 3 obtained from one realization interpolated from the pilot points is shown in Figure 21. This shows that the median value of Kh for layer 1 is about 21 m/d and that for layer 3 is 4.4 m/d. Similarly, the distribution of horizontal and vertical hydraulic conductivity realisations for the aquitard layer is shown in Figure 22. Single realisations of Ss and Sy are shown in Figure 23 and Figure 24, respectively.

There is higher variability of hydraulic conductivity in the calibrated field for Layer 1 compared to Layer 3. While Figure 19 shows that both prior and posterior distributions span the entire range of the parameter values, distributions at many pilot points were constrained by the available observations, especially in Layer 1 given considerable number of groundwater head observations. For example, prior and posterior distributions of Sy at 9 different pilot points is shown in Figure 25. The prior and posterior distribution of drain conductance multiplier values is shown in Figure 26.

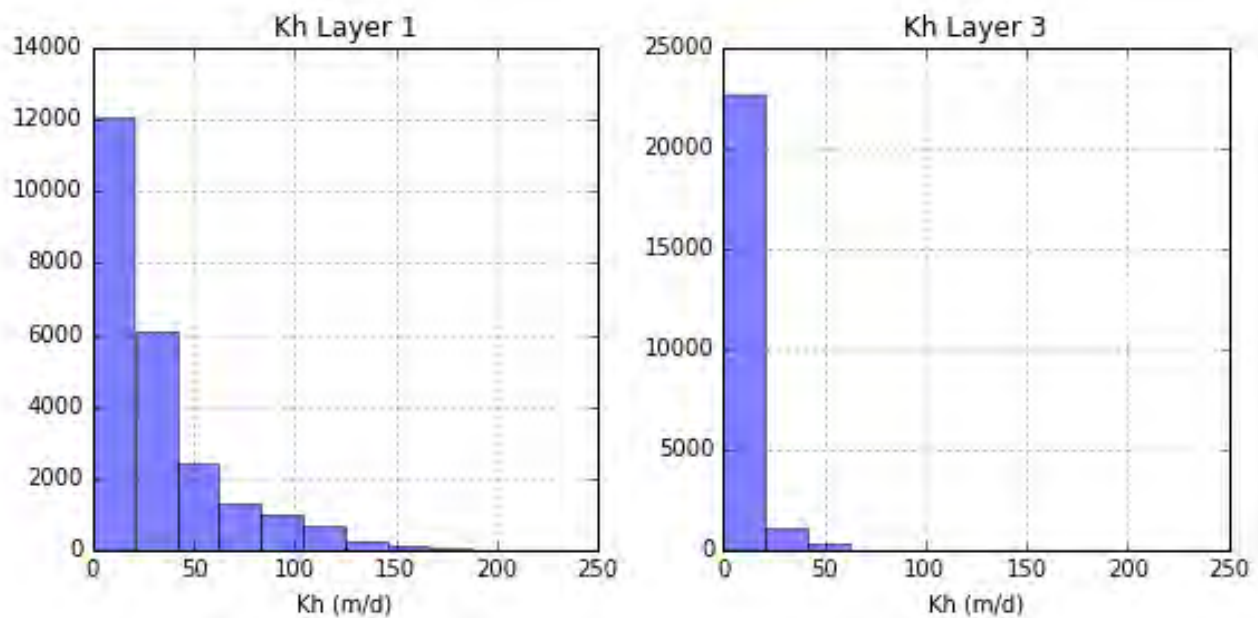


Figure 20 One realization of Kh values for layer 1 and 3 interpolated from the pilot points.

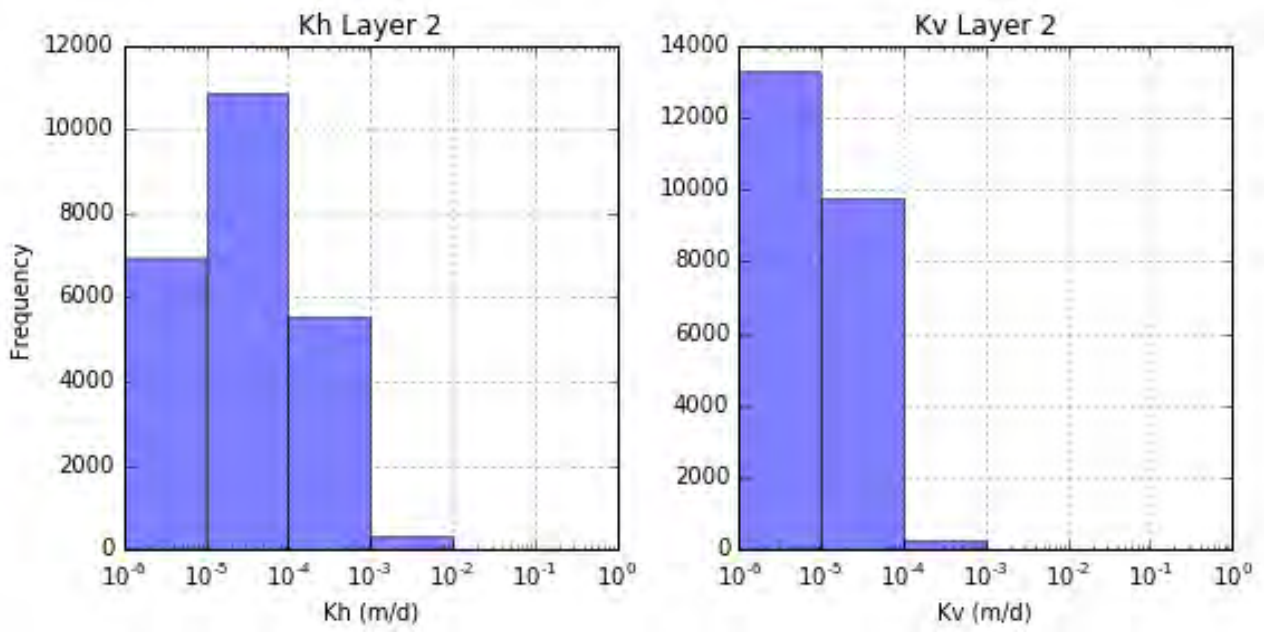


Figure 21: Distribution of horizontal and vertical conductivity realization for the aquitard layer (Layer 2)

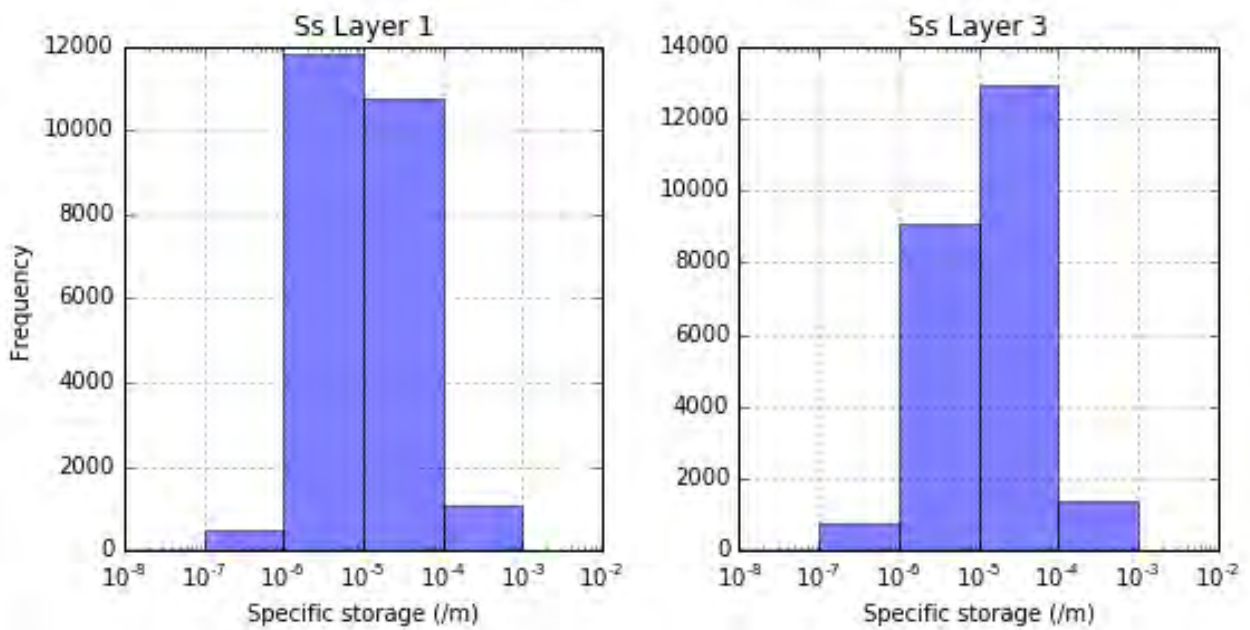


Figure 22 One realization of Ss values for layer 1 and 3 interpolated from the pilot points.

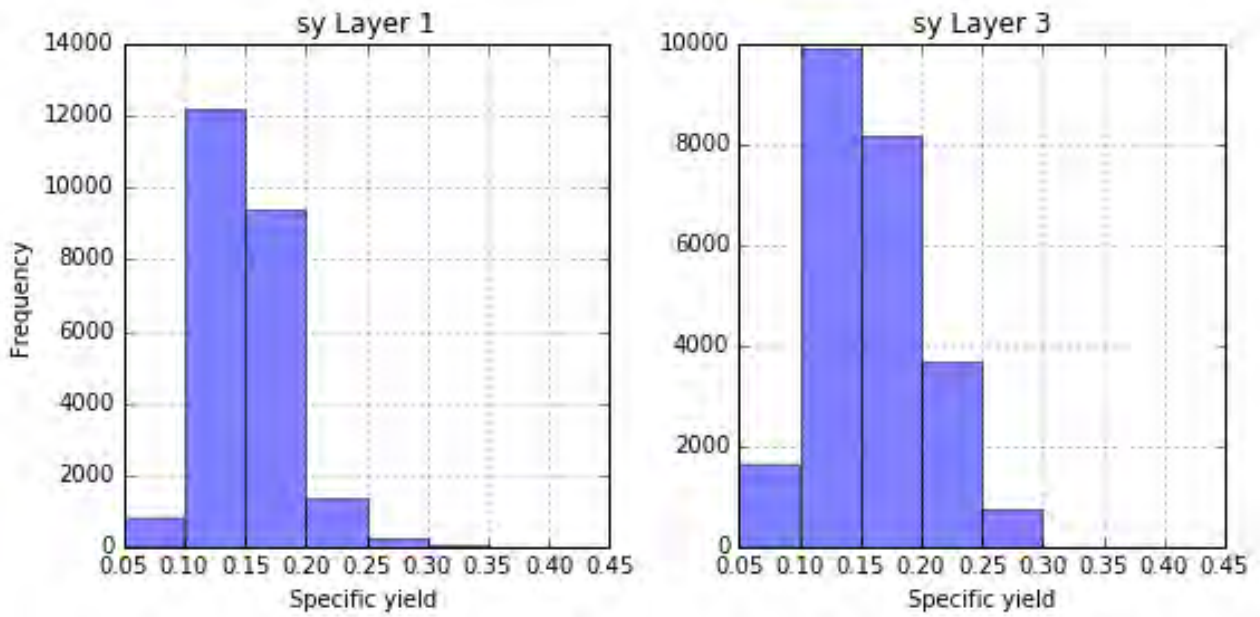


Figure 23 One realization of Sy values for layer 1 and 3 interpolated from the pilot points.

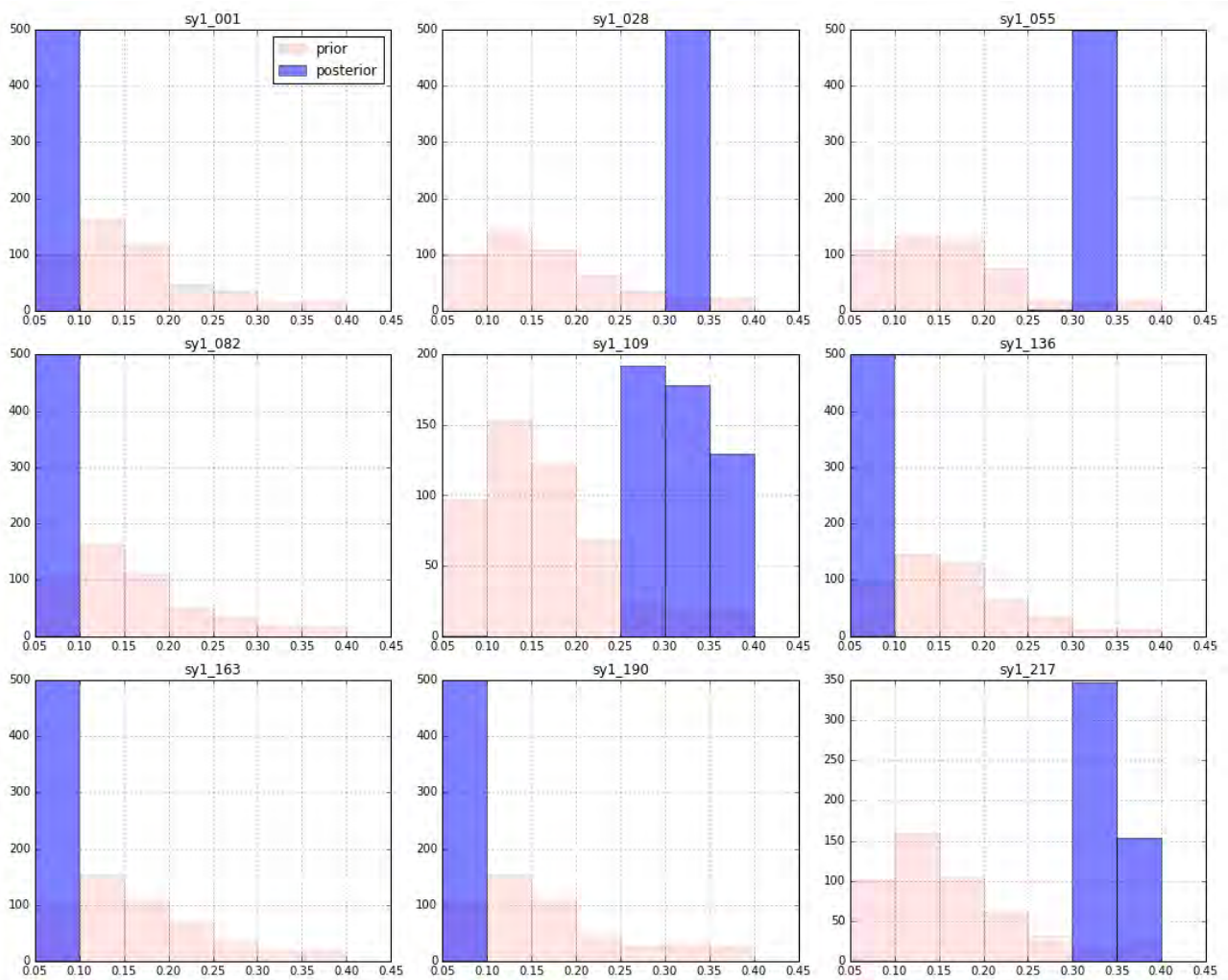


Figure 24: Distribution of specific yield parameter at 9 pilot points in model layer 1

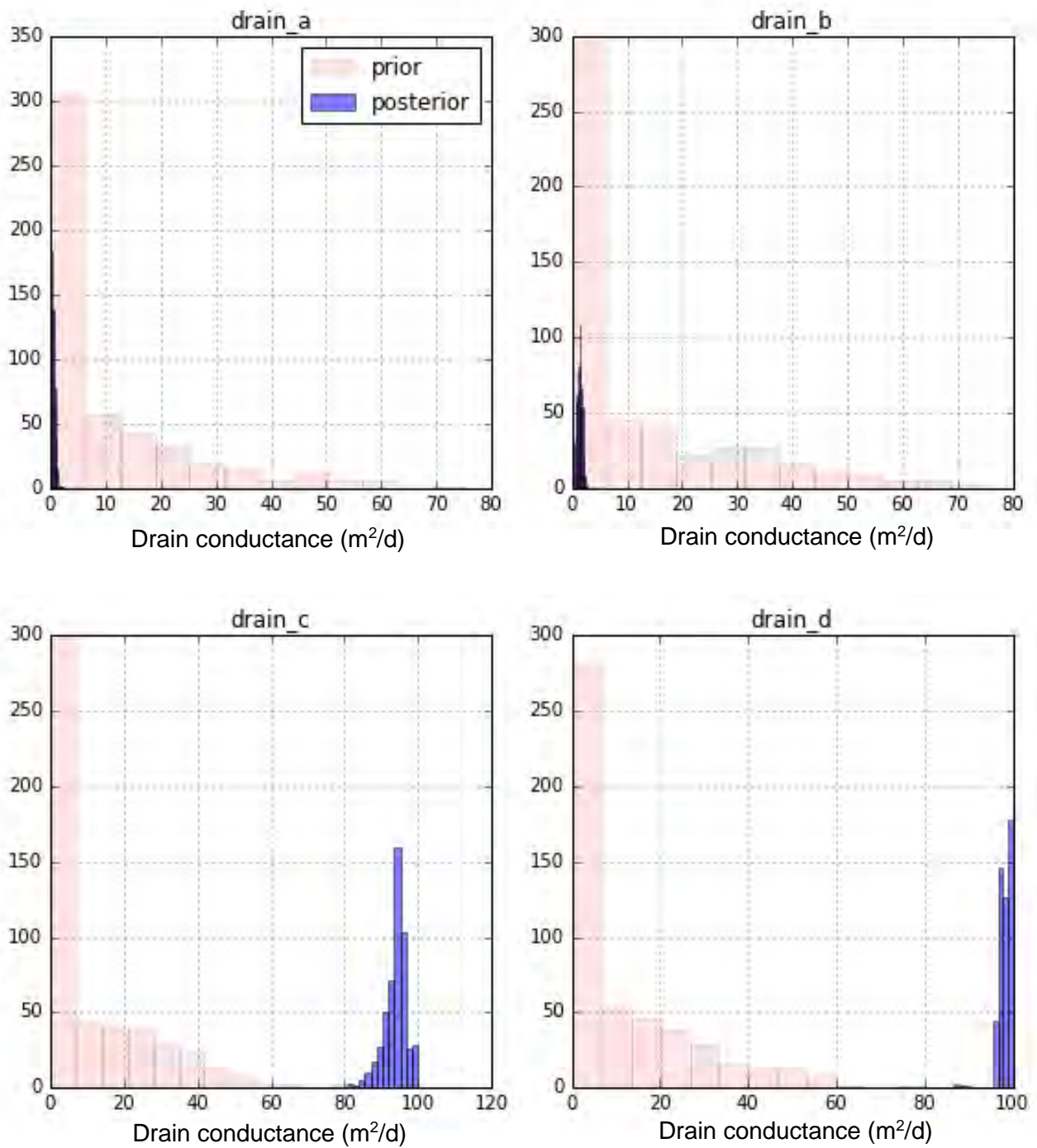


Figure 25: Prior and posterior distributions of drain conductance parameter.

The time series of observed and simulated groundwater heads at 6 observations locations is shown in Figure 27.

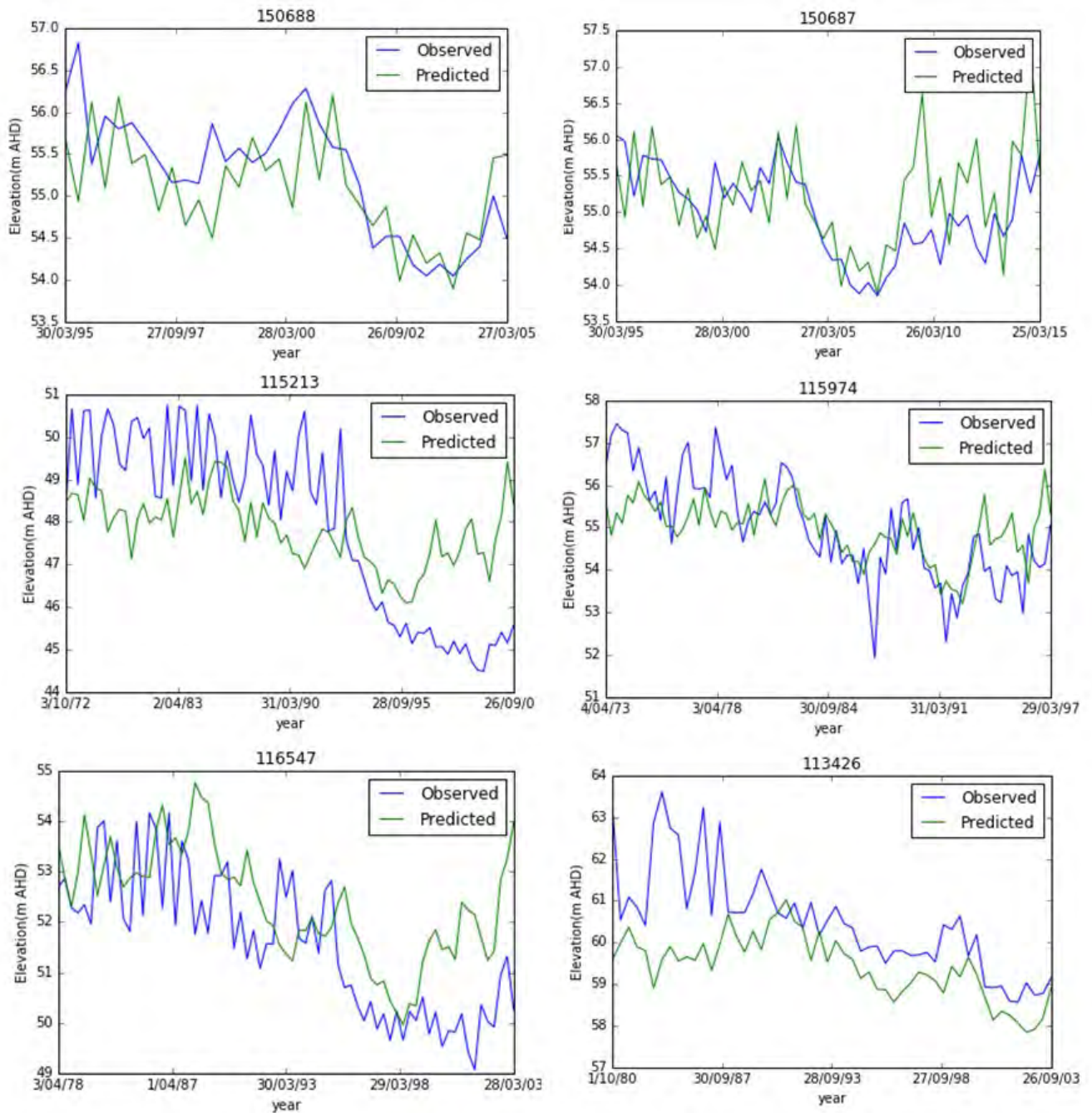


Figure 26: Time series of observed and modelled groundwater levels in selected bores where observations span across different lengths of periods

An additional Monte Carlo simulation of the model was undertaken using the NetR package to evaluate the effects of NetR parameters. The model set-up remained similar to the initial calibration run except that the recharge package was replaced by the NetR package with the inclusion of two parameters to govern the effect of net recharge on the overall water balance. It was found that the available groundwater head observations were useful in constraining these two parameters. The prior and posterior distribution of the `str_d` and `str_f` parameters are shown in Figure 28 and Figure 29 respectively. A full round of calibration and uncertainty analysis was not undertaken using this set up of the model. Instead, rejection sampling was undertaken to identify the 100 best parameters sets that resulted in the least values of the objective function. The prior

and posterior distributions of the objective function resulting from this analysis is shown in Figure 30.

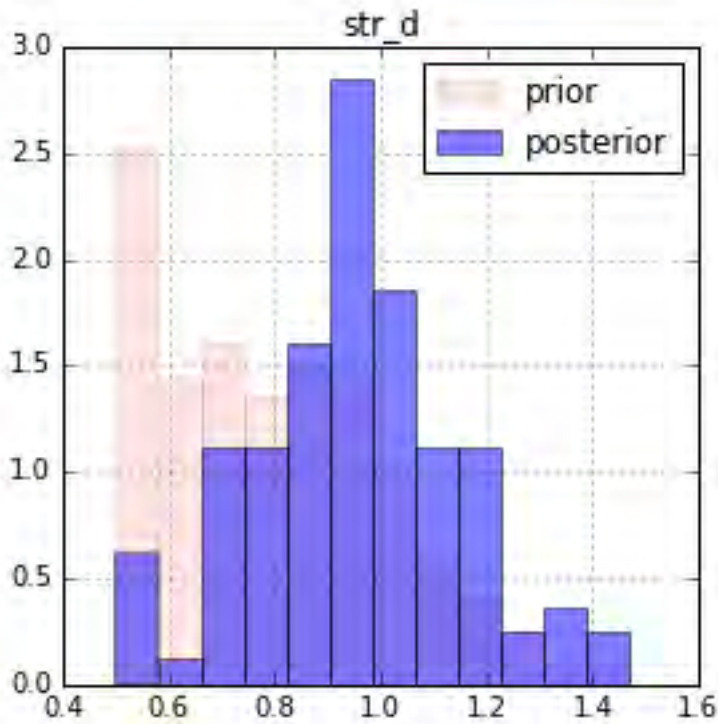


Figure 27: Prior and posterior distribution of str_d parameter for the NetR package. The str_d is a unitless multiplier for the depth component of the NetR function.

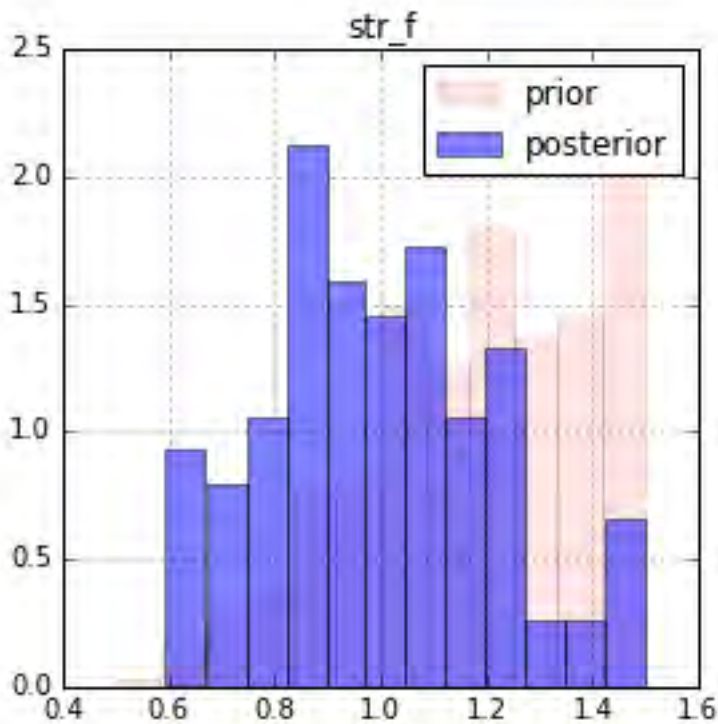


Figure 28: Prior and posterior distribution of the str_f parameter for the NetR package. The str_f is a unitless multiplier for the flux component of the NetR function.

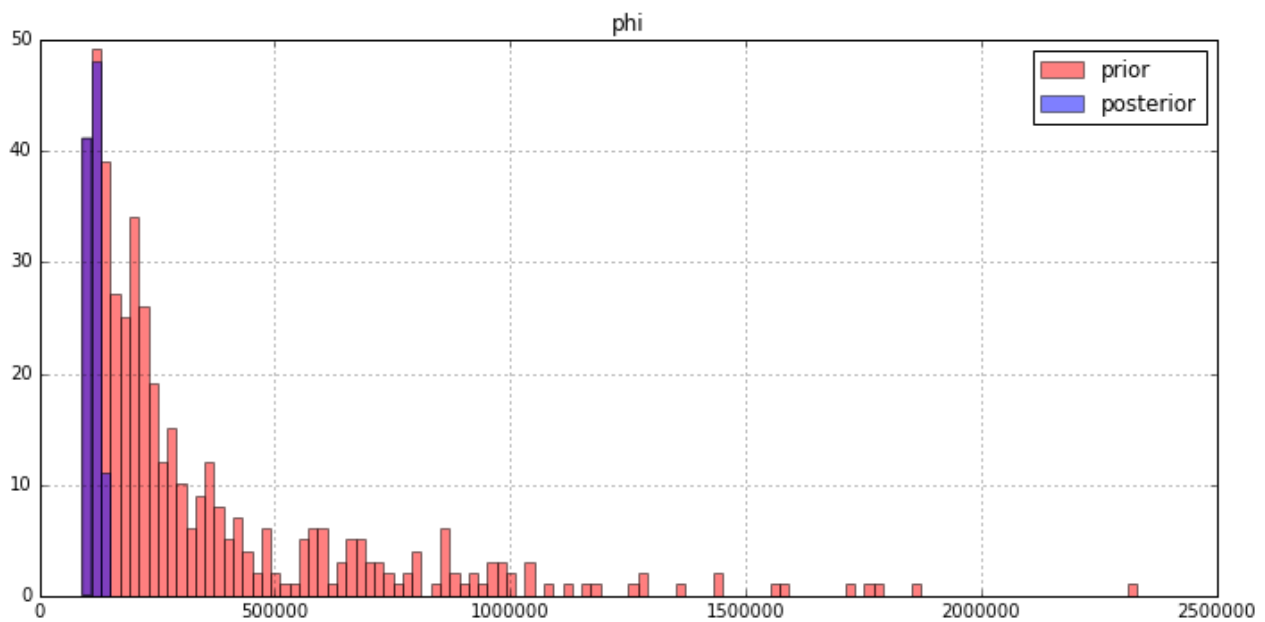


Figure 29: Prior and posterior distribution of objective function obtained from the Monte Carlo simulation using the NetR package

The posterior parameter sets that resulted from the calibration and uncertainty analysis were used in the scenario analysis to simulate the groundwater head and flux changes resulting from groundwater extraction for the gas development. The results from this scenario analysis are discussed in Section 4 of this report. These parameter sets were also used in the GISERA companion project on contamination risk assessment for particle tracking analysis to investigate travel times and distances.

The post-calibration comparison of modelled and observed drain fluxes showed that the model produced drain fluxes at a similar rate as those observed, with a general trend of overestimation (Figure 31). Very little data was available for Drain A (A2391001 Bakers Range South Drain at Phillips Road) in the northwest of the child model extent. Although the 2003 and 2004 drain fluxes matched well, observations showed little to no drain fluxes from then until 2009 (Figure 31a). It is unclear whether this is due to a lack of gauge data or model overestimation. In the north east of the child model extent Drain B (A2390536 Drain C at upstream of Coonawarra) the model predicted higher drainage rates than suggested from gauged observations (Figure 31b). This suggests that the piezometric surface may have been overestimated in this region. For Drain C (A2390515 Bakers Range South Drain at Robe-Penola Road), the modelled drain flow was generally higher than the observed flux with some years matching well, particularly around the late 1980s to the early 1990s (stress periods 38 to 42) (Figure 31c).

The post-calibration comparison of drain fluxes increases confidence that the model outputs and parameterisation are reasonable. The general trend of overestimation may indicate that the depth to groundwater in the model is somewhat shallow. The modelled flux did not account for any channel losses or evaporation from the drains, however, not all of the minor drains were captured in the drain network that was modelled. Therefore, this comparison should be taken as a guide for the order of magnitude of the drain fluxes, rather than expecting that they match perfectly.

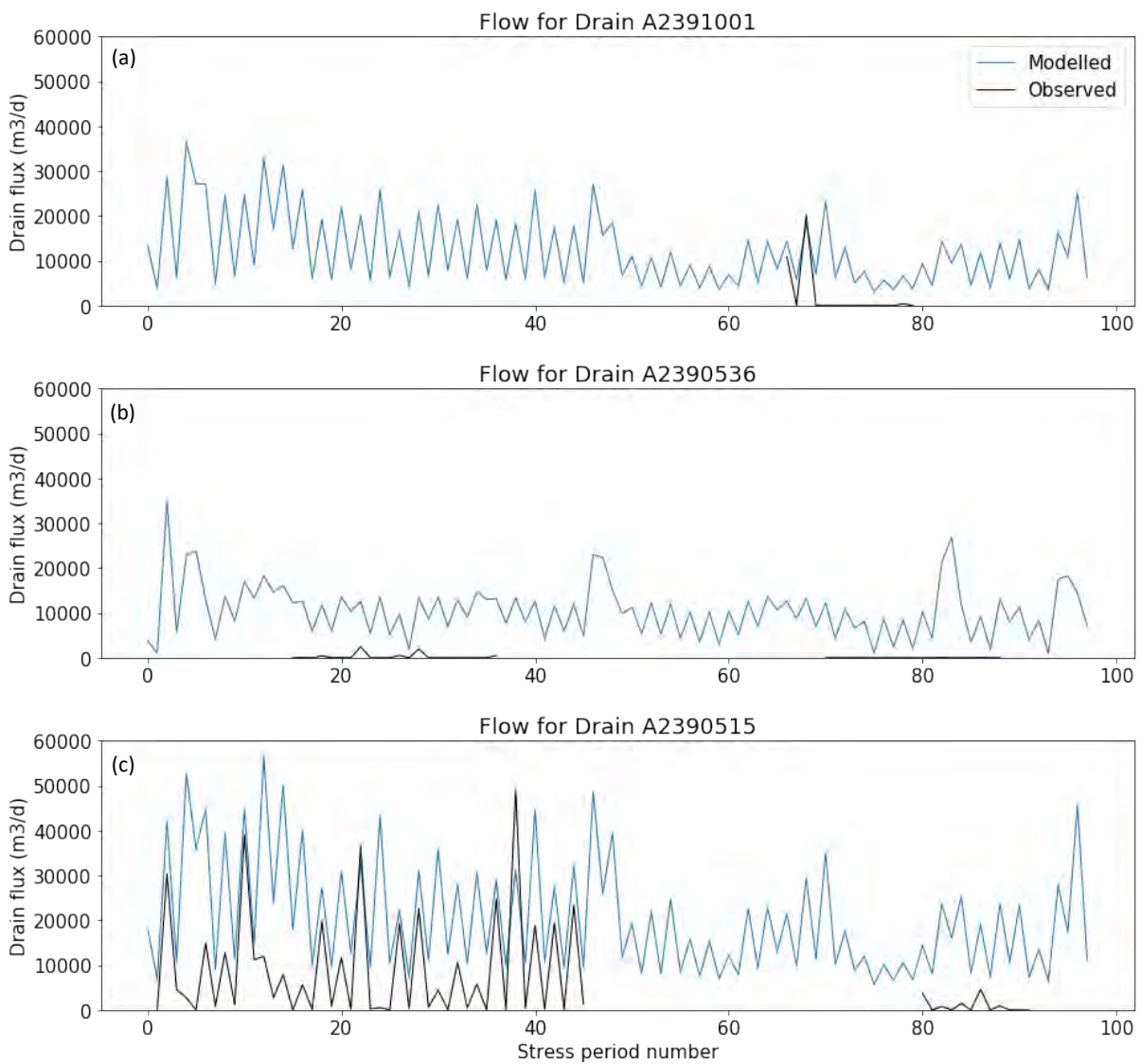


Figure 30 Modelled and observed drain fluxes for drain gauges (a) A2391001 Bakers Range South Drain at Phillips Road (b) A2390536 Drain C at upstream of Coonawarra and (c) A2390515 Bakers Range South Drain at Robe-Penola Road.

4 Probabilistic water balance and scenario analysis

The calibrated model was used to estimate the drawdown and water balance impacts of conventional gas well development at Dombey 1, Haselgrove 4 and Nangwarry 1.

4.1 Scenarios

The model was run for 100 years after the initial 49 years of history matching. The assumptions in the modelling were that:

1. Current land use would remain constant (2019 levels, represented by the 2010 – 2015 SA Landcover data).
2. Groundwater extraction from existing wells would remain constant at the 2019 levels for the next 100 years.
3. General head boundary conditions would remain constant at the 2019 values.
4. Net recharge would cycle through the first 49 years to the end of the modelling period. This was considered as an acceptable assumption as the effects of a changing climate would be cancelled out in the drawdown calculation; this allowed the impacts to be assessed for both drier and wetter periods.
5. Drain locations, depths and conductance remain constant for the 100-year future modelling period.

Both the water budget for the year where groundwater was extracted for the construction of three gas wells, and drawdown due to this extraction were assessed in this report. Drawdown was chosen as it is independent of future land use and climatic changes, assuming it is not significantly altered by land clearing for well pads. The water balance and drawdown impacts of the water supply for the three gas wells: Dombey 1, Haselgrove 4 and Nangwarry 1 (Table 3) were assessed for extraction rates of 2 ML for the first year to represent water requirements for drilling and construction. The following 99 years have no extraction from the water supply wells (Figure 27).

Table 3 Gas well locations, and locations of potentially greatest drawdown.

Well Name	easting	northing	row	col	lay
Dombey	464297	5867752	40	33	1
Haselgrove 4	485046	5856154	123	79	1
Nangwarry	487614	5847302	133	115	3

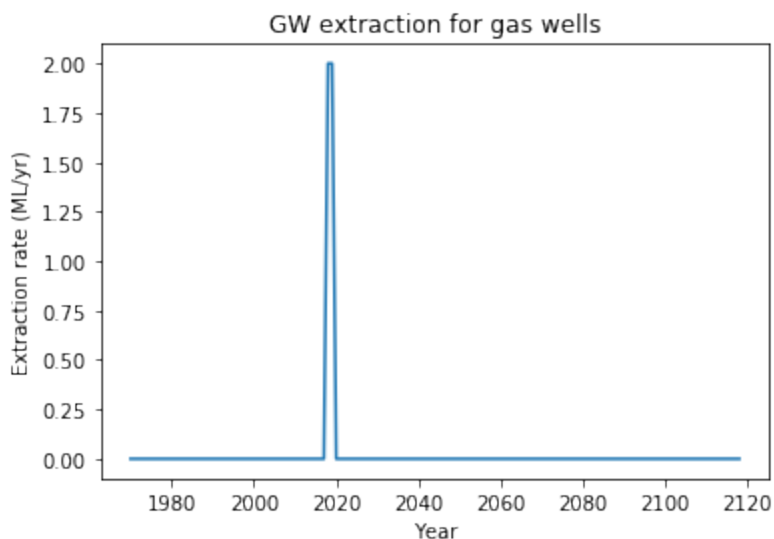


Figure 31 Groundwater extraction scenario for the three gas wells.

4.2 Groundwater heads

Piezometric surface outputs from the model show that groundwater heads are highest on the eastern side of the model, declining west towards the coast (Figure 30).

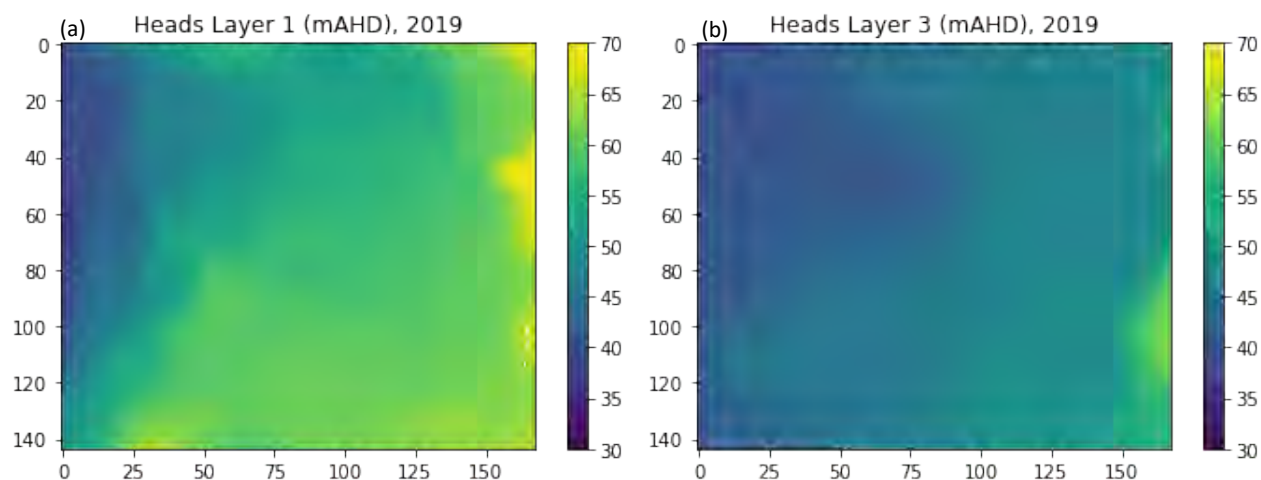
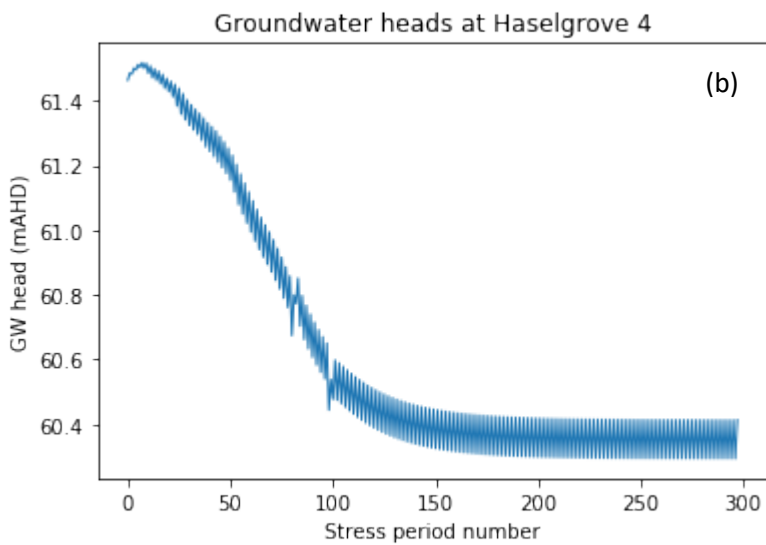
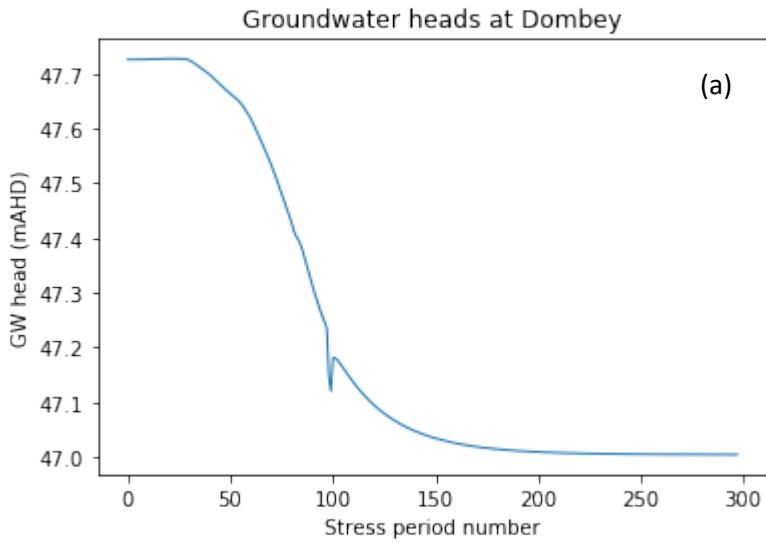


Figure 32 Groundwater heads for one realisation of the South East child model, unconfined aquifer, (a) Layer 1 and (b) Layer 3.

Groundwater heads at the Dombey well decreased over the 149-year modelling period by around 0.7 m (Figure 32a). This is likely to be due to increased groundwater pumping and changes in land use in the initial 49-year history matching period. The drawdown of around 0.1 m from the scenario of groundwater extraction for gas well development is evident but small.

Groundwater heads at the Haselgrove 4 well site also decreased by around 1.0 m over the 149-year modelling period (Figure 32b). Seasonal oscillation in head is also apparent due to the seasonal groundwater pumping of nearby extraction bores. The drawdown is also apparent at Haselgrove 4, but it is of the same order of magnitude as the seasonal changes due to pumping in surrounding wells.

Groundwater heads in the confined aquifer at the Nangwarry well site also decreased, but only by around 5 mm over the 149-year modelling period (Figure 33c). There are also slight changes in head over time due to the seasonal effects of nearby pumping. Drawdown due to gas well development was around 0.3 m.



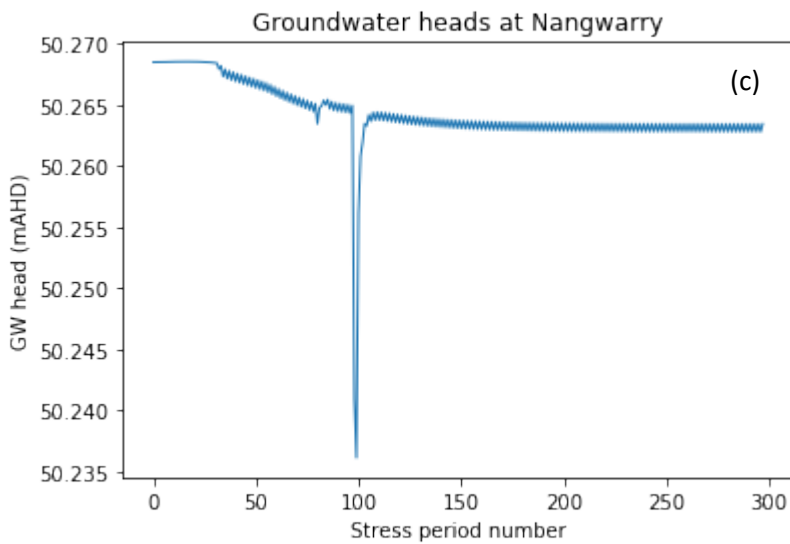
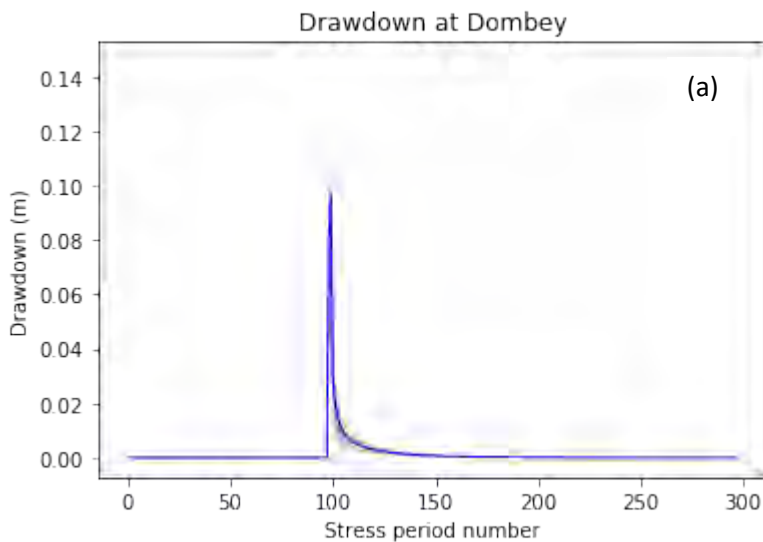


Figure 33 One realisation of the groundwater heads at the location of the gas wells, Dombey (a), Haselgrove 4 (b) and Nangwarry (c)

4.3 Drawdown

Maximum drawdown will occur at the location of the groundwater extraction. Drawdown from the pumping scenarios, including the uncertainty bounds (in grey) is shown in Figure 34. Median drawdown at the Dombey 1 and Haselgrove 4 wells was 0.095 m with uncertainty bounds of 0.05 m to 0.142 m (Figure 34 a and b). Median drawdown at Nangwarry 1 was 0.03 m (Figure 34 c) with uncertainty bounds of 0.018 m to 0.042 m. There is a 95% chance that the maximum drawdown will be less than 0.14 m at Dombey 1 and Haselgrove 4, and less than 0.04 m at Nangwarry 1.



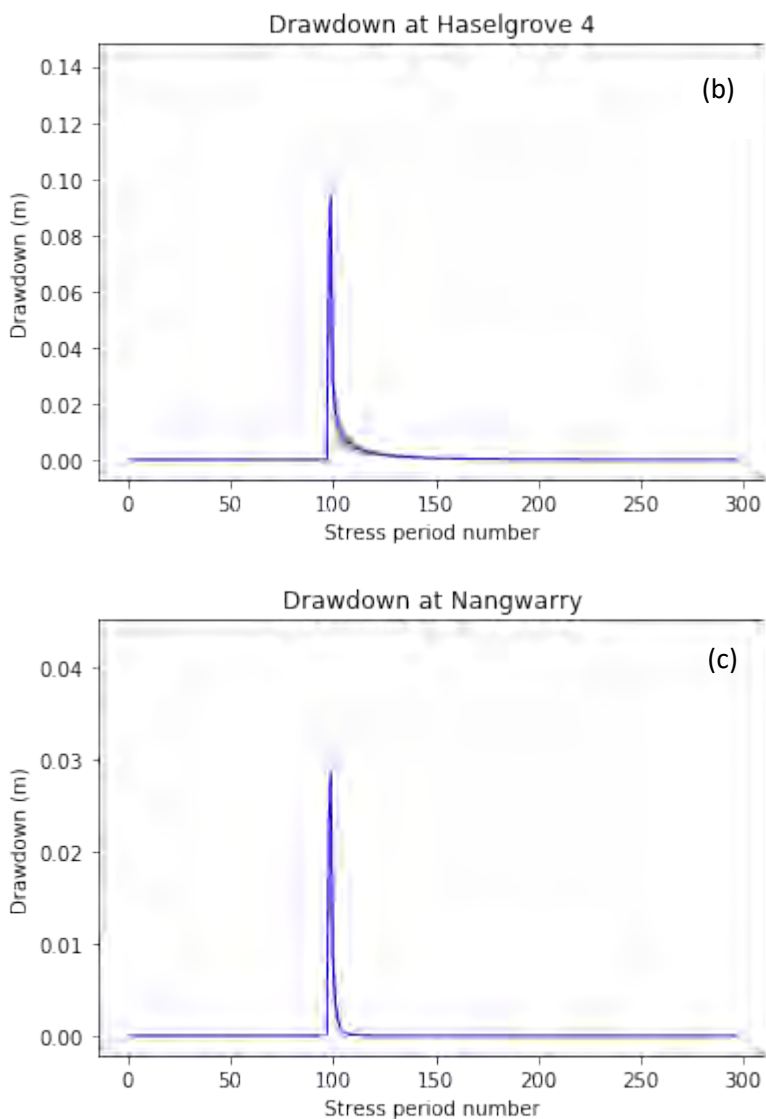


Figure 34 Drawdown at the three well sites showing the average drawdown in blue, and uncertainty bands in grey, for Dombey (a), Haselgrove 4 (b) and Nangwarry (c).

Drawdown at distances of 500 m and 1 km from the gas wells are indicated in Figure 35. Modelling suggested that there is a 95% chance that drawdown would be less than 0.1 m at distances larger than 500 m from Dombey 1, and less than 0.09 m at distances larger than 500 m from Haselgrove 4. There is a 95% chance that drawdown would be less than 0.032 m at distances larger than 500 m from Nangwarry 1 well.

For distances of more than one kilometre from the wells, modelling indicated a 95% likelihood of drawdown being less than 0.09 m, 0.07 m and 0.032 m from Dombey 1, Haselgrove 4, and Nangwarry 1, respectively. The high hydraulic conductivity of the region has resulted in very low drawdown overall.

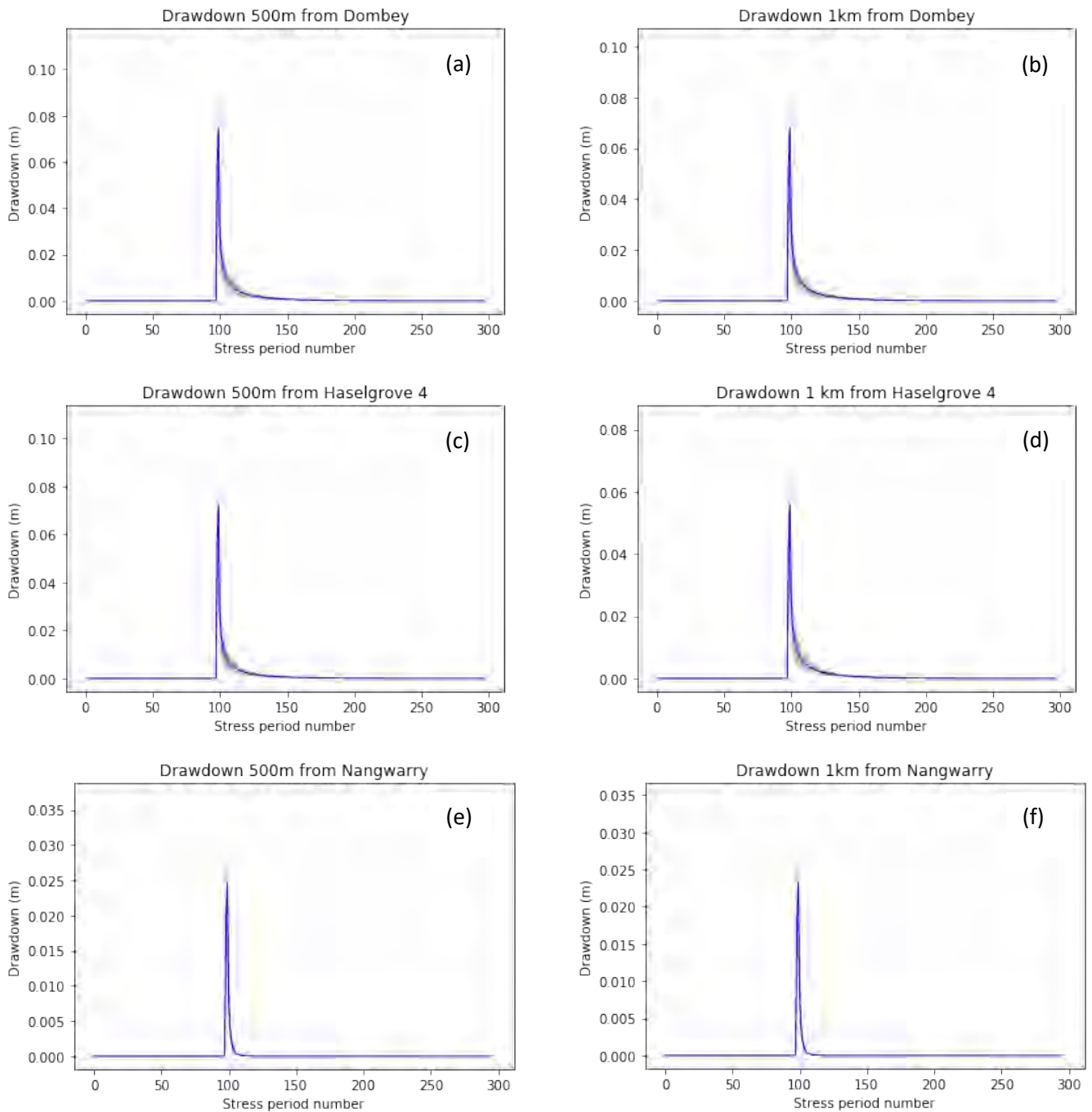


Figure 35 Drawdown at a distance of 500 m (a, c and e) and one km (b, d and f) from each of the three well sites showing the average drawdown in blue, and uncertainty bands in grey, for Dombey (a,d), Haselgrove 4 (b,e) and Nangwarry (c,f).

4.4 Well pumping rates

Summer groundwater extraction rates for agricultural, stock and domestic, town water supply and gas well development purposes were summed up and reported on a cell by cell basis (Figure 36). Summer pumping ranged from close to zero up to 4 ML per model cell. The pumping scenarios for the gas well development during the summer six-month stress period were 1 ML in comparison. There are 32 model cells with pumping rates greater than this. The proposed gas well extractions represent 3% of the summer extraction rate within the child model extent and 9% of the annual

extraction. On a scale of the whole of the South East, the water extraction is likely to represent a much lower percentage.

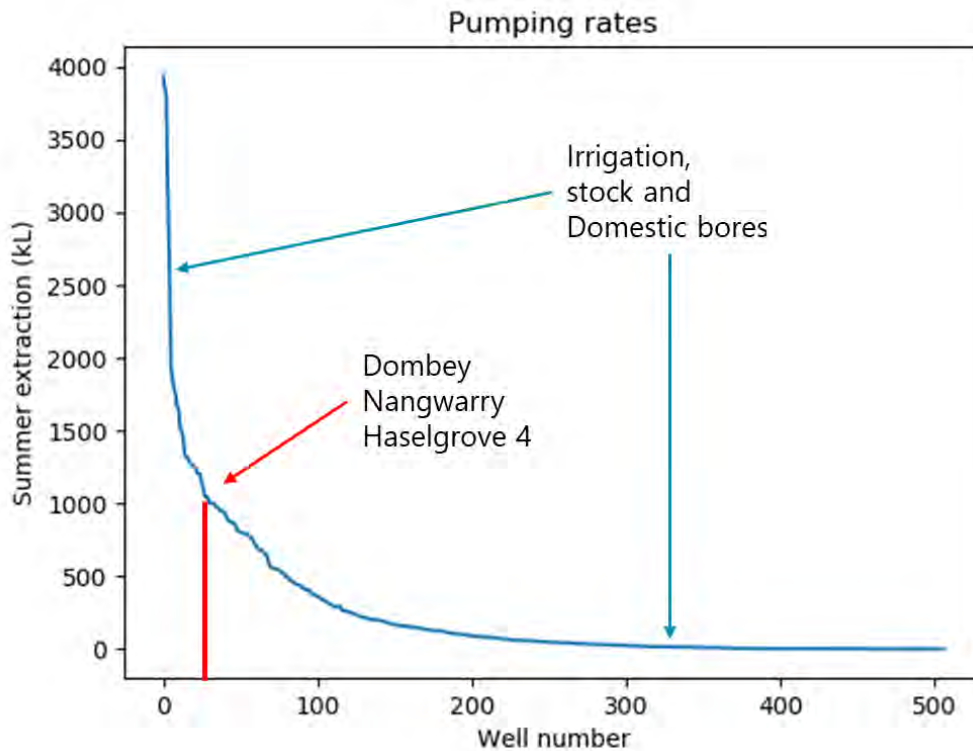


Figure 36 Histogram of the summer pumping rates from existing irrigation, stock and domestic wells within the child model extent, and the expected summer pumping rates at the Dombey, Haselgrove 4 and Nangwarry wells. Note that this only includes existing wells from within the child model extent, and not for the whole of the South East.

4.5 Water balance

Figure 36 shows the average annual water balance for the region covered by the child model, including the extraction for the gas well development scenarios, which only occur for a single year. This indicates the maximum contribution of the gas wells to the water balance. For subsequent years, the contribution of the gas wells would be zero. Change in storage is the largest component of the water balance outflows, followed by drains and irrigation, stock and domestic wells (Figure 37). The inflows to the annual water balance were dominated by net recharge, which constituted 68% of inflows to the model (Figure 38). Change in storage due to seasonal variation was the second highest inflow. Extraction for the gas well development was 1.7% of the annual average water balance. Note that in Figure 37 and Figure 38, the net recharge does not represent the total recharge and evapotranspiration, only the averaged positive and negative components of the net recharge to the groundwater. Whether net recharge is positive or negative will vary spatially and temporally through the model domain.

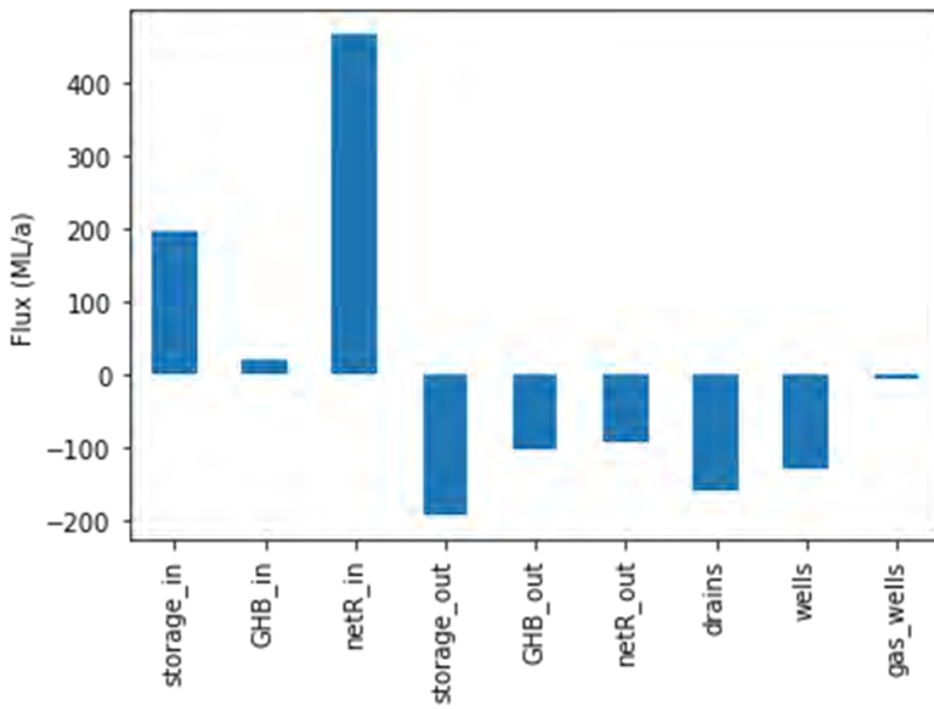


Figure 37 Water balance for the child model extent comparing the gas well extraction rate for the single year of construction to the annual average water balance over the 100-year model run time. It includes changes in groundwater storage (storage in and out), flows across the general head boundaries (GHB in and out), net Recharge NetR in and out, groundwater intercepted by the drains (drains), pumping from existing wells (wells) and pumping from the Dombey, Haselgrove 4 and Nangwarry wells (gas_wells).

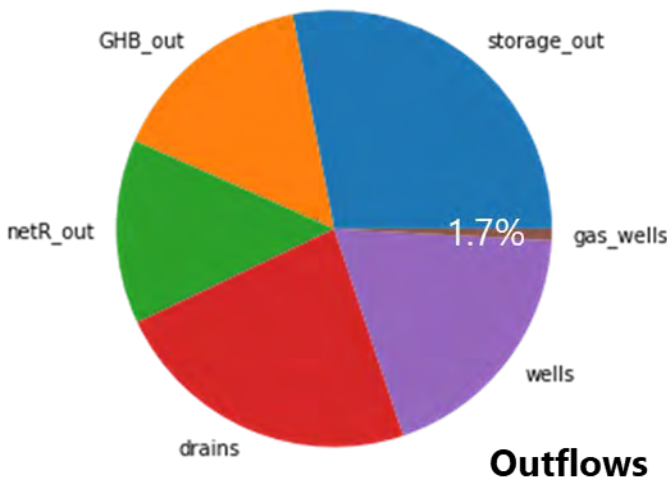
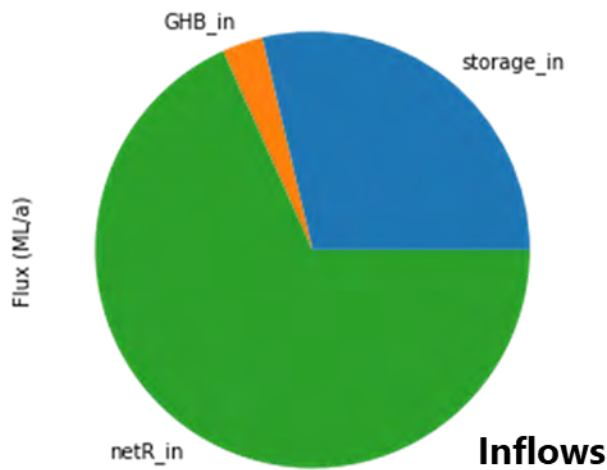


Figure 38 Water balance for the child model extent comparing the gas well extraction rate for the single year of construction to the annual average water balance over the 100-year model run time shown as inflows to the child model and outflows. The groundwater extraction for the gas wells makes up 1.7% of the total for the year of construction, and 0% for all other years.

4.6 Net recharge

Net recharge varied across the model domain based on soil and land use types, climate and depth to groundwater table (Figure 39). The climatic divide between Mt Burr data (south west corner) and Penola data (north east data) is clear in Figure 39b. Higher rates of NetR (both recharge and ET dominant) are associated with shallow groundwater, particularly where the groundwater intersects the land surface (Figure 40). Net recharge was also influenced by land cover (Figure 10) and soil type (Figure 11).

Across the child model domain, the average annual net recharge was 22 mm/year. By comparison, the CMRSET data for the South East region represented by the South East regional water balance model produced an estimated overall net recharge of 44 mm/year (Doble, et al., 2015, Doble, et al., 2017).

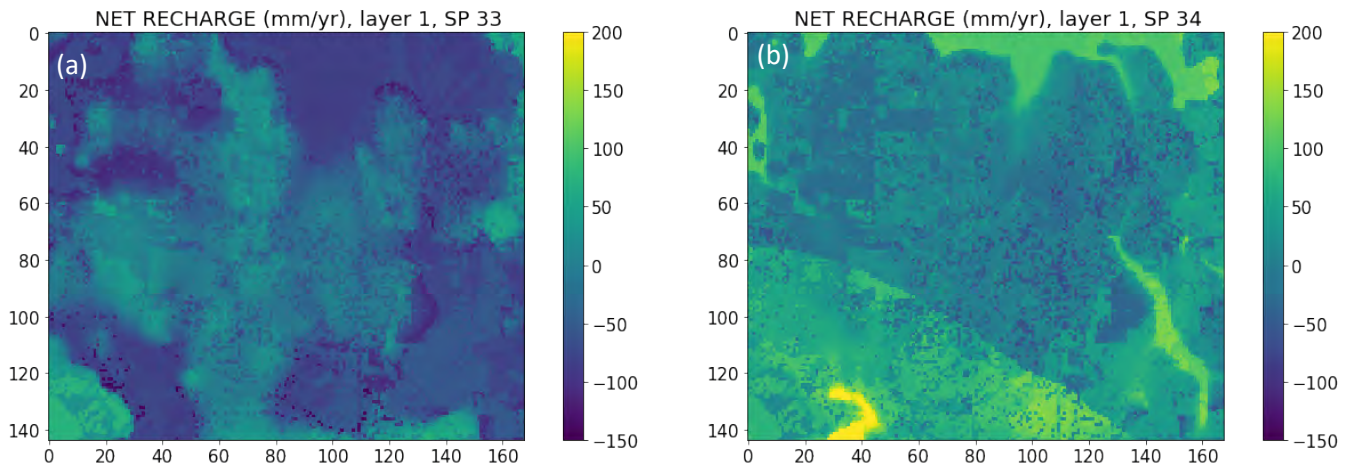


Figure 39 One realisation of the net recharge for the child model extent during the dry summer season (a) and the wet winter season (b). Note the change from ET dominant conditions (a) to recharge dominant conditions (b) and the NW-SE line demarking the change between Mount Burr and Penola climate data in (b).

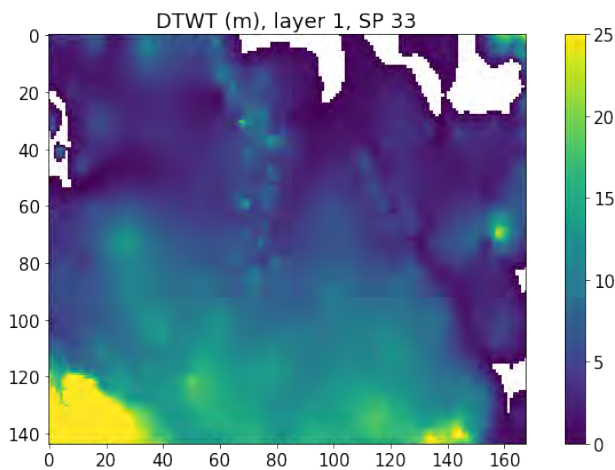


Figure 40 Depth to groundwater in stress period 33 of the model for the same realisation in Figure 39.

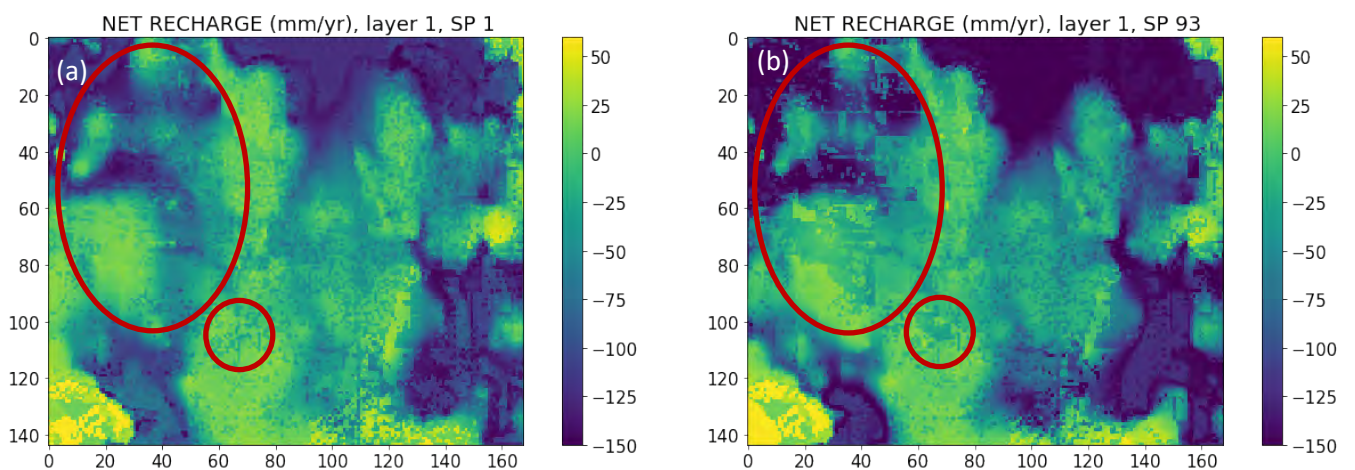


Figure 41 One realisation of the net recharge for the child model extent (summer season, ET dominant) in 1970 (a) and 2016 (b). Red ovals indicate areas where forestry development has taken place.

Figure 42 and Figure 43 show the water balance components for the last 18 stress periods (9 years) of modelling for seasonally varying and annual NetR inputs respectively. Net recharge and the associated change in storage were the dominant water balance components. The seasonally varying NetR results show NetR(purple) varying from recharge dominant (positive) to ET dominant (negative) with each six-monthly stress period. The storage (pink) varied in opposite sync with the net recharge as the groundwater depth rose and fell seasonally in response to the recharge and discharge.

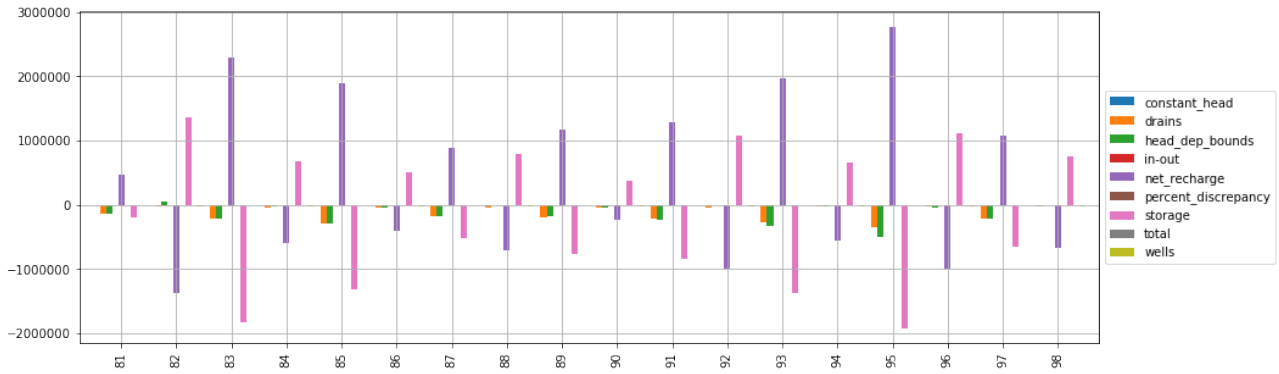


Figure 42 Water balance from the groundwater model with seasonally changing NetR curves, for the last 18 stress periods of the history matching period (2000 - 2019). Net recharge inflows and outflows and changes in storage are relatively larger due to the seasonally changing NetR curves.

The annual NetR results show net recharge (occurring in paired, six-monthly stress periods) vary depending on the relative rainfall and PET for the year (Figure 43). Generally, the net recharge is positive (recharge dominant). As NetR is averaged for each year, it is smaller in comparison to the other water balance components, including drains and well extraction. Head dependent boundary inputs and outputs were of the same order of magnitude as the drains, and mostly negative. The head boundary conditions were based on results from the regional scale groundwater model, and these could be improved by recalibrating the regional scale model with the same NetR package inputs. Well extraction alternated from high in summer to low in winter and increased over time as the area of land under irrigation expanded.

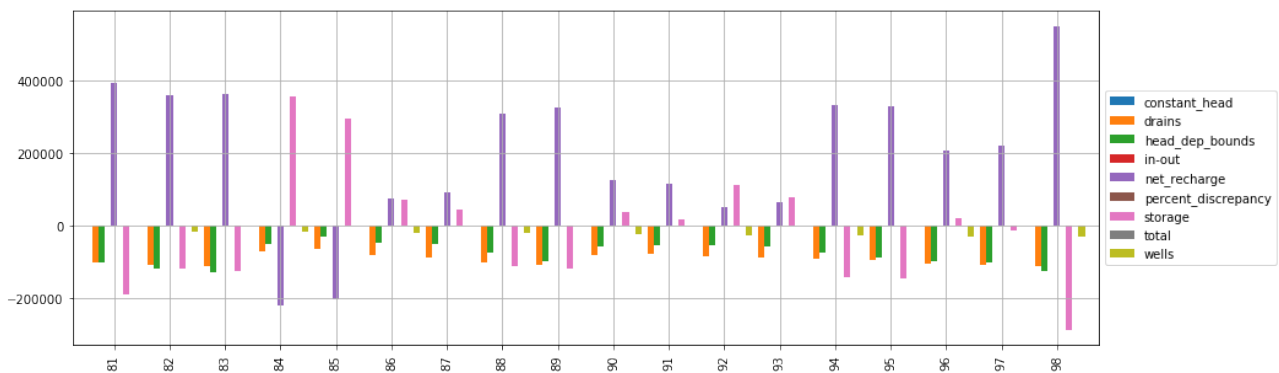


Figure 43 Water balance from the groundwater model with annually changing NetR curves, for the last 18 stress periods of the history matching period (2000 - 2019). Net recharge inflows and outflows are relatively larger due to the seasonally changing NetR curves.

5 Conclusions

The work described in this report was undertaken for a region around Penola in the South East of South Australia, to quantify the potential impacts on groundwater resources from conventional gas well and carbon dioxide well development. A child model was developed based on the hydrostratigraphy and parameterisation of the Kingston calibration of the South East regional water balance model and the Wattle Range groundwater model. The child model covered a region near Penola that included three gas well sites, namely, Haselgrove 4, Nangwarry 1 and Dombey 1. The model domain extended 36 km east-west and 42 km north-south, thus covering a total area of 1512 km². The flow domain was conceptualised as a three-layer system, comprising of the unconfined Tertiary Limestone Aquifer, the Upper Tertiary Aquitard and the Tertiary Confined Sand Aquifer.

The model was developed using FloPy, a Python based interface for the USGS MODFLOW 2005 groundwater flow model. History matching was undertaken from May 1970 to May 2019. Future scenario analysis runs were for a period of 149 years, from May 1970 to May 2119, assuming a historical warm up time of 49 years a gas well development period of one year, operational lifetime of 40 years and duration of potential impact of 100 years.

The NetR package was coded into MODFLOW-NWT, which provided a more stable framework for modelling wetting and drying processes associated with shallow groundwater. Modelling required a similar computational effort as the standard MODFLOW-NWT but included the emulated unsaturated zone processes associated with NetR. The NetR inputs were calibrated with PEST, standard software for groundwater model calibration and uncertainty software, using stretch and shift parameters on the NetR – DTW curves.

The water consumption associated with the construction and operation of the Dombey 1, Haselgrove 4 and Nangwarry 1 gas wells were found to have minimal impacts on the water balance of the South East. The maximum drawdown in the unconfined Tertiary Limestone Aquifer at the Dombey 1 and Haselgrove 4 sites, under the planned extraction scenario had a 95% chance of being less than 14 cm. The maximum drawdown in the confined Tertiary Confined Sands Aquifer at the Nangwarry site in the confined aquifer has a 95% chance of being less than 4 cm. At more than one kilometre away from the extraction wells, the drawdown reduced to having a 95% chance of being less than 9 cm, 7 cm and 3 cm from Dombey 1, Haselgrove 4 and Nangwarry 1 respectively. The high hydraulic conductivity of the region resulted predominantly in very low drawdowns.

The magnitude of drawdown was comparable to the seasonal changes in groundwater elevation with a rapid recovery of groundwater head after cessation of pumping. The proposed water extraction volumes for the construction of the three wells extractions represent around 1.7% of the water balance outflows of the modelled flow domain for a single year with no further extraction in subsequent years. At the scale of the entire Otway Basin, the extraction is likely to represent far less than 1.7% of the water budget. The drawdown from the construction these wells is therefore unlikely to impact any assets in the region.

Net recharge emulation was used to incorporate spatial and temporal changes in rainfall, soil types and land cover into the model and capture recharge and ET behaviour where groundwater is shallow. This project represents a first-time implementation of the NetR package in a fully transient mode with changing land use and climate data. Furthermore, it is also the first time that the NetR – DTW curves have been included in model calibration.

The development of the finer scale child model allowed stochastic Particle Tracking analyses to be carried out to identify flow paths and flow rates that underpin the modelling of solute transport undertaken in the companion GISERA SE contamination project (Rassam, et al., 2020).

6 Appendices

6.1 Land use change

The following maps (Figures 44 to 49) show the original South Australian Land Cover Layers (Willoughby, et al., 2018)

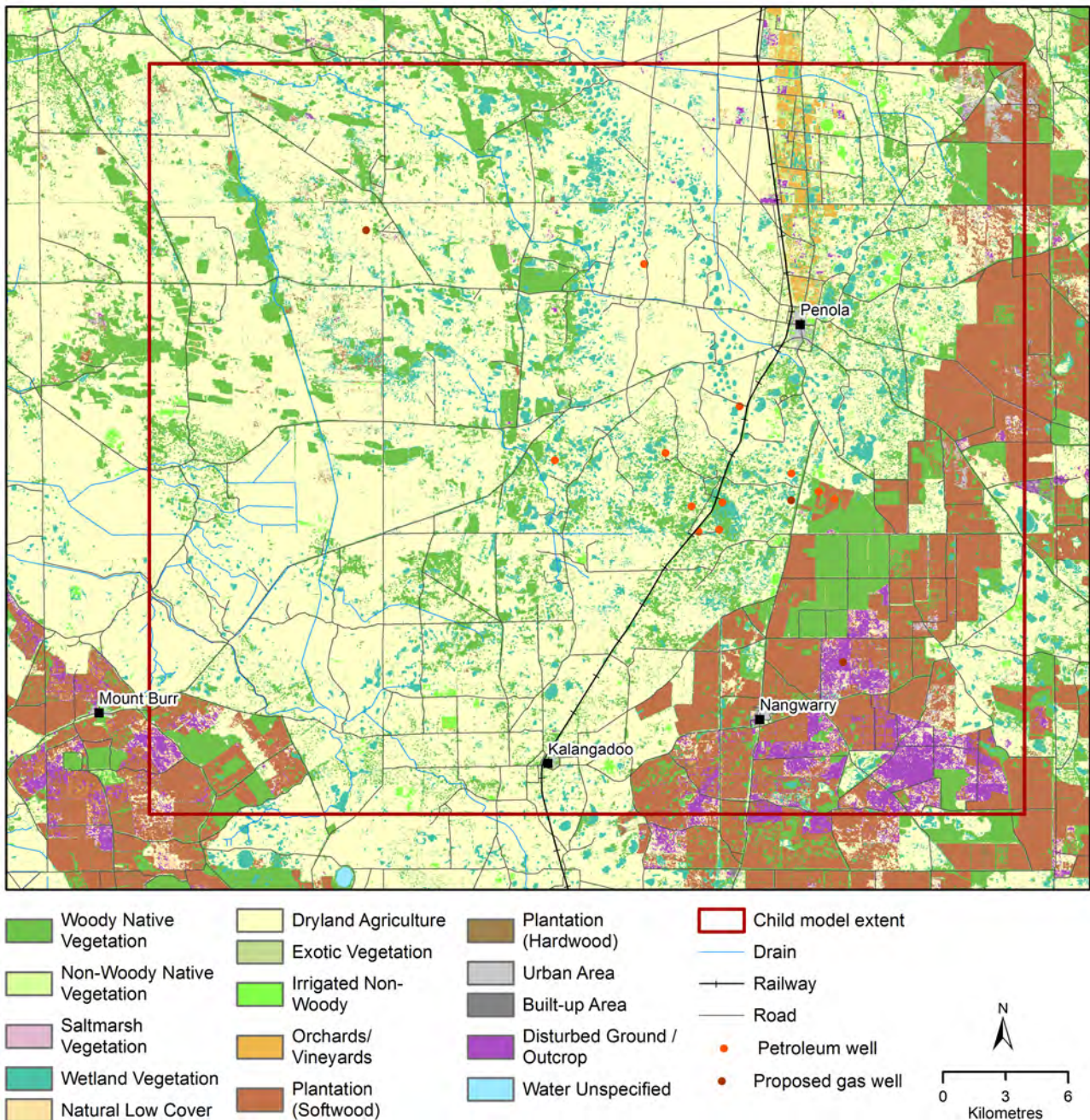


Figure 44 Most likely land cover for the Penola region from 1987 to 1990

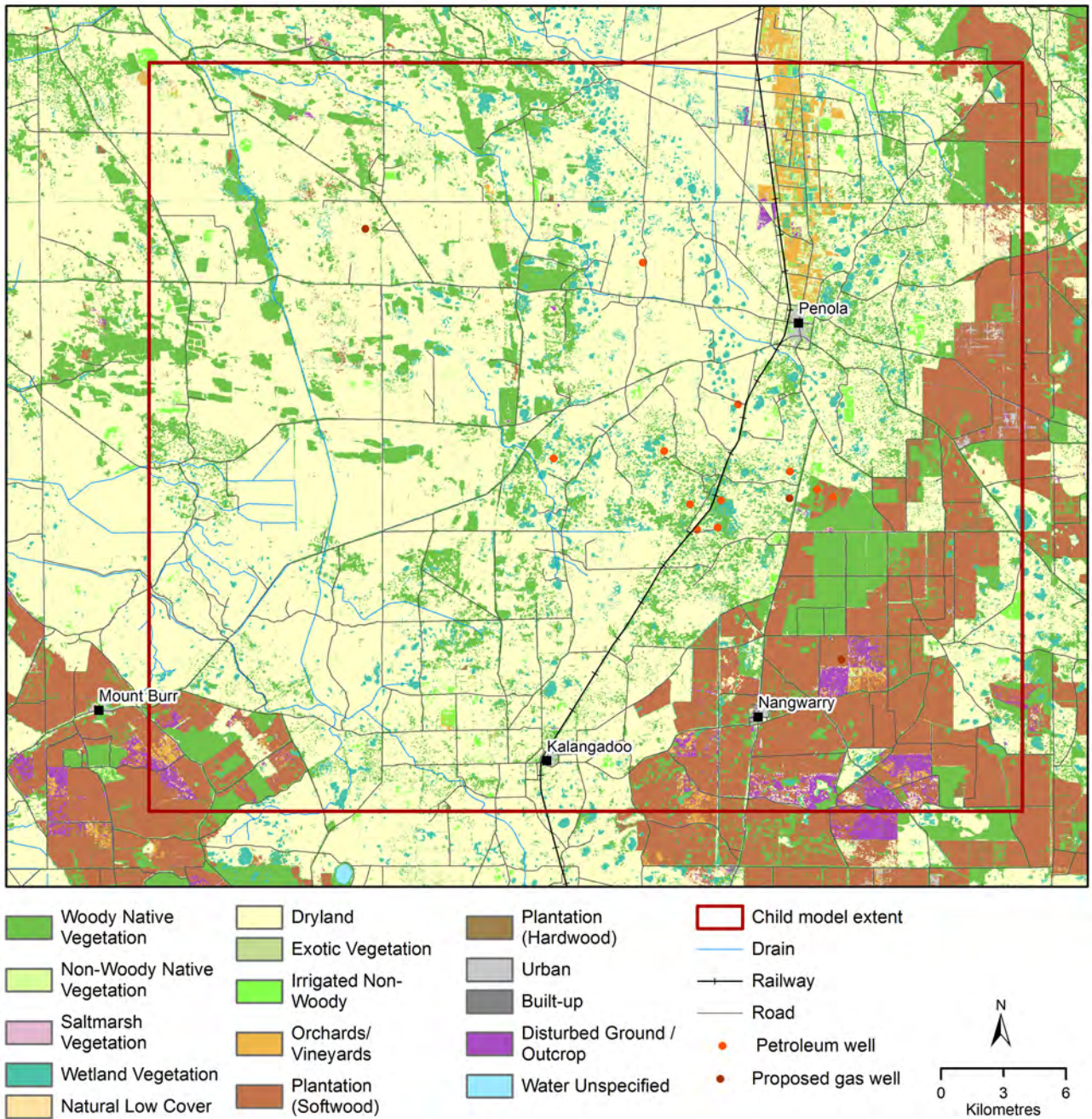


Figure 45 Most likely land cover for the Penola region from 1990 to 1995

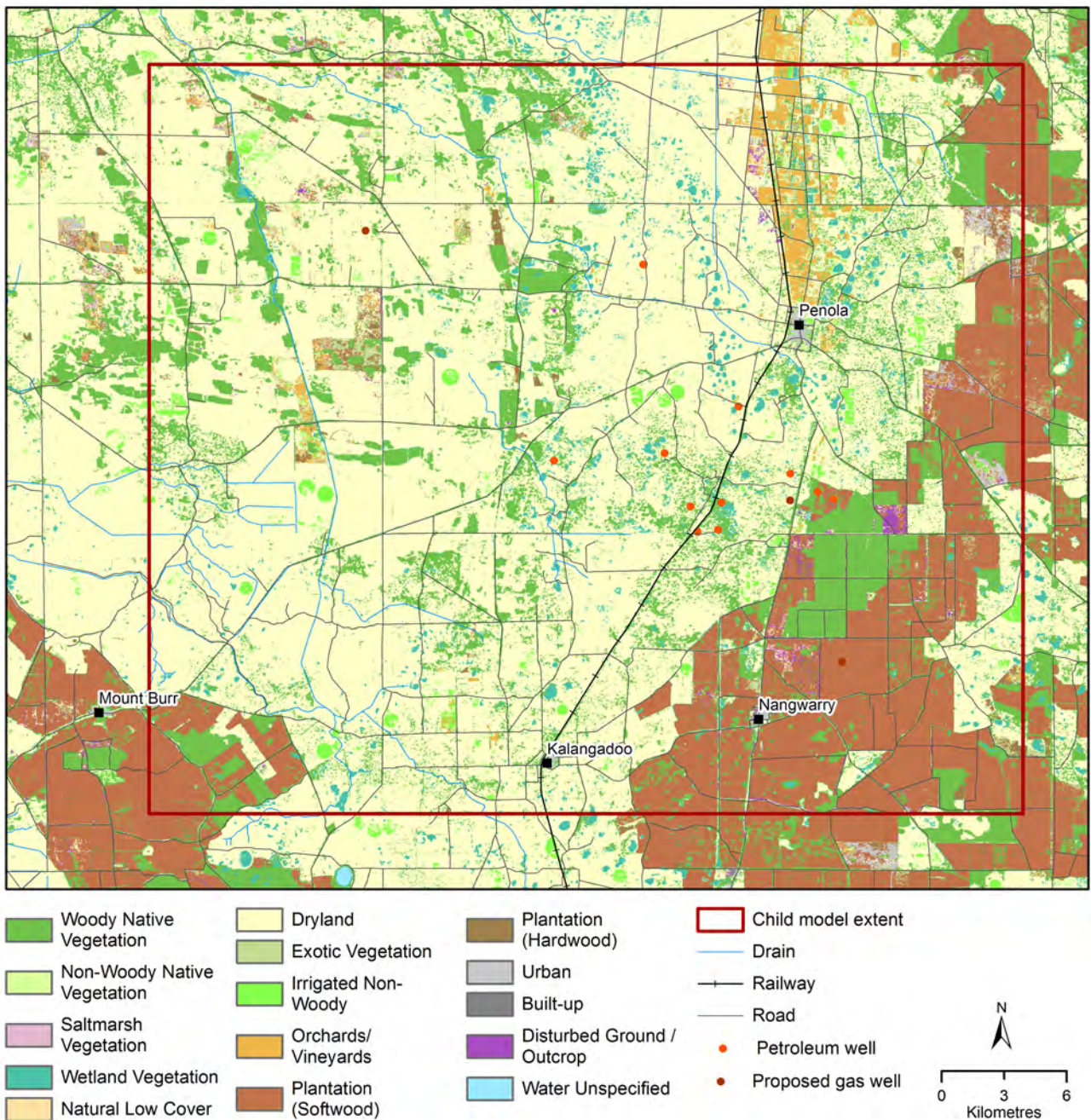


Figure 46 Most likely land cover for the Penola region from 1995 to 2000

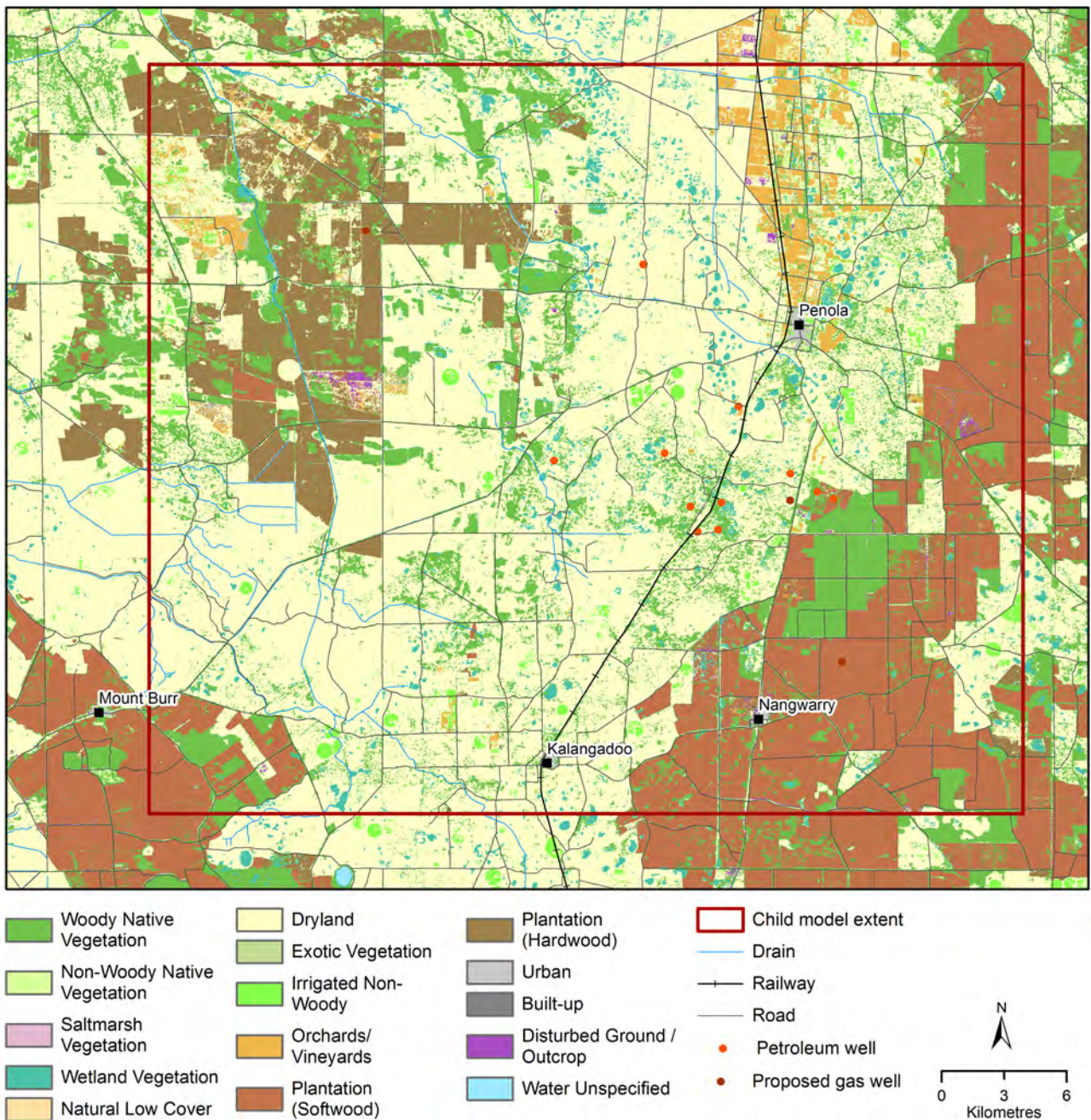


Figure 47 Most likely land cover for the Penola region from 2000 to 2005

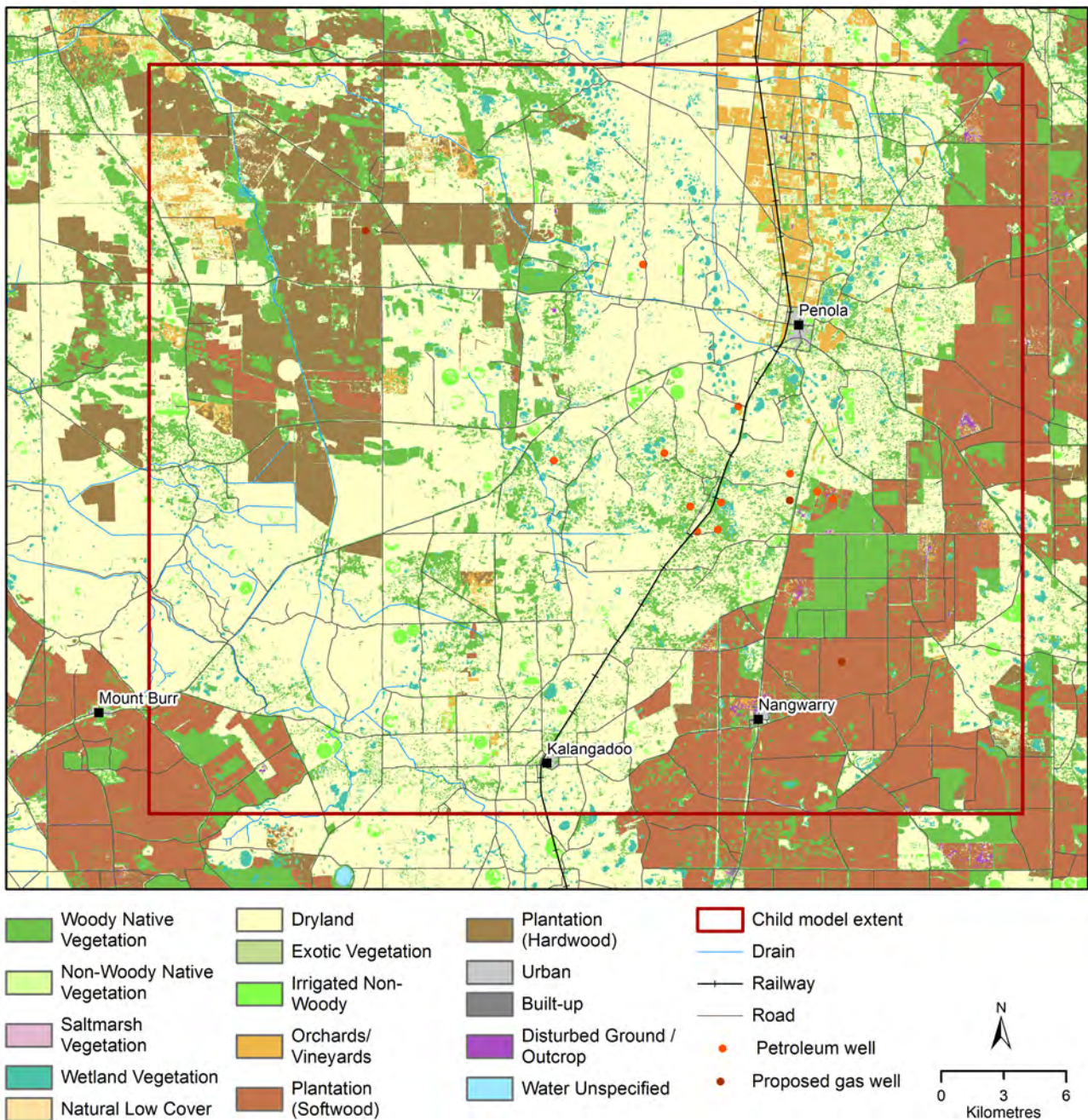


Figure 48 Most likely land cover for the Penola region from 2005 to 2010

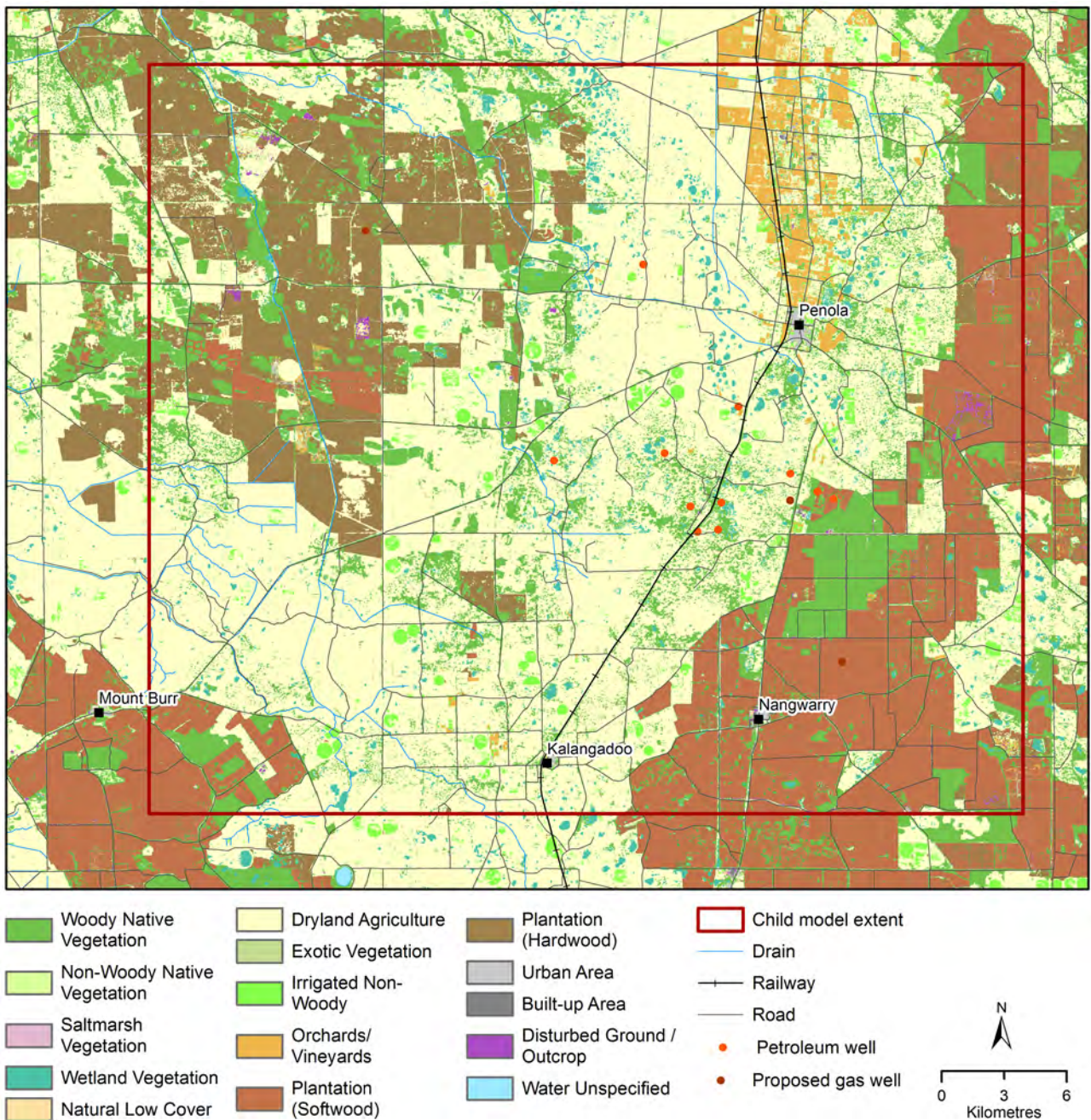


Figure 49 Most likely land cover for the Penola region from 2010 to 2015

6.2 Land use change updated for the NetR package

The following maps (Figures 50 to 55) show the most likely land covers that were aggregated to the seven land use types used in the NetR modelling.

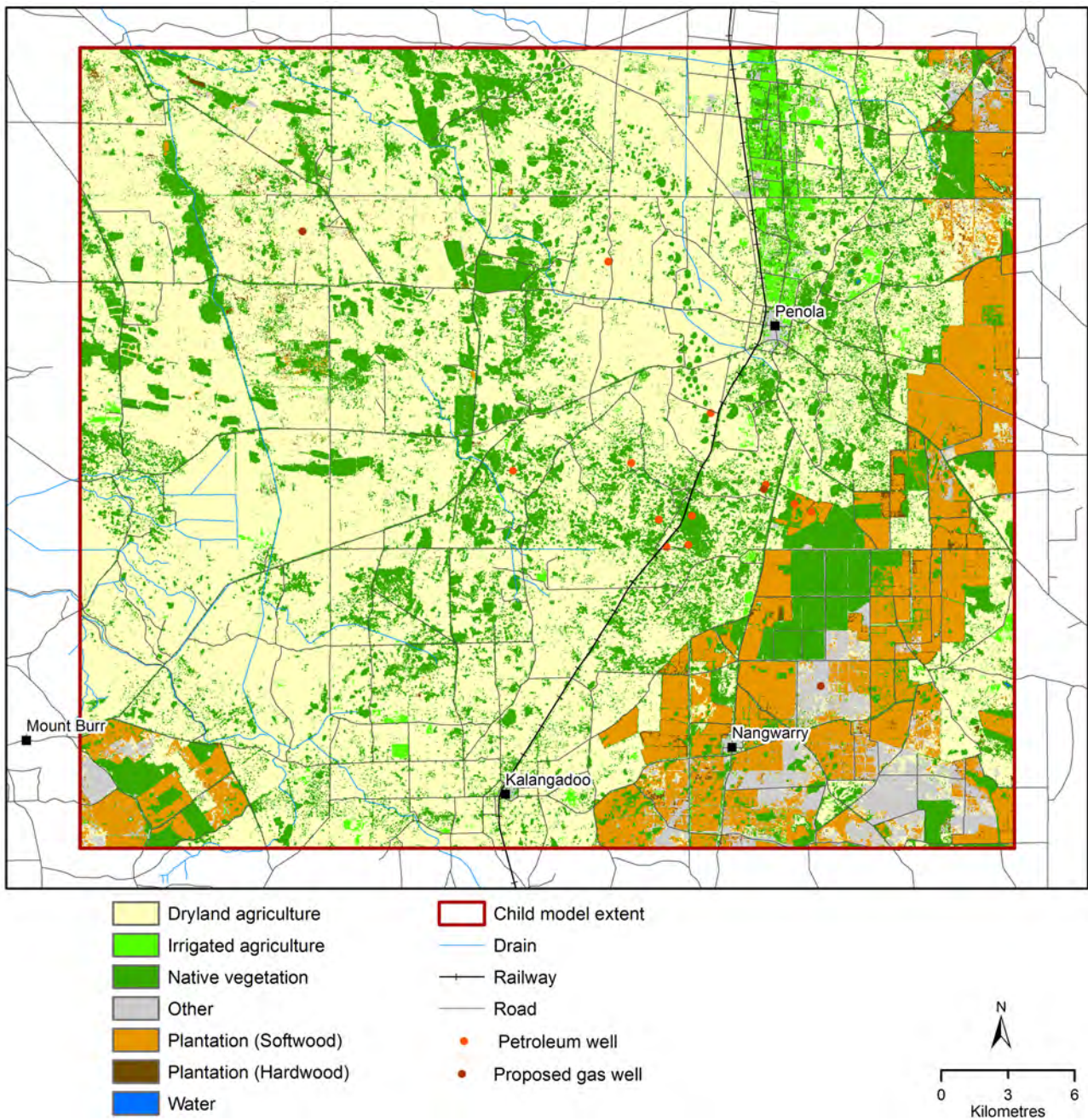


Figure 50 Most likely land cover aggregated for the child model from 1987 to 1990

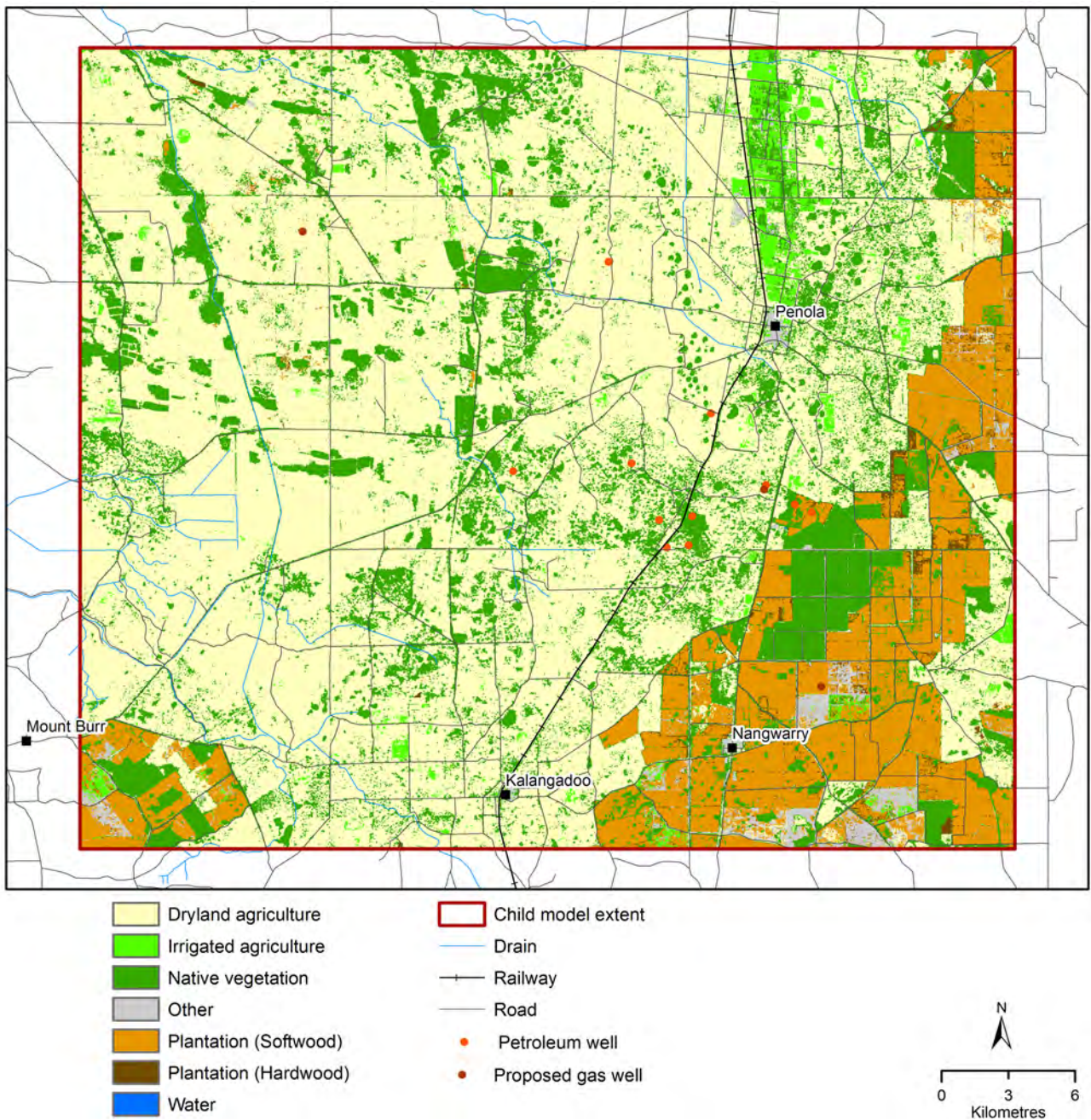


Figure 51 Most likely land cover aggregated for the child model from 1990 to 1995

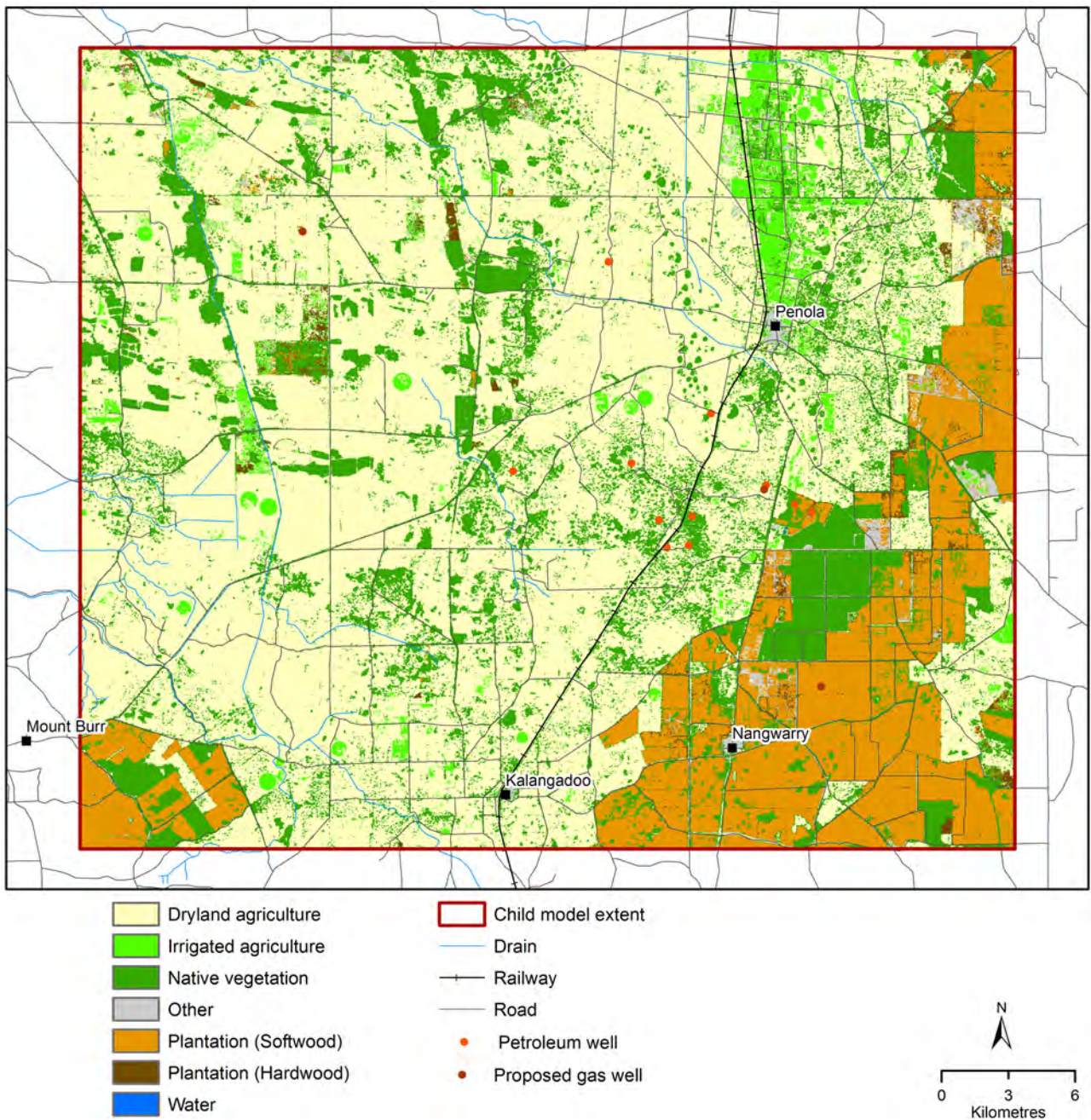


Figure 52 Most likely land cover aggregated for the child model from 1995 to 2000

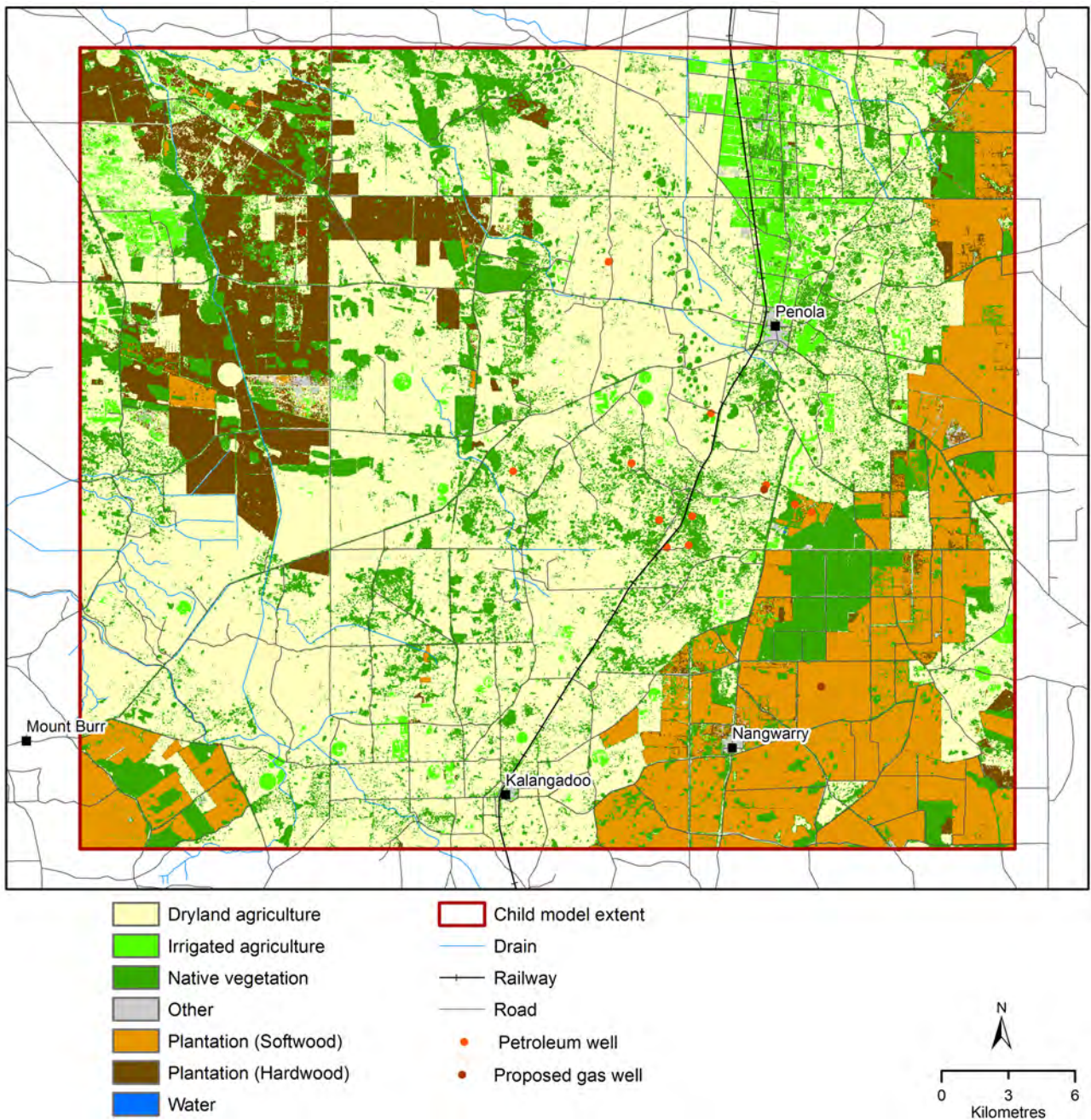


Figure 53 Most likely land cover aggregated for the child model from 2000 to 2005

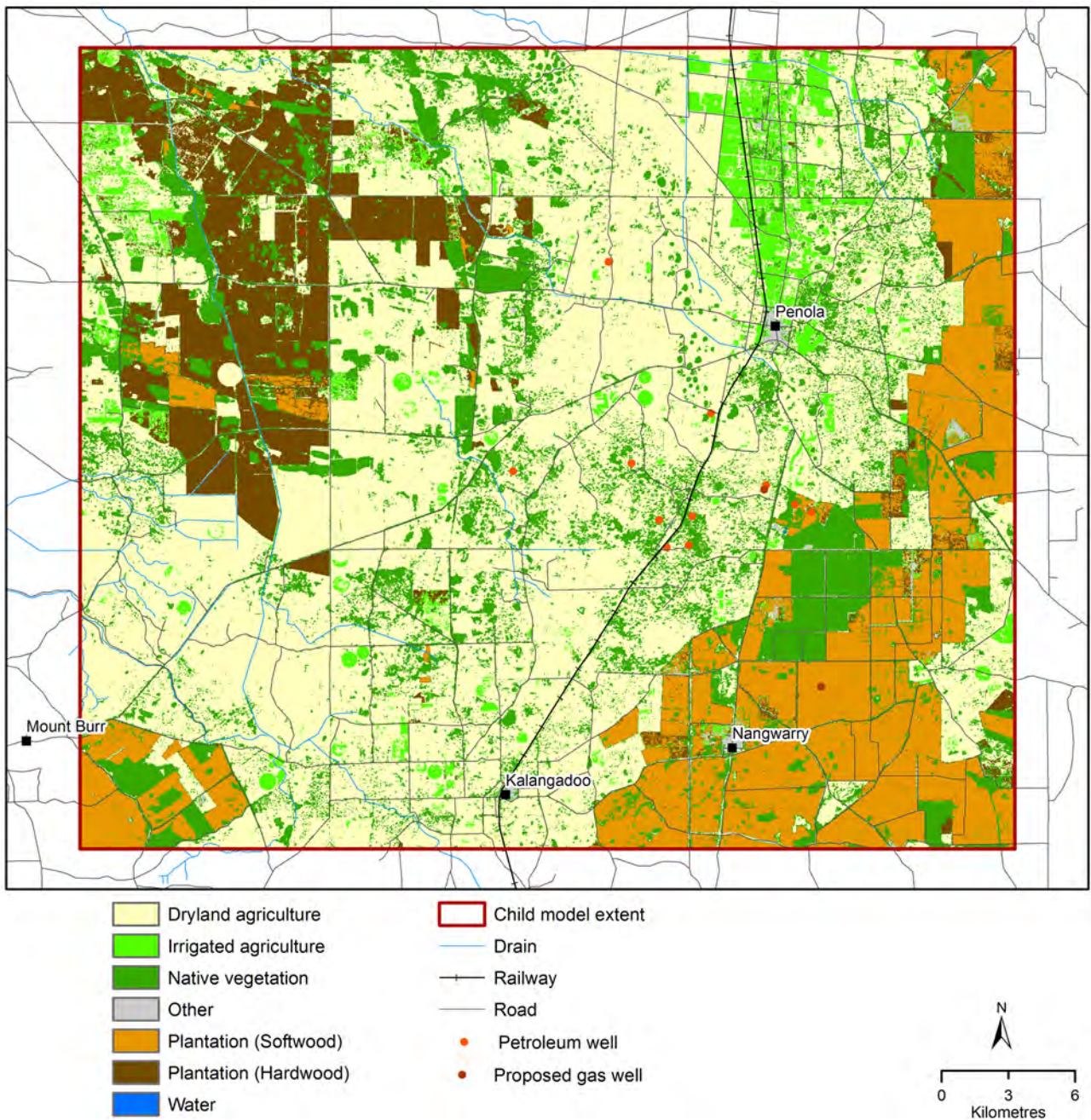


Figure 54 Most likely land cover aggregated for the child model from 2005 to 2010

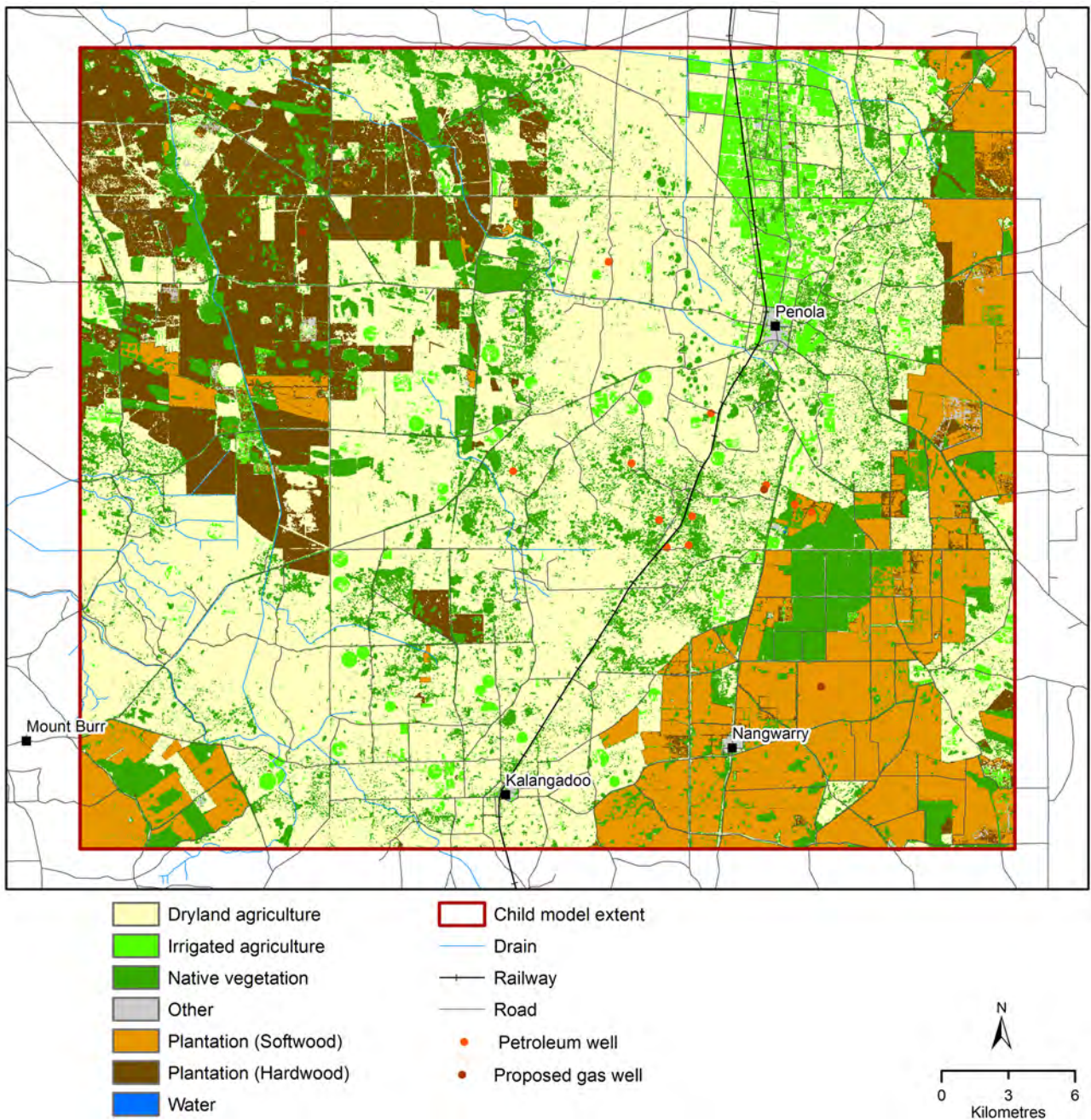
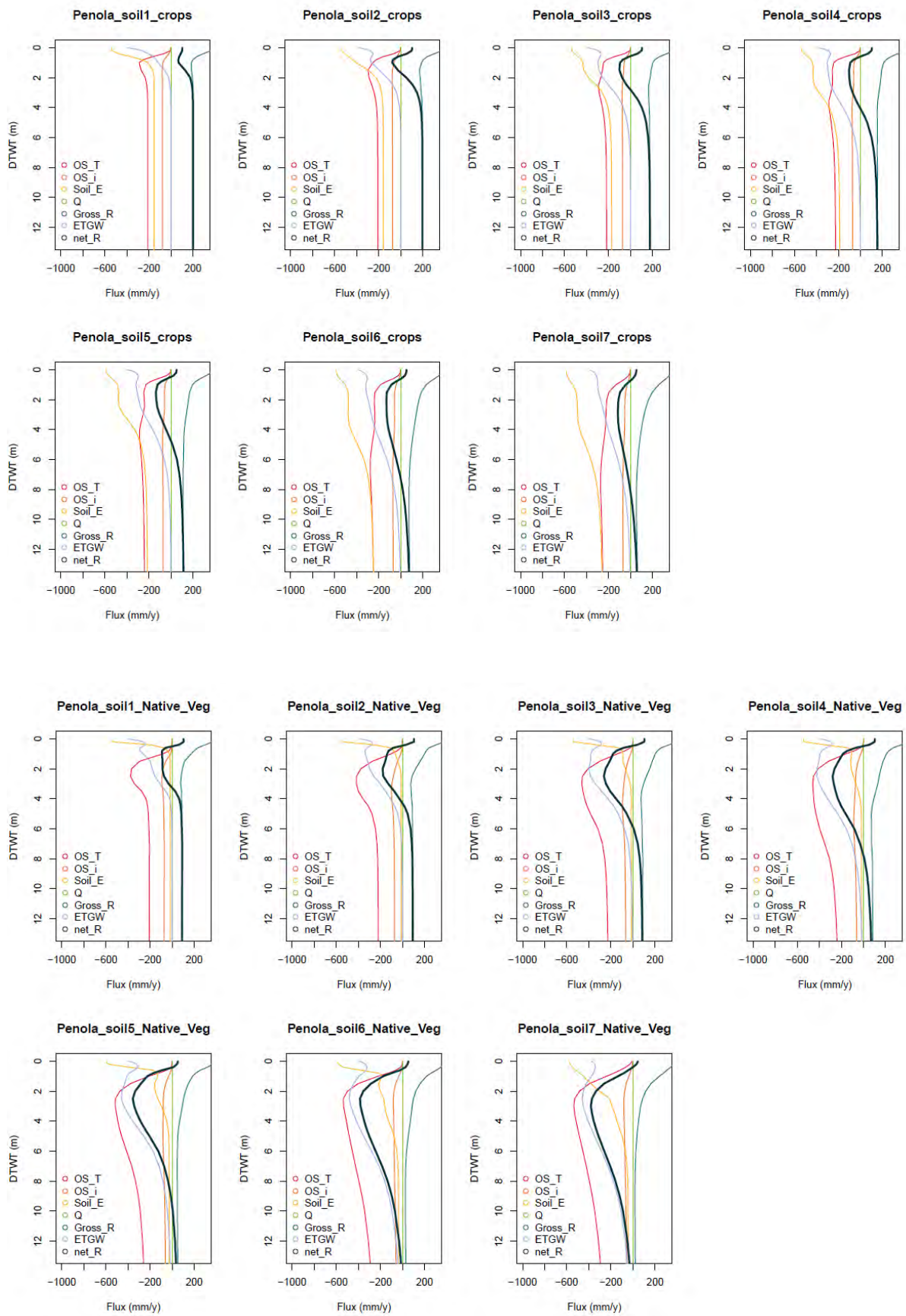
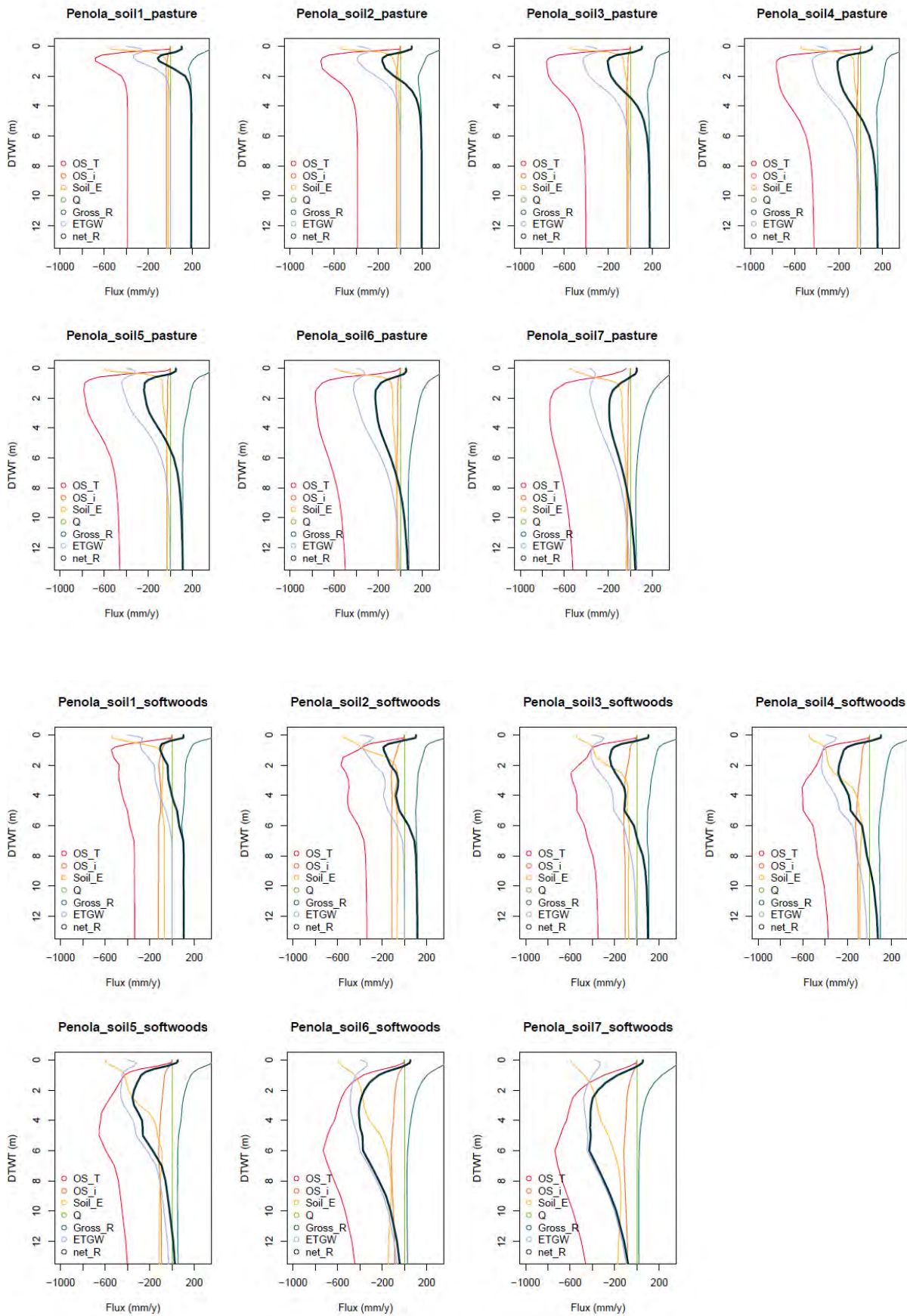


Figure 55 Most likely land cover aggregated for the child model from 2010 to 2015

6.3 Average annual NetRcurves





7 References

- Ahrens J, Geveci B, Law C (2005) Paraview: An end-user tool for large data visualization. *The visualization handbook* 717
- Bakker M, Post V, Langevin CD, Hughes JD, White JT, Starn JJ, Fienen MN (2016) Scripting MODFLOW model development using Python and FloPy. *Groundwater* 54: 733–739 DOI 10.1111/gwat.12413
- Brown K, Harrington GA, Lawson J (2006) Review of groundwater resource condition and management principles for the Tertiary Limestone Aquifer in the South East of South Australia, DWLBC Technical report 2006/02, Government of South Australia, Department of Water, Land and Biodiversity Conservation, Mount Gambier. .
- Chen Y, Oliver DS (2012) Ensemble randomized maximum likelihood method as an iterative ensemble smoother. *Mathematical Geosciences* 44: 1-26
- Cook PG, Miller A, Shanafield M, Simmons CT (2016) Predicting Water Resource Impacts of Unconventional Gas Using Simple Analytical Equations. *Groundwater*: n/a-n/a DOI 10.1111/gwat.12489
- Dawes W, Zhang L, Dyce P (2004) WAVES v3.5 User Manual CSIRO Land and Water, Canberra, pp. 30.
- Doble RC, Pickett T, Crosbie RS, Morgan LK (2015) A new approach for modelling groundwater recharge in the South East of South Australia using MODFLOW Goyder Institute for Water Research Technical Report 15/26.
- Doble RC, Pickett T, Crosbie RS, Morgan LK, Turnadge C, Davies PJ (2017) Emulation of recharge and evapotranspiration processes in shallow groundwater systems. *Journal of Hydrology* 555: 894-908 DOI <https://doi.org/10.1016/j.jhydrol.2017.10.065>
- Harbaugh AW (2005) MODFLOW-2005, the US Geological Survey modular ground-water model: The ground-water flow process US Department of the Interior, US Geological Survey Reston, VA, USA
- Hutton C, Wagener T, Freer J, Han D, Duffy C, Arheimer B (2016) Most computational hydrology is not reproducible, so is it really science? *Water Resources Research* 52: 7548-7555
- Ince DC, Hatton L, Graham-Cumming J (2012) The case for open computer programs. *Nature* 482: 485 DOI 10.1038/nature10836
- Johnston RM, Barry SJ, Bleys E, Bui EN, Moran CJ, Simon DAP, Carlile P, McKenzie NJ, Henderson BL, Chapman G, Imhoff M, Maschmedt D, Howe D, Grose C, Schoknecht N, Powell B, Grundy M (2003) ASRIS: the database. *Australian Journal of Soil Research* 41: 1021-1036
- Morgan LK, Harrington N, Werner AD, Hutson J, Woods J (2015) South East Regional Water Balance Project – Phase 2, Development of a Regional Groundwater Flow Model. Goyder Institute for Water Research Technical Report Series No. 15/38, pp. 138.
- Niswonger RG, Panday S, Ibaraki M (2011) MODFLOW-NWT, a Newton formulation for MODFLOW-2005. *US Geological Survey Techniques and Methods* 6: A37
- Rassam D, Sreekanth J, Gonzalez D, Mallants D, Doble R (2020) Groundwater contamination vulnerability and modelling analysis of onshore gas water quality impacts for southeast SA, CSIRO Land and Water.
- White JT (2018) A model-independent iterative ensemble smoother for efficient history-matching and uncertainty quantification in very high dimensions. *Environmental Modelling & Software* 109: 191-201

- Willoughby N, Thompson D, Royal M, Miles M (2018) South Australian Land Cover Layers: an Introduction and Summary Statistics. DEW Technical report 2018/01. Government of South Australia, Department for Environment and Water, Adelaide.
- Wood C (2017) Lower Limestone Coast forest water accounting groundwater model, DEWNR Technical report 2017/14, Government of South Australia, Department of Environment, Water and Natural Resources, Adelaide
- Wood C, Pierce D (2015) South East confined aquifer modelling investigations - Kingston groundwater management area, DEWNR Technical report 2015/48, Government of South Australia, through Department of Environment, Water and Natural Resources, Adelaide.
- Wood G, Way D (2011) Development of the Technical Basis for a Regional Flow Management Strategy for the South East of South Australia, DFW Report 2011/21, Government of South Australia, through Department for Water, Adelaide.

CONTACT US

t 1300 363 400
+61 3 9545 2176
e csiroenquiries@csiro.au
w www.csiro.au

AT CSIRO, WE DO THE EXTRAORDINARY EVERY DAY

We innovate for tomorrow and help improve today – for our customers, all Australians and the world.

Our innovations contribute billions of dollars to the Australian economy every year. As the largest patent holder in the nation, our vast wealth of intellectual property has led to more than 150 spin-off companies.

With more than 5,000 experts and a burning desire to get things done, we are Australia's catalyst for innovation.

CSIRO. WE IMAGINE. WE COLLABORATE.
WE INNOVATE.